

**Yale University**  
**EliScholar – A Digital Platform for Scholarly Publishing at Yale**

---

Yale Medicine Thesis Digital Library

School of Medicine

---

January 2015

# Skeletal Maturity Assessment: Calcaneal Apophyseal Ossification

Allen Nicholson

Follow this and additional works at: <http://elischolar.library.yale.edu/ymtdl>

---

## Recommended Citation

Nicholson, Allen, "Skeletal Maturity Assessment: Calcaneal Apophyseal Ossification" (2015). *Yale Medicine Thesis Digital Library*. 2003.

<http://elischolar.library.yale.edu/ymtdl/2003>

This Open Access Thesis is brought to you for free and open access by the School of Medicine at EliScholar – A Digital Platform for Scholarly Publishing at Yale. It has been accepted for inclusion in Yale Medicine Thesis Digital Library by an authorized administrator of EliScholar – A Digital Platform for Scholarly Publishing at Yale. For more information, please contact [elischolar@yale.edu](mailto:elischolar@yale.edu).

# **Skeletal Maturity Assessment: Calcaneal Apophyseal Ossification**

A Thesis Submitted to the Yale University School of Medicine in  
Partial Fulfillment of the Requirements for the Degree of Doctor of  
Medicine

By

Allen D. Nicholson

2015

## **Abstract**

**Background:** Skeletal maturity scoring systems are used to gauge the amount of growth that a child has experienced and the amount of growth that remains. Studies have shown that skeletal maturity is more closely linked to time of peak height velocity (PHV) than chronological age. At PHV, skeletal maturity is very similar between children regardless of sex. Determination of PHV is important for orthopaedic decisions such as timing of epiphysiodesis and risk of scoliosis curve progression. However, the few existing systems of maturity assessment that can identify PHV have limitations preventing them from being used clinically or from predicting PHV beginning at an early age. Ossification of the calcaneal apophysis has never been fully characterized. We examined the ossification sequence of the calcaneus in relation to timing of peak height velocity (PHV). We compare calcaneal apophyseal ossification to other systems of maturity assessment including the Sanders hand score and the modified Oxford hip score. Also, we compare calcaneal apophyseal ossification to the ossification sequence of the plantar and thenar sesamoids, the triradiate cartilage (TRC), and the iliac apophysis.

**Methods:** Ninety-four healthy children (forty-nine females and forty-five males) between ages three and eighteen were followed longitudinally through their growth with annual serial radiographs and physical examinations. We had approximately seven hundred serially acquired sets of foot, hip, and hand radiographs. PHV was calculated using the height measurements of each child. We compared to PHV the extent of calcaneal apophyseal ossification, iliac crest apophyseal ossification, Sanders hand scores, thenar and plantar sesamoid appearance, the TRC, and modified Oxford hip scores using radiographs taken on the same day annually over a minimum five year period.

**Results:** Excursion of the calcaneal apophysis begins with appearance of the ossification center approximately five years prior to PHV and can be divided into six stages that occur over a seven year period. Four of six stages of calcaneal apophyseal ossification and two of eight stages of the Sanders system occur prior to PHV. The areas of overlap of the calcaneal and Sanders stages allow the two maturity systems to be combined for superior localization of maturity. The plantar and thenar sesamoids offer the ability to quickly deduce maturity and clarify stages of the calcaneal and Sanders systems. If the plantar sesamoids are present, and the thenar sesamoids are absent, the child is in between 1.35 to 0.12 years before PHV. Calcaneal stages 0-3, and Sanders hand scores 1-2 are associated with modified Oxford hip scores indicating substantial risk of contralateral SCFE.

**Conclusions:** Ossification of the calcaneal apophysis can determine skeletal maturity around the time of adolescence. The calcaneal system can best identify maturity in the five years prior to PHV whereas the Sanders system better localizes maturity in time after PHV. Combinations of maturity systems allow for more precise localization of maturity than single systems alone. The calcaneal, Sanders system, and TRC can stratify children at high risk of contralateral SCFE. Identification of the most suitable maturity system to answer a clinical question depends on the certainty of the maturity indicator and the strength of the clinical association. If a maturity indicator is certain, and the clinical association of the maturity indicator is strong, additional maturity measurements are not needed. However, if either the maturity indicator or the clinical association is uncertain, further certainty can be obtained by considering a second maturity marker in conjunction, as shown through the improved power of the combined calcaneal/Sanders system for identification of PHV and prediction of contralateral SCFE.

## **Acknowledgements**

I would like to thank the coauthors of this work.

Coridon M. Huez, MD<sup>1</sup>, James O. Sanders, MD<sup>2</sup>, Raymond W. Liu, MD<sup>3</sup>, Daniel R.  
Cooperman, MD<sup>1</sup>

1. Department of Orthopaedics and Rehabilitation, Yale School of Medicine, PO Box 208071, New Haven, CT 06510
2. Department of Orthopaedics, University of Rochester School of Medicine, 601 Elmwood Ave, Box 665, Rochester, NY 14642
3. Department of Orthopaedics, Case Western Reserve University School of Medicine, 11100 Euclid Ave, Cleveland, OH 44106

### **Source of Funding**

We received a grant from POSNA which allowed us to digitize the images and identify the PHV. I received research funding from Yale University School of Medicine during the time I conducted this research.

# Table of Contents

	Page
<b>Introduction</b>	<b>1</b>
<b>Chapter 1</b> - Relationship of Calcaneal and Iliac Apophysis Ossification to Peak Height Velocity Timing in Adolescents	<b>8</b>
<b>Chapter 2</b> - Relationship of Calcaneal Apophyseal Ossification and Sanders Hand Scores to Peak Height Velocity Timing in Adolescents	<b>26</b>
<b>Chapter 3</b> - Digital and Analog Markers of Skeletal Maturity: The Clinical Utility of the Thenar and Plantar Sesamoids	<b>44</b>
<b>Chapter 4</b> - Translating Between Systems of Skeletal Maturity: The Prognostic Power of Skeletal Maturity for Prediction of Contralateral SCFE	<b>69</b>
<b>Discussion</b>	<b>96</b>
<b>References</b>	<b>101</b>

## **Introduction**

Determination of skeletal maturity is important when addressing the problems of growing children. Skeletal maturity scoring systems are used to gauge the amount of growth that a child has experienced and the amount of growth that remains. Remaining growth is more closely related to skeletal maturity than to chronological age.<sup>1-6</sup> Accurate maturity determination is often at the heart of pediatric orthopedics and improved methods will better inform epiphysiodesis timing, risk of contralateral slipped capital femoral epiphysis (SCFE), and risk of scoliosis progression.<sup>7,8</sup> With newer methods of harnessing growth to correct deformities, understanding where a child is in their growth sequence will become more important.

Skeletal maturation occurs in an orderly fashion but at different ages in different children.<sup>9</sup> The methods of determining “skeletal age” were first described by Todd<sup>10</sup> and have subsequently become part of standard usage through the Todd successor, the Greulich and Pyle atlas.<sup>9,11</sup> The Todd hand atlas and the Greulich and Pyle atlas describe a method of determining “skeletal age” from radiographs of the hand. The subjects used for these atlases were from the Bolton-Brush study conducted by Dr. T. Wingate Todd at Western Reserve University from 1926 to 1942.<sup>9,11</sup> The Bolton-Brush study was a longitudinal documentation of growth and development of 4,435 healthy children and adolescents who had serial radiographs taken biannually or annually of the skull, left shoulder, elbow, wrist and hand, hip, knee, and foot, and had anthropometric data such as height, weight, and menarche recorded at each visit. The widely used Greulich and Pyle hand atlas of skeletal maturity grouped the children of the Bolton-Brush study by sex and chronological age, and then determined an “average” appearance of the bones of the hand

for each age category.<sup>9</sup> The Greulich and Pyle atlas remains one of the most commonly used system of skeletal maturity to date, and involves comparison of hand radiographs to references in the atlas to establish the “skeletal age” of the child.

However, the concept of skeletal age defined by the Greulich and Pyle atlas and other similar atlases is problematic with males and females maturing at different ages and a wide standard deviation in maturation within each sex.<sup>12</sup> Studies have noted a wide variation in “bone age” for the same subjects when graded by different observers.<sup>13-15</sup> In addition, there have been concerns that these atlases are less relevant in the modern day due to the age of the atlases and the use of primarily white children for the database.<sup>16-18</sup> However, the majority of studies have shown that the Greulich and Pyle atlas is largely applicable to modern children, although less accurate around the time of puberty.<sup>12, 19, 20</sup> The Greulich and Pyle atlas, and other similar “bone age” atlases were developed prior to the work of Tanner, which delineated the importance of the adolescent growth spurt and particularly the timing of maximum height growth, the peak height velocity (PHV), as a uniform marker of maturity during adolescence.<sup>21, 22</sup>

Tanner developed the concept of peak height velocity and created clinical longitudinal standards of growth.<sup>21, 23</sup> Since Tanner first defined PHV, several studies have shown that skeletal maturity is more closely related to the timing of PHV than chronological age.<sup>1-6</sup> At PHV, skeletal maturity between different children, regardless of sex, is very similar. In 1975 Tanner developed a method of measuring skeletal maturity using radiographs of the hand, known as the Tanner-Whitehouse II (TW-II) method.<sup>23</sup> There are key differences between the Tanner-Whitehouse method and the Greulich and Pyle approach. Whereas the Greulich and Pyle approach establishes a series of “average”



hand radiographs for each age to which radiographs taken in clinic can be compared, the Tanner-Whitehouse method grades each ossification center of the hand individually. The Tanner-Whitehouse method establishes twenty regions of interest in the hand, each region of which is divided into discrete morphologic stages. Based on the appearance of each ossification center, and the sex of the child, a score is assigned to each ossification center. The individual scores are then added for an overall maturity score. There are commonly used variations of this system such as the carpal system which considers only the carpal ossification centers or the Radio-Ulnar and Short bones (RUS) system which disregards the carpal ossification centers.<sup>12</sup>

In 2001 Tanner published an updated version of his popular skeletal maturity assessment system, known as the TW-III, that had new longitudinal growth standards.<sup>22</sup> The descriptions and ratings of each morphological grade of the ossification centers remain the same, but the population growth charts were updated for modern children. Tanner's TW-III RUS system has been shown by Sanders to be the skeletal maturity system most closely linked with adolescent idiopathic scoliosis (AIS) curve progression.<sup>4</sup> Children with a digital skeletal age (DSA) of 400-425 are at time of PHV.<sup>4</sup> Although the TW-III can accurately identify PHV, it is too complex for clinical use.<sup>12, 22, 23</sup> The Tanner-Whitehouse system requires scoring of several ossification centers with required familiarity of small morphological changes, and access to complex scoring tables. The complexities of the scoring system can cause significant inter-rater variability.<sup>24</sup> Sanders suggests that the TW-III is more appropriate for a research study than clinical use unless reliable, rapid computerized measurements can be obtained.<sup>12</sup>

In 2008 Sanders developed a simplified scoring of the hand based on the TW-III system designed for clinical use.<sup>4</sup> He established a series of eight reference descriptors that can be used to gauge maturity in a clinical setting and can be used for prognostic information concerning adolescent idiopathic scoliosis curve progression.<sup>12</sup> Use of these eight archetypes is more straightforward than using the formal TW-III system and correlates more strongly with AIS curve progression than either the Risser sign or the Greulich and Pyle bone age atlas. Sanders followed twenty-two girls with AIS for two years through their growth spurt and established prognostic information of the likelihood of AIS curve progression that would require surgery, which he defined as greater than fifty degrees. Based on a child's Sanders hand score and AIS curvature, probability of curve progression eventually requiring surgery can be estimated. However, the majority of the Sanders hand stages occur after PHV has been reached, making this system less useful for prediction of how much time children have until they reach PHV.

In addition to skeletal maturity systems that assess ossification of the hand, there are several other widely-used systems for other ossification centers in the body. The Risser system uses excursion of the iliac apophysis to predict remaining vertebral growth, and is perhaps the most widely used skeletal maturity system other than the Greulich and Pyle hand atlas.<sup>25</sup> Although the Risser system correlates poorly with scoliosis curve acceleration, it remains commonly used due the availability of pelvic radiographs from those used in the assessment of scoliosis curves and its utility in delineating the end of the risk period for curve progression.<sup>26-30</sup> However, excursion of the iliac apophysis first begins after PHV, preventing the Risser system from predicting maturity before PHV.<sup>31</sup> Another system, the Oxford method, grades nine ossification centers surrounding the hip

and has been used for analysis of SCFE.<sup>32</sup> Loder found that SCFE occurs within a narrow range of bone age as determined by Oxford hip scores.<sup>33</sup> Recent literature has explored use of the modified Oxford hip score, which grades five ossification centers surrounding the hip, for prediction of contralateral SCFE.<sup>7, 8, 34</sup> Modified Oxford hip scores of 16-18 are strongly predictive of contralateral SCFE.<sup>7, 8</sup> Two other popular systems include the Sauvegrain method, and the modified Sauvegrain method, which explore ossification of the elbow.<sup>5, 35, 36</sup>

The majority of skeletal maturity systems such as the Greulich and Pyle hand atlas, or the Tanner-Whitehouse III hand scores, rely on accurately judging a series of morphological changes of bones to establish skeletal maturity.<sup>9, 22</sup> The sequence of regular morphological changes of an ossification center can be considered an analog radiographic feature. Analog radiographic features can create potential for inter-rater disagreement due to varying judgment of the morphological appearance. Depending on the complexity of the skeletal maturity system and the familiarity of the rater, this can result in large inter-rater errors, as described by Cundy *et al.* for the Greulich and Pyle system.<sup>13</sup>

Certain skeletal maturity systems also feature digital radiographic features, bony features that are either absent or present. Many bones can serve as digital systems of assessment, in that they are absent and later appear, or certain parts of them appear such as the epiphyses. Digital markers are simple, and can sometimes be used by themselves in the absence of other radiographic features. However, the majority of ossification centers appear early during development. The plantar and thenar sesamoids have unique potential to be considered for use as a digital assessment method because they develop

later, around the time of PHV. The time period around the adolescent growth spurt is often of the most interest to the pediatric orthopedist, as this is the time period most associated with scoliosis curve progression, SCFE, and epiphysiodesis.<sup>4,33</sup>

There are many systems of skeletal maturity assessment, several of which have been linked to specific clinical uses. However, there is a considerable need for a skeletal maturity system that can predict how much time children have before reaching PHV beginning at an early age. There are only a few existing systems of skeletal maturity assessment that can identify PHV. However, they each have limitations. TW-III RUS scores of 400-425 are indicative of PHV, but the TW-III system is cumbersome and complex, making it ill-suited for clinical use.<sup>12, 22, 23</sup> Sanders describes PHV as occurring between Sanders 2 and 3 hands.<sup>12</sup> However, this only leaves two potential Sanders stages before PHV, which limits the time preceding PHV during which maturity can be predicted. Charles and Dimgelio described a modified Sauvegrain method using only ossification of the olecranon of the elbow. The Charles and Dimgelio system describes PHV as occurring when the olecranon is fully fused. Their system can identify maturity relative to PHV beginning up to two years before PHV. However, this time period is very limited, and this system cannot identify how far children are after PHV. Thus, there remains a considerable need in pediatric orthopaedics to create a skeletal maturity system that is simple enough for clinical use, and can identify how far before and after PHV children are over a significant time range.

We recently developed a method of scoring excursion of the calcaneal apophysis that resembles the widely used Risser grading system of the iliac apophysis, and is able to localize skeletal maturity during the time before and after PHV has been reached.<sup>37</sup> The

calcaneal apophysis ossifies in an orderly and consistent fashion over seven years that can be well characterized as six different stages occurring during narrow intervals, four of which occur prior to PHV. Our system is simple to use, reproducible, and can identify maturity well before PHV has been reached.

In the following work we explore creation of the calcaneal system, its use for identification of PHV, and compare it to existing systems of maturity assessment such as the Risser system, the Sanders hand scores, the Oxford hip score, and closure of the triradiate cartilage (TRC). We explore the potential for combined skeletal maturity systems, such as the calcaneal and Sanders scores, for improved localization of skeletal maturity. We explore the difference between digital and analog skeletal maturity systems, as well as the value digital markers have by themselves and as adjuncts to analog maturity systems. We also use the calcaneal system, Sanders hand scores, and TRC to identify children at risk of contralateral slipped capital femoral epiphysis (SCFE).

## **Chapter 1 - Relationship of Calcaneal and Iliac Apophysis Ossification to Peak Height Velocity Timing in Adolescents**

### **Introduction**

The purpose of the present study is to evaluate one particular ossification center, the calcaneal apophysis, and compare it to both the timing of the PHV and to the commonly used Risser sign of iliac apophyseal ossification maturation.<sup>25</sup> We describe a fundamental physiologic process that, to our knowledge, has not previously been characterized and explore its utility as a system of assessing skeletal maturity.

### **Materials and Methods**

We reviewed 728 serial foot radiographs from ninety-four children (forty-nine females and forty-five males) between ages three to eighteen years, who were studied under the direction of Dr. T. Wingate Todd by the Brush Foundation at Western Reserve University from 1926 to 1942.<sup>9, 11</sup> These children were part of a prospective, longitudinal assessment of growth in healthy children living in Cleveland, Ohio, some of whom entered the study in infancy, and many of whom were followed to the end of growth. They had serial x-rays taken of their skull and left shoulder, elbow, wrist and hand, hip, knee, and foot on multiple occasions. In addition, other types of anthropometric data were gathered whenever the children received x-rays such as height and weight. Heights were measured using a stadiometer with standardized measurement technique allowing consistency in measurements over time and between observers. Greulich and Pyle utilized the hand x-rays in this database to create their bone age atlas.<sup>9</sup> All children

accepted for the study were selected on the basis of their freedom from gross physical or mental defects and the promise of the parents to permit their children to participate until completion of the study.<sup>9,11</sup> Children were recruited primarily through the Cleveland area schools and through referral from family physicians. The families were above average in economic and educational status.<sup>11</sup> The majority of subjects were white (92.2%), and the rest were black (7.7%) and a negligible representation of other racial groups.<sup>11</sup>

We identified ninety-four subjects followed for over a decade with consecutive radiographs made at least yearly from age of ten to fifteen years, who had height data available at the time of each radiograph. We chose this age range as that most associated with the PHV which also corresponds to the usual age range when children present with adolescent idiopathic scoliosis and for leg length equalization procedures. Peak height velocity has been calculated for each of the individuals using serial height measurements, after the approach of Tanner and Davies.<sup>21</sup> The patients' heights were measured annually around the time of puberty. The velocity of growth in cm/yr was calculated from the height measurements and curves were fit using a cubic spline to determine the maximum velocity during adolescent growth as representing the peak height velocity. The subject's age of this value was used for the timing of the PHV.

Annual lateral foot radiographs were digitally enhanced to adjust the contrast and achieve better clarity of the calcaneus. We examined the degree of ossification of the calcaneal apophysis. We assessed the extent of fusion of the apophysis as it occurred. We divided the process into six stages, as shown in Figure 1.1. Stage 0 - no ossification of the calcaneal apophysis. Stage 1 - the calcaneal apophysis covers < 50% of the

metaphysis. Stage 2 - the apophysis covers  $\geq 50\%$  of the metaphysis but does not fully cover the plantar surface. The radiolucent interval between the apophysis and metaphysis is wider near the areas of plantar and dorsal extension than in the central region. Stage 3 - the apophysis has extended fully over the plantar surface (within two mm of the calcaneal concavity) and continues to extend over the dorsal surface with no signs of fusion. There is a narrow and relatively uniform radiolucent interval between the apophysis and metaphysis, and the plantar sesamoids are present on an AP radiograph. Stage 4 - fusion of the apophysis to the metaphysis begins. Stage 5 - fusion is complete. We also examined the corresponding Risser signs for each subject using matching pelvic radiographs that were taken at the same time as each foot radiograph. Microsoft Excel 2013 was used to calculate confidence intervals.

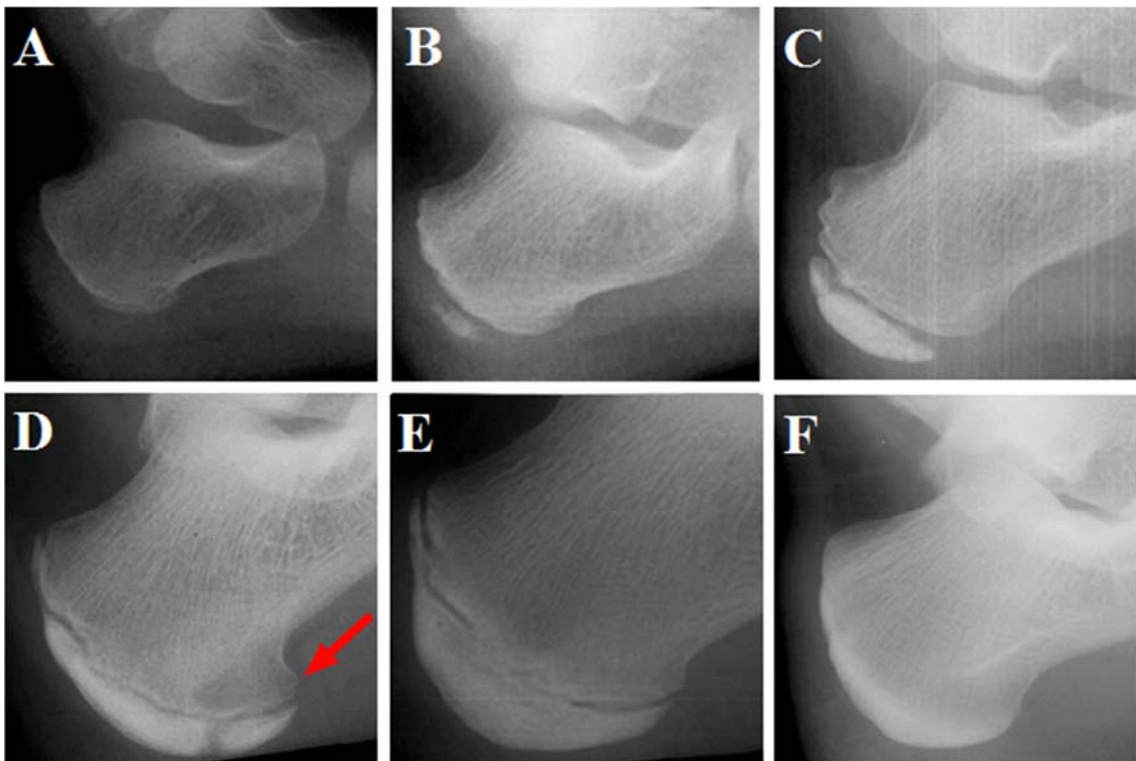


**Figure 1.1. Ossification of the calcaneal apophysis**



Reprinted with permission from Nicholson AD, Liu RW, Sanders JO, Cooperman DR. Relationship of Calcaneal and Iliac Apophysis Ossification to Peak Height Velocity Timing in Children. *The Journal of Bone & Joint Surgery*. 2015-01-21; 97:147-54.

(A) Stage 0 - No ossification of the apophysis is evident.

(B) Stage 1 - The apophysis extends more quickly over the plantar than dorsal surface. The apophysis in this figure covers  $< 50\%$  of the metaphysis.

(C) Stage 2 - The apophysis covers  $\geq 50\%$  of the metaphysis but has not extended to the plantar edge. The radiolucent interval between the apophysis and metaphysis is wider near the areas of plantar and dorsal extension than in the central region.

(D) Stage 3 - Complete extension over the plantar surface is seen when the apophysis extends within 2 mm of the plantar edge of the calcaneal concavity, as shown by the red arrow. There is a narrow and relatively uniform radiolucent interval between the apophysis and metaphysis.

(E) Stage 4 - Fusion of the apophysis is occurring, but there are still visible intervals between the apophysis and metaphysis. Fusion begins in the central region of the interval between the apophysis and metaphysis.

(F) Stage 5 - Fusion of the apophysis is complete.

The radiographs were blinded and 120 images of the calcaneus and 120 images of the hip were selected using a random-number generator. Two observers then viewed the radiographs on a high-resolution computer monitor and independently graded the calcaneal stage and the extent of iliac apophyseal ossification. Microsoft Excel 2013 was used to calculate inter-rater reliability and intra-rater reliability.

The author of this thesis performed the grading of images, the calculations, and the writing for these articles, with excellent guidance from his coauthors, principally Dr. Cooperman. Dr. Cooperman and Dr. Huez often graded additional sets of images for verification of accuracy and calculation of inter-rater reliability, as described in the methods section of each chapter. Chapter 1 of this thesis has been published in JBJS, Chapter 2 has been submitted to JBJS, and some data from Chapter 4 has been published in JPO in a different article. Chapter 3 will be submitted to JBJS along with Chapter 4.

## **Results**

Ossification of the calcaneal apophysis occurs in a very orderly fashion with the ossification center first appearing 4.7 years (95% CI -5.2, -4.2) before PHV. Ossification begins with the appearance of small osseous particles on the central surface of the metaphysis (stage 1). The years before the PHV and the range of ages for each calcaneal stage are shown in Table 1.1. Representative radiographs of each stage of ossification are shown in Figure 1.1. The apophysis and metaphysis undergo reciprocal shaping as ossification occurs. The apophysis spreads across the plantar surface more quickly than the dorsal surface (stage 1 and 2). The interval between the apophysis and metaphysis is typically not uniform during these stages, with a wider interval near the regions of extension than in the central region.

**Table 1.1 - Ossification of calcaneus with respect to PHV**

		Timing Relative to PHV (yr)		
	n	Mean	95% CI	Range
Stage 0	45	-6.06	-6.36 to -5.75	-8.5 to -3.8
Stage 1	91	-3.69	-3.95 to -3.43	-6.3 to -0.9
Stage 2	108	-1.93	-2.11 to -1.75	-4.6 to 0.0
Stage 3	85	-0.86	-1.01 to -0.71	-3.2 to 0.9
Stage 4	151	0.69	0.56 to 0.81	-1.8 to 3.0
Stage 5 (first appearance)*	75	2.11	2.00 to 2.23	1.1 to 3.2

\*There were 173 stage 5 calcanei radiographs that occurred after the first appearance of stage 5 and were not used for the calculations of the first appearance of stage 5.

The apophysis typically reaches the plantar edge before completing excursion over the dorsal region (stage 3). Complete extension over the plantar surface is defined as the apophysis extending within 2 mm of the plantar edge of the calcaneal concavity. Stage 3 can be further characterized by a narrow and relatively uniform interval between the apophysis and metaphysis as well as the presence of the plantar sesamoids on an AP radiograph as shown in Figure 1.2. 96% of stage 3 calcanei had the plantar sesamoids present on an AP radiograph. The plantar sesamoids first appear 0.98 years before PHV (95% CI -1.19, -0.78) while stage 3 occurs 0.86 years (95% CI -1.0, -0.7) years before PHV. Fusion of the apophysis to the metaphysis (stage 4) begins shortly after the plantar surface of the metaphysis is covered. Fusion of the apophysis occurs over the next 2

years (stage 4) and the apophysis is typically fully fused 2.1 years (95% CI 2.0, 2.2) after PHV (stage 5). Fusion begins in the middle of the apophysis and proceeds outward.



**Figure 1.2. A stage 3 calcaneus showing the appearance of the plantar sesamoids (red arrows).**

Reprinted with permission from Nicholson AD, Liu RW, Sanders JO, Cooperman DR.

Relationship of Calcaneal and Iliac Apophysis Ossification to Peak Height Velocity

Timing in Children. *The Journal of Bone & Joint Surgery*. 2015-01-21; 97:147-54.

Extension of the apophysis has reached within 2 mm of the concavity of the plantar aspect of the calcaneus, the interval between the apophysis and metaphysis is narrow and relatively uniform, and the plantar sesamoids are present. The plantar sesamoids

(indicated by red arrows) appear on an AP radiograph during the transition from stage 2 to stage 3 and 96% of stage 3 calcanei in the cohort had the plantar sesamoids present.

During late stage 3 or stage 4 many calcanei (46% of our cohort) have a secondary ossification center appear on the dorsal surface that connects with the primary ossification center forming a thin strip, as shown in Figure 1.3. Approximately half of our cohort (43%) did not develop a secondary ossification center and excursion continued in a linear manner from the primary ossification center across the dorsal surface. A small part (10%) of our cohort never had the apophysis cover the final dorsal region of the metaphysis.

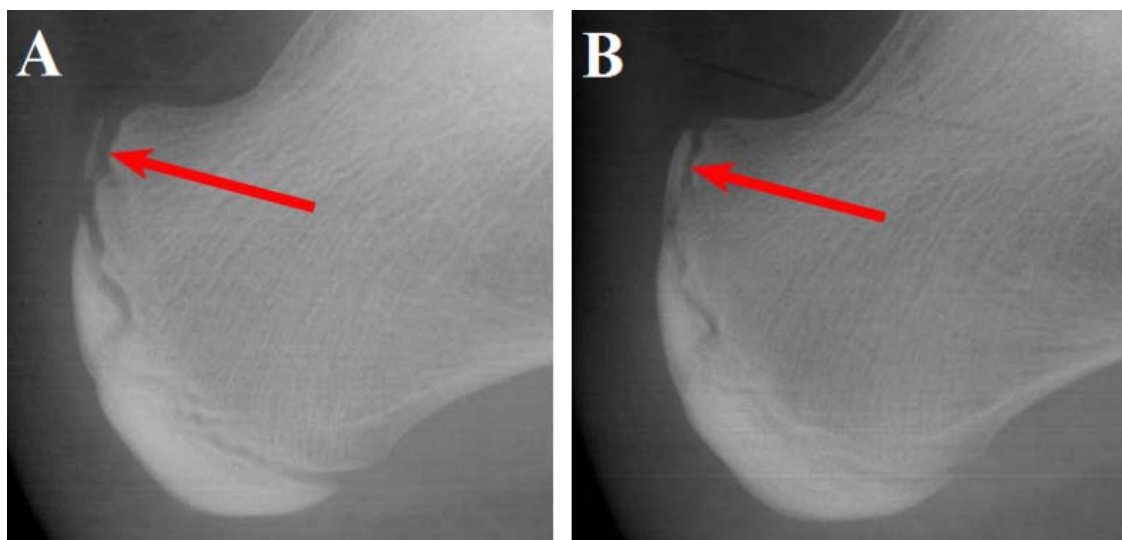


**Figure 1.3. Ossification of the dorsal surface of the calcaneal apophysis**

Reprinted with permission from Nicholson AD, Liu RW, Sanders JO, Cooperman DR. Relationship of Calcaneal and Iliac Apophysis Ossification to Peak Height Velocity Timing in Children. *The Journal of Bone & Joint Surgery*. 2015-01-21; 97:147-54.

(A) Some calcanei have a secondary ossification center form in the dorsal region (red arrow) during late stage 3 or stage 4. This calcanei corresponds to stage 4 due to fusion in the central region.

(B) Ossification of the secondary ossification center forms a thin strip (red arrow).

The timing of calcaneal stages 0, 3, 4, and 5 with respect to the PHV did not differ significantly between sexes as shown in Table 1.2. Stage 1 and 2 had a slight difference between sexes as shown in Table 1.2. Ossification of the calcaneus with respect to chronological age is shown in Table 1.3. The chronological age for each calcaneal stage occurred approximately two years later for males than for females. Inter-rater reliability and intra-rater reliability for determination of calcaneal stage were calculated with  $\kappa$  values of 0.90 and 0.96, respectively.

**Table 1.2 - Ossification of calcaneus with respect to PHV by sex**

		Timing Relative to PHV (yr)		
<b>Female</b>	n	Mean	95% CI	Range
Stage 0	24	-6.19	-6.51 to -5.86	-7.57 to -4.82
Stage 1	54	-3.87	-4.21 to -3.53	-6.35 to -1.22
Stage 2	58	-2.06	-2.31 to -1.80	-4.64 to 0.04
Stage 3	43	-0.88	-1.10 to -0.65	-2.50 to 0.88
Stage 4	80	0.70	0.51 to 0.89	-1.49 to 3.05
Stage 5 (first appearance)	38	2.14	1.97 to 2.32	1.06 to 3.24
<b>Male</b>	n	Mean	95% CI	Range
Stage 0	21	-5.91	-6.45 to -5.37	-8.55 to -3.84
Stage 1	37	-3.43	-3.80 to -3.05	-5.93 to -0.91
Stage 2	50	-1.79	-2.04 to -1.54	-4.55 to -0.38
Stage 3	42	-0.84	-1.04 to -0.64	-3.20 to 0.17
Stage 4	71	0.67	0.51 to 0.83	-1.79 to 2.16
Stage 5 (first appearance)	37	2.09	1.94 to 2.23	1.34 to 3.18

**Table 1.3 - Ossification of calcaneus with respect to chronological age by sex**

		Age (yr)		
<b>Female</b>	n	Mean	95% CI	Range
Stage 0	24	4.75	4.37 to 5.13	3.10 to 7.01
Stage 1	54	7.20	6.80 to 7.60	4.50 to 11.02
Stage 2	58	9.29	8.98 to 9.60	7.01 to 12.27
Stage 3	43	10.46	10.17 to 10.76	7.99 to 13.13
Stage 4	80	12.03	11.79 to 12.27	9.01 to 15.01
Stage 5 (first appearance)	38	13.44	13.14 to 13.74	11.04 to 16.02
<b>Male</b>	n	Mean	95% CI	Range
Stage 0	21	6.95	6.37 to 7.53	3.78 to 9.05
Stage 1	37	9.64	9.27 to 10.01	7.92 to 12.01
Stage 2	50	11.59	11.37 to 11.81	10.00 to 13.04
Stage 3	42	12.57	12.27 to 12.87	10.06 to 14.98
Stage 4	71	13.85	13.64 to 14.07	12.00 to 16.07
Stage 5 (first appearance)	37	15.24	14.96 to 15.51	13.88 to 17.02

A comparison of the calcaneal system and the Risser system in relation to time from PHV is shown in Figure 1.4. The Risser sign is still grade 0 at the time fusion of the calcaneal apophysis begins (stage 4). Although Risser grade 1 and calcaneal grade 3 appear to overlap in Figure 1.4, no individual child was Risser grade 1 and calcaneal grade 3. The overlap is a reflection of the variability between children but not within children. Excursion of the iliac crest apophysis began during fusion of the calcaneal



apophysis (stage 4) for 41% of the cohort and after the calcaneal apophysis had completed fusion (stage 5) for 59% of the cohort. Inter-rater reliability and intra-rater reliability for determination of the Risser sign were calculated with  $\kappa$  values of 0.77 and 0.95, respectively.

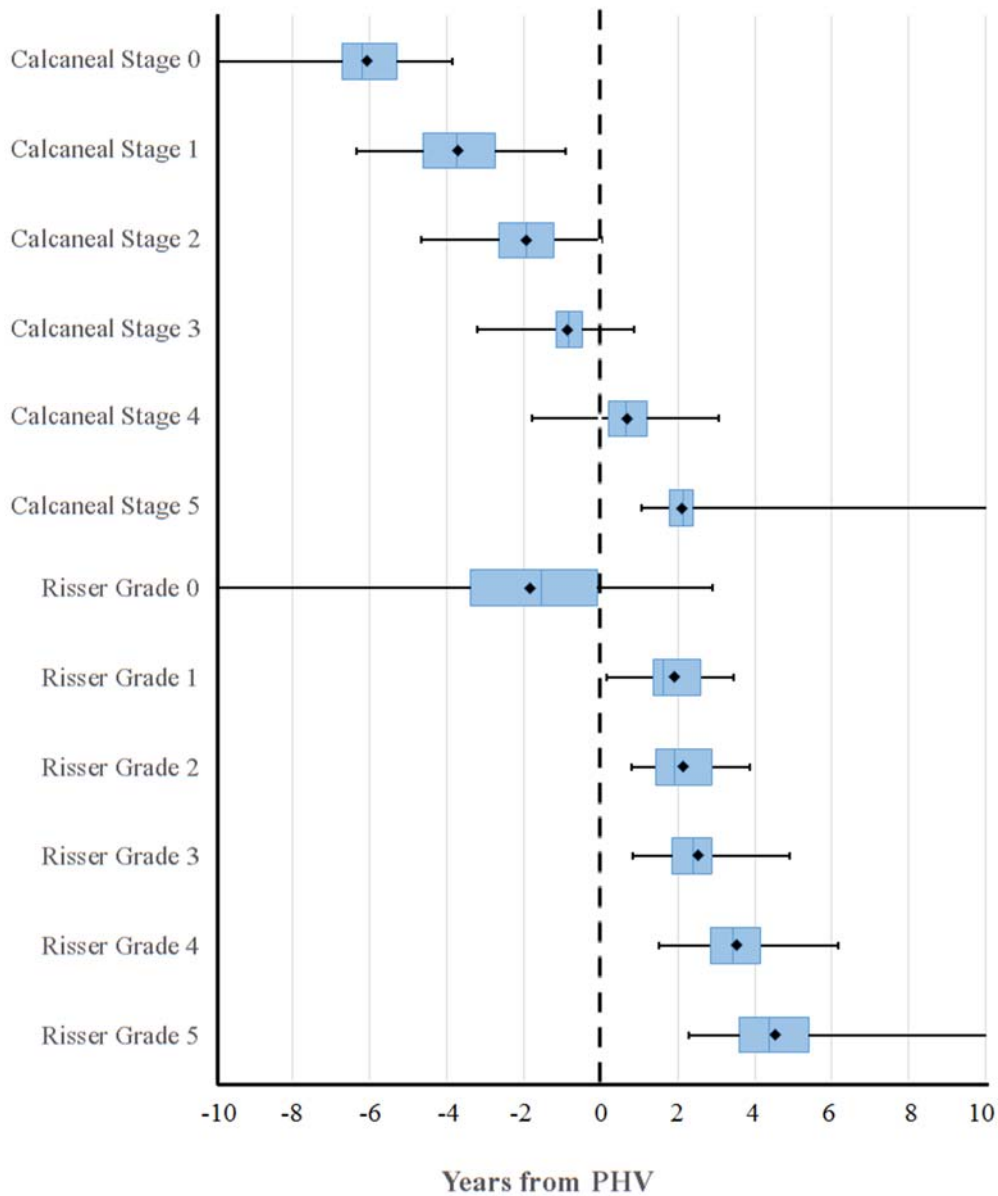


**Figure 1.4. Comparison of calcaneal staging and the Risser system with respect to PHV**

Reprinted with permission from Nicholson AD, Liu RW, Sanders JO, Cooperman DR.

Relationship of Calcaneal and Iliac Apophysis Ossification to Peak Height Velocity

Timing in Children. *The Journal of Bone & Joint Surgery*. 2015-01-21; 97:147-54.

A box and whiskers plot of the age with respect to PHV for the calcaneal stages and the Risser grades. The black lines represent the range for each examined sequence, while the blue box represents the middle 50% of data. The blue line in the middle of each box represents the median, while the black diamond represents the mean. Calcaneal stage 0 and Risser grade 0 have their lower age ranges extended to -10 years from PHV to represent that they are scores of immaturity and children will have that score from birth. Calcaneal stage 5 and Risser grade 5 have their upper age ranges extended to +10 years from PHV to represent that they represent scores of full maturity. The row for calcaneal stage 5 represents the first appearance of full calcaneal fusion for each child.

## **Discussion**

Several methods of assessing skeletal maturity exist, but the most commonly used are the hand-wrist skeletal ages from the Greulich and Pyle atlas and the Tanner-Whitehouse-III method of individual bone scoring.<sup>9,22</sup> The Greulich and Pyle atlas established a series of reference hand radiographs that can be used to establish a bone age through comparison to the reference radiographs. This system can be complex to use in clinical practice. These complexities can result in large interobserver error, as shown by Cundy *et al.*<sup>13</sup> Additionally, this work was prior to the understanding of PHV delineated by Tanner, and height velocity information was not used.<sup>21,22</sup> The TW-III scoring system has previously been identified as the scoring system most useful for predicting curve

acceleration in adolescent idiopathic scoliosis during early adolescence by Sanders *et al.*<sup>4</sup>

<sup>12</sup> Potential difficulties for use of this system include the complexity of the calculations and required familiarity with the scoring system.<sup>24</sup>

One of the most widely used clinical scoring systems is the Risser system, which uses excursion of the iliac crest apophysis to determine skeletal maturity.<sup>25</sup> This system has limited value for predicting PHV because it typically appears after the peak height velocity, but it is widely used by orthopaedic surgeon due to its simplicity and its utility in predicting the end of spinal growth.<sup>26, 28-30</sup> Other systems have explored use of ossification of the elbow for identification of PHV. The Sauvegrain method uses a 27-point scoring system of the elbow, and has been shown to identify the period when adolescents are beginning the deceleration phase of growth.<sup>35, 36</sup> Hans *et al.* studied twenty children (ten females and ten males) that had serial elbow x-rays and well documented PHVs.<sup>5</sup> When a Sauvegrain score of 26 was reached, all of the twenty children were past PHV. Dimeglio studied the Sauvegrain method and popularized the use of the olecranon apophysis alone, a part of the Sauvegrain scoring system. According to Dimeglio, the olecranon apophysis completely fuses at PHV.<sup>20, 35</sup> Dimeglio suggests using the olecranon apophyseal fusion sequence alone to determine the PHV in patients who are Risser 0.<sup>20</sup> This method is used by some, but if the first x-ray a physician sees shows fusion, it is unclear how one would determine how long the apophysis has been fused, creating uncertainty about the PHV. An ideal osteologic marker would allow for accurate identification of the period of growth immediately prior to the PHV as well as after, while being simple enough to allow for widespread adoption.

An atlas of skeletal development of the foot was developed by Hoerr *et al.* in 1962 using the children from the same Bolton Brush study used by Greulich and Pyle.<sup>38</sup> Hoerr *et al.* created a comprehensive skeletal reference in which he identified appearance of ossification centers and ossification patterns. This atlas was created prior to the understanding of PHV delineated by Tanner.<sup>21,22</sup> The method of Hoerr *et al.* relies on comparison to reference plates to determine skeletal ages. They found that the calcaneal apophysis is the last ossification center to appear in the foot and is one of the last to fuse, although they do not specifically comment on the process of calcaneal ossification.<sup>38</sup> Hackman *et al.* recently evaluated the accuracy of the Hoerr atlas for age estimation of a Scottish population, finding a strong correlation between estimated age and chronological age.<sup>39</sup> Other than the atlas from Hoerr *et al.* and the recent work of Hackman *et al.*, the foot has been minimally investigated.

Ossification of the calcaneal apophysis is a physiologic process that has never been fully described or explored as an assessment of skeletal maturity. We fully characterize ossification of the calcaneal apophysis. Excursion of the calcaneal apophysis occurs in a consistent fashion that includes appearance of the ossification center, spread of the apophysis in a plantar-dominant fashion, regular changes to the appearance of the interval between the apophysis and metaphysis, and consistent patterns of fusion. Calcaneal apophysis ossification can be clearly and consistently delineated into six distinct physiologic stages. The six stages of calcaneal apophysis ossification occur at regular intervals in relation to PHV, as shown in Figure 1.4. The stages of calcaneal apophysis ossification are consistent between children regardless of sex.

The consistency of calcaneal apophysis ossification makes this process suitable for assessment of skeletal maturity and PHV. For instance, calcaneal stage 3 occurs 0.86 years before the PHV within a narrow time frame whereas calcaneal stage 4, an actively fusing calcaneal apophysis, typically occurs after PHV. Four of the six stages of calcaneal apophyseal ossification occur before PHV has been reached, allowing identification of this crucial time period. Skeletal maturity assessment allows for prediction of remaining growth and determination of appropriate orthopedic interventions. For instance, maturity systems allow for assessment of the risk of curve progression in idiopathic scoliosis and the likelihood of a unilateral SCFE progressing to a bilateral one.<sup>2, 7, 8, 12</sup> The maximum growth rate at adolescence is known as peak height velocity, and has been shown to be closely related to skeletal maturity. Investigators have found strong evidence that skeletal maturity is more closely related to PHV than chronological age.<sup>2-4, 40-42</sup> Identification of PHV also has direct clinical implications. Sanders *et al.* found that the period of PHV has a high correlation with the curve acceleration phase of scoliosis.<sup>4</sup> Additionally, he suggests that posterior spine fusion done prior to PHV will result in crankshaft whereas posterior spine fusion done after PHV will not.<sup>1</sup>

The calcaneal system is similar to the familiar and straightforward Risser sign in that it uses extension of the apophysis to assess maturity. Although the Risser sign correlates poorly with scoliosis curve acceleration, it remains the most commonly used tool for the assessment of skeletal maturity due to its simplicity, the availability of pelvic radiographs from those used in the assessment of scoliosis curves, and its usefulness in delineating the end of the risk period for curve progression, Risser Stage 5.<sup>26-30</sup> The

benefits of the calcaneal system compared to the Risser system are clearly shown in Figure 1.4 - calcaneal stages occur within narrow windows that transpire before and after PHV whereas the Risser grades occur exclusively after PHV and have significant overlap between grades. The calcaneal system has the simplicity of the Risser system with the added benefits of not requiring gonadal exposure to radiation and being more useful for delineation of concrete stages of skeletal maturity in relation to PHV.

A possible limitation of this study concerns the age of the collection used, and that the radiographs may not be representative of modern children. There is evidence that children are reaching puberty at earlier ages.<sup>43</sup> However, our study design compares calcaneal apophyseal signs to PHV rather than chronological age, which would compensate for the earlier onset of puberty in modern children. PHV also allows males and females to be compared directly. There may also be concerns that the children were potentially unhealthy or malnourished. However, the children who participated in the Bolton Brush study were from the advantaged of their time and were required to be of good health.<sup>9, 11</sup>

Ossification of the calcaneal apophysis has never been comprehensively described. We fully characterize this fundamental physiologic process and examine its suitability for assessment of skeletal maturity. The calcaneal apophysis ossifies in an orderly and consistent fashion that can be well characterized as six different stages, four of which happen before PHV has been reached. The calcaneal stages occur during narrow intervals in relation to PHV, allowing the calcaneal system to be used for assessment of skeletal maturity. The orderly spread of the calcaneal apophysis across the plantar end of the metaphysis (stage 3) can be monitored through serial lateral

radiographs of the foot and can alert the surgeon that the PHV is imminent. This information can aid the surgeon in determining optimal treatments for scoliosis, improve estimation of epiphysiodesis timing, and assist with treatment plans for other disorders of maturation.

## **Chapter 2 – Relationship of Calcaneal Apophyseal Ossification and Sanders Hand Scores to Peak Height Velocity Timing in Adolescents**

### **Introduction**

Two methods of assessing skeletal maturity, a simplified scoring system of the hand and calcaneal apophyseal ossification, have recently been described that can determine maturity relative to peak height velocity and are simple enough for clinical use.<sup>12,37</sup> Sanders developed a simplified scoring of the hand based on the TW-III system, which he previously identified as closely correlated with adolescent idiopathic scoliosis curve progression.<sup>4</sup> He established a series of eight reference descriptors that can be used to gauge maturity in a clinical setting and can be used for prognostic information concerning AIS curve progression.<sup>12</sup> Use of these eight archetypes is more straightforward than using the formal TW-III system and correlates more strongly with idiopathic scoliosis curve progression than either the Risser sign or the Greulich and Pyle bone age atlas.

We recently developed a method of scoring excursion of the calcaneal apophysis that resembles the widely used Risser grading system of the iliac apophysis, and is able to localize skeletal maturity during the time before PHV has been reached.<sup>37</sup> The calcaneal apophysis ossifies in an orderly and consistent fashion that can be well characterized as six different stages occurring during narrow intervals, four of which occur prior to PHV.

The purpose of this study is to compare the Sanders hand scores to those of the calcaneal apophysis. We will evaluate the relationship of both systems to timing of peak height velocity in adolescents. We will explore the utility of using the Sanders and



calcaneal systems in combination for establishment of maturity relative to peak height velocity.

## **Materials and Methods**

We studied 738 serial foot and 694 serial hand radiographs from ninety-four children (forty-nine females and forty-five males) ages three to eighteen years, who were evaluated under the direction of Dr. T. Wingate Todd by the Brush Foundation at Western Reserve University from 1926 to 1942.<sup>9, 11</sup> These patients are the same as those previously used in the description of calcaneal apophyseal ossification.<sup>37</sup> The Bolton-Brush study is described in chapter 1 as are calculations for our present study.

The calcaneal apophysis scoring was described previously and is shown in Figure 1.1.<sup>37</sup> The Sanders method is summarized in Figure 2.1.<sup>12</sup> The Sanders stages correspond to Greulich and Pyle atlas standards, as shown in Table 2.1. Sanders stage 1 occurs when the digital epiphyses of the hand are not all wider than the metaphyses. The epiphysis of the middle phalanx of the 5<sup>th</sup> digit is often the last to cover the metaphysis. Stage 2 occurs when all digital epiphyses fully cover the metaphyses. Stage 3 occurs when the preponderance of digits are capped and the second through fifth metacarpal epiphyses are wider than their metaphyses. Stage 4 occurs when any of the distal phalangeal physes are closing. Stage 5 occurs when all distal phalangeal physes are closed but the middle and proximal phalangeal physes remain open. Stage 6 occurs when the middle or proximal phalangeal physes are closing. Stage 7 occurs when all physes are closed except for the distal radial physis (ignoring the ulna). Stage 8 occurs when all physes are closed.

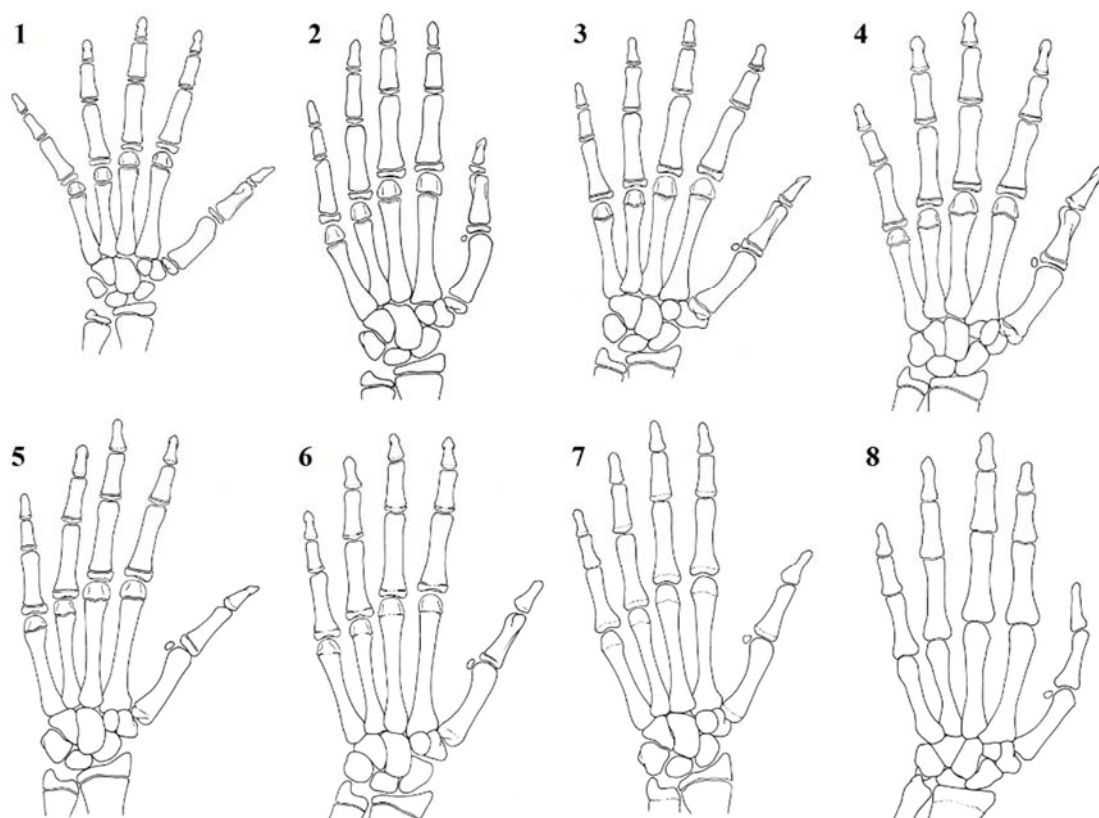


**Figure 2.1. Sanders hand scores**

Reprinted with permission from Sanders JO, Khoury JG, Kishan S, Browne RH, Mooney III JF, Arnold KD, et al. Predicting scoliosis progression from skeletal maturity: a simplified classification during adolescence. *The Journal of Bone & Joint Surgery*. 2008;90(3):540-53.

Stage 1 – All of the digital epiphyses of the hand are not covered.

Stage 2 – All digital epiphyses fully cover the metaphyses.

Stage 3 – The preponderance of digits are capped and the second through fifth metacarpal epiphyses are wider than their metaphyses.

Stage 4 – Any of the distal phalangeal physes are closing.

Stage 5 – All distal phalangeal physes are closed but the other physes remain open.

Stage 6 – The middle or proximal phalangeal physes are closing.

Stage 7 – All physes are closed except for the distal radial physis (ignoring the ulna).

Stage 8 – All physes are closed.

**Table 2.1 – Sanders stages compared to Greulich and Pyle reference**

<b>Sanders Stage</b>	<b>Stage Description</b>	<b>Greulich and Pyle Female Reference</b>	<b>Greulich and Pyle Male Reference</b>
1	Juvenile slow	Standard 17 (8yr + 10 mo)	Standard 22 (12 yr + 6 mo)
2	Preadolescent slow	Standard 18 (10 yr)	Standard 23 (13 yr)
3	Adolescent rapid – early	Standard 19, 20 (11 yr and 12 yr)	Standard 24, 25 (13 yr + 6 mo and 14 yr)
4	Adolescent rapid – late	Standard 21 (13 yr)	Standard 26 (15 yr)
5	Adolescent steady – early	Standard 22 (13 yr + 6 mo)	Standard 27 (15 yr + 6 mo)
6	Adolescent steady – late	Standard 23 (14 yr)	Standard 28 (16 yr)
7	Early mature	Standard 24 (15 yr)	Standard 29 (17 yr)
8	Mature	Standard 26 (17 yr)	Standard 31 (19 yr)

We graded each radiograph with their respective Sanders or calcaneal stage. Of the 738 calcaneal radiographs and 694 hand radiographs, there were 626 pairs of hand

and foot radiographs taken at the same sessions, and for these the Sanders hand scores and calcaneal scores were combined. Six individuals graded 30 hand radiographs for calculation of  $\kappa$  using the Sanders system.<sup>12</sup>  $\kappa$  of the calcaneal system was described in chapter 1. Microsoft Excel 2013 was used to calculate confidence intervals as well as  $\kappa$  coefficients.

## **Results**

Ossification of the calcaneal apophysis occurs in an orderly fashion over a seven-year period, with each calcaneal stage occurring during discrete and regular intervals with respect to PHV. The chronological sequence of the calcaneal and Sanders stages is shown in Table 2.2 and Figure 2.2. The majority of the calcaneal stages occur earlier than the Sanders stages. Ossification of the hand from Sanders stage 2 to Sanders stage 8 occurred over a 5 year period. Sanders stage 1 is a very long stage, whereas Sanders stages 2 and 3 occur at regular intervals over 12 month periods. Sanders stages 4 to 6 occur rapidly in a little more than a 1 year period. It was rare to see an adolescent with two annual hand radiographs from Sanders stages 4-6. Sanders stage 7 is a longer stage, typically lasting 1-2 years.

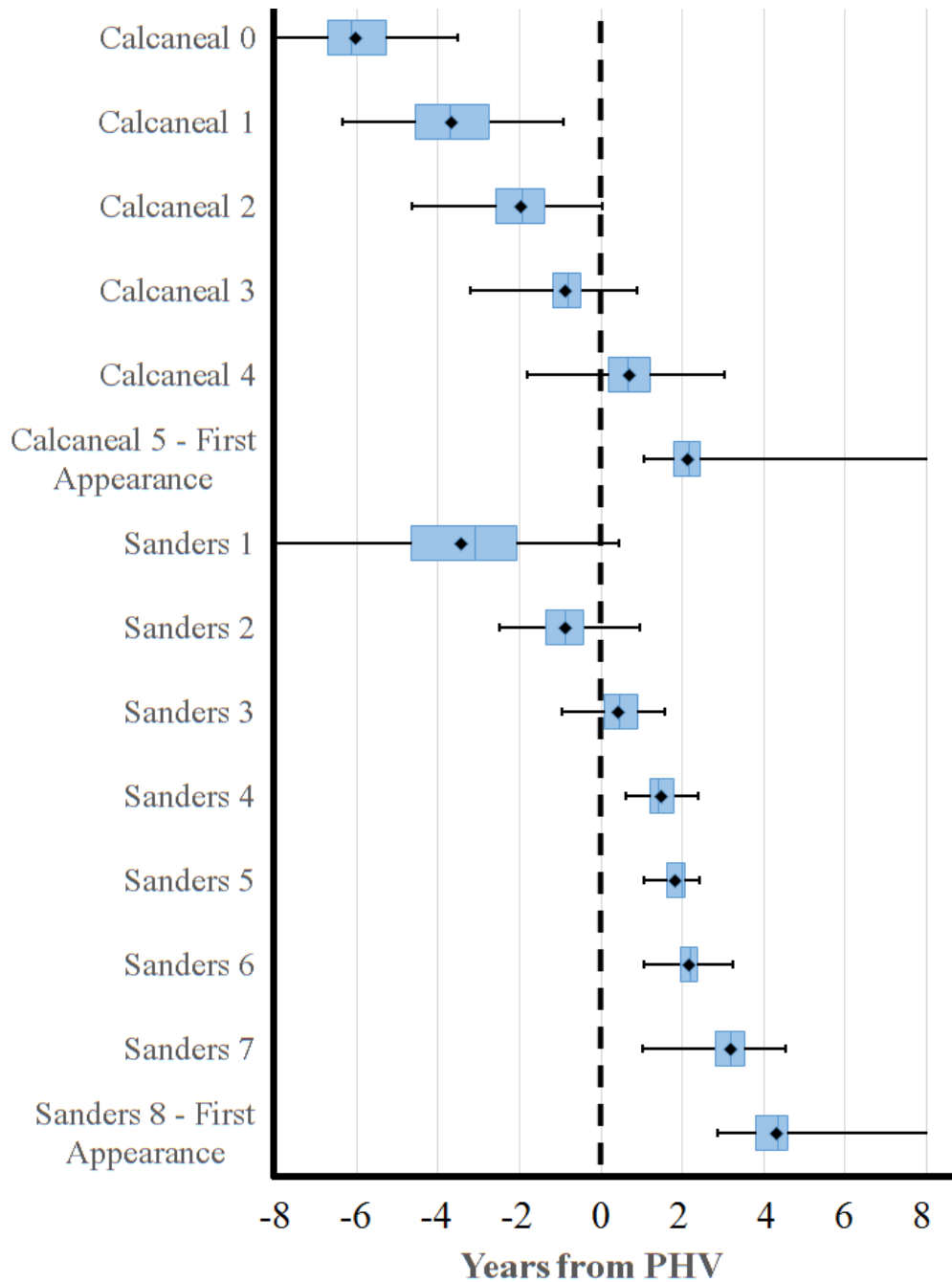


**Figure 2.2.** A box and whiskers plot of the age with respect to PHV for the calcaneal stages and the Sanders hand scores. The black lines represent the range for each examined sequence, while the blue box represents the middle 50% of data. The blue line in the middle of each box represents the median, while the black diamond represents the mean. Calcaneal stage 0 and Sanders stage 1 have their lower age ranges extended to -8

years from PHV to represent that they are scores of immaturity and children will have that score from birth. Calcaneal stage 5 and Sanders stage 8 have their upper age ranges extended to +8 years from PHV to represent that they represent scores of full maturity. The row for calcaneal stage 5 and Sanders stage 8 represent the first appearance of that stage for each child.

**Table 2.2 – Age from PHV for each stage of the calcaneal and Sanders systems**

		Timing Relative to PHV (yr)		
Stage	n	Mean	95% CI	Range
Calcaneal 0	48	-6.01	-6.31 to -5.70	-8.55 to -3.51
Calcaneal 1	94	-3.67	-3.92 to -3.42	-6.35 to -0.91
Calcaneal 2	111	-1.95	-2.12 to -1.79	-4.64 to 0.02
Calcaneal 3	85	-0.87	-1.03 to -0.72	-3.20 to 0.88
Calcaneal 4	157	0.70	0.58 to 0.82	-1.79 to 3.05
Calcaneal 5 - First Appearance*	78	2.14	2.03 to 2.25	1.06 to 3.24
Sanders 1	236	-3.42	-3.64 to -3.19	-8.55 to 0.44
Sanders 2	93	-0.86	-1.00 to -0.72	-2.51 to 0.95
Sanders 3	99	0.44	0.33 to 0.56	-0.97 to 1.56
Sanders 4	40	1.48	1.35 to 1.60	0.62 to 2.37
Sanders 5	13	1.83	1.61 to 2.05	1.07 to 2.43
Sanders 6	42	2.16	2.03 to 2.29	1.06 to 3.24
Sanders 7	105	3.19	3.07 to 3.31	1.03 to 4.53
Sanders 8 - First Appearance**	38	4.30	4.08 to 4.53	2.85 to 6.95

\*First appearance of calcaneal stage 5. There were 165 radiographs of stage 5 calcanei that were taken after the first appearance of calcaneal stage 5 and were not used for the calculation of the first appearance of calcaneal stage 5.

\*\*First appearance of Sanders stage 8. There were 28 radiographs of Sanders stage 8 hands that were taken after the first appearance of Sanders stage 8 and were not used for the calculation of the first appearance of Sanders stage 8.

The Sanders method and calcaneal staging both occur as a regular sequence of events with respect to PHV. The mean age with respect to PHV for each calcaneal and Sanders stage is shown in Table 2.2 and Figure 2.2. Four of six calcaneal stages occur before PHV whereas six of eight Sanders stages occur after PHV. PHV happens between calcaneal stages 3 and 4, and Sanders stages 2 and 3. Calcaneal stage 3 and Sanders stage 2 have similar mean ages before PHV, with calcaneal stage 3 occurring 0.87 years (95% CI, 1.03 to 0.72 years) before PHV and Sanders 3 occurring 0.86 years (95% CI, 1.00 to 0.72 years) before PHV. Calcaneal stage 4 and Sanders stage 3 also have similar mean ages after PHV, with calcaneal stage 4 occurring on average 0.70 years (95% CI, 0.58 to 0.82 years) after PHV and Sanders stage 3 occurring on average 0.44 years (95% CI, 0.33 to 0.56 years) after PHV. Calcaneal stage 0 and Sanders stage 1 are both the earliest stages in their respective systems, and the average years with respect to PHV are a reflection of the sample population rather than a true mean for each stage.

Calcaneal stages show strong correlation to the Sanders stages ( $r^2 = 0.72$ ). The distribution of Sanders scores with respect to calcaneal stages is shown in Figure 2.3 and Table 2.3. The distribution of calcaneal stages with respect to Sanders scores is shown in Figure 2.4 and Table 2.4. All of calcaneal stage 0 radiographs (100%) correspond with Sanders stage 1 radiographs. The majority of calcaneal stage 1 radiographs (98.8%) also correspond to Sanders stage 1 radiographs. Calcaneal stage 2 is predominantly Sanders



stage 1 (74.7%) with a minority (25.3%) Sanders stage 2. The majority of calcaneal stage 3 correspond (61.8%) to Sanders stage 2, with a minority corresponding to Sanders stage 1 (22.4%) and Sanders stage 3 (15.8%). The majority of calcaneal stage 4 are equivalent (59.7%) to Sanders stage 3, with minorities equivalent to Sanders stage 2 (13.4%), Sanders stage 4 (17.9%), and Sanders stage 5 (4.5%). Calcaneal 5 is the mature calcaneal stage and is present for Sanders stages 4-8.

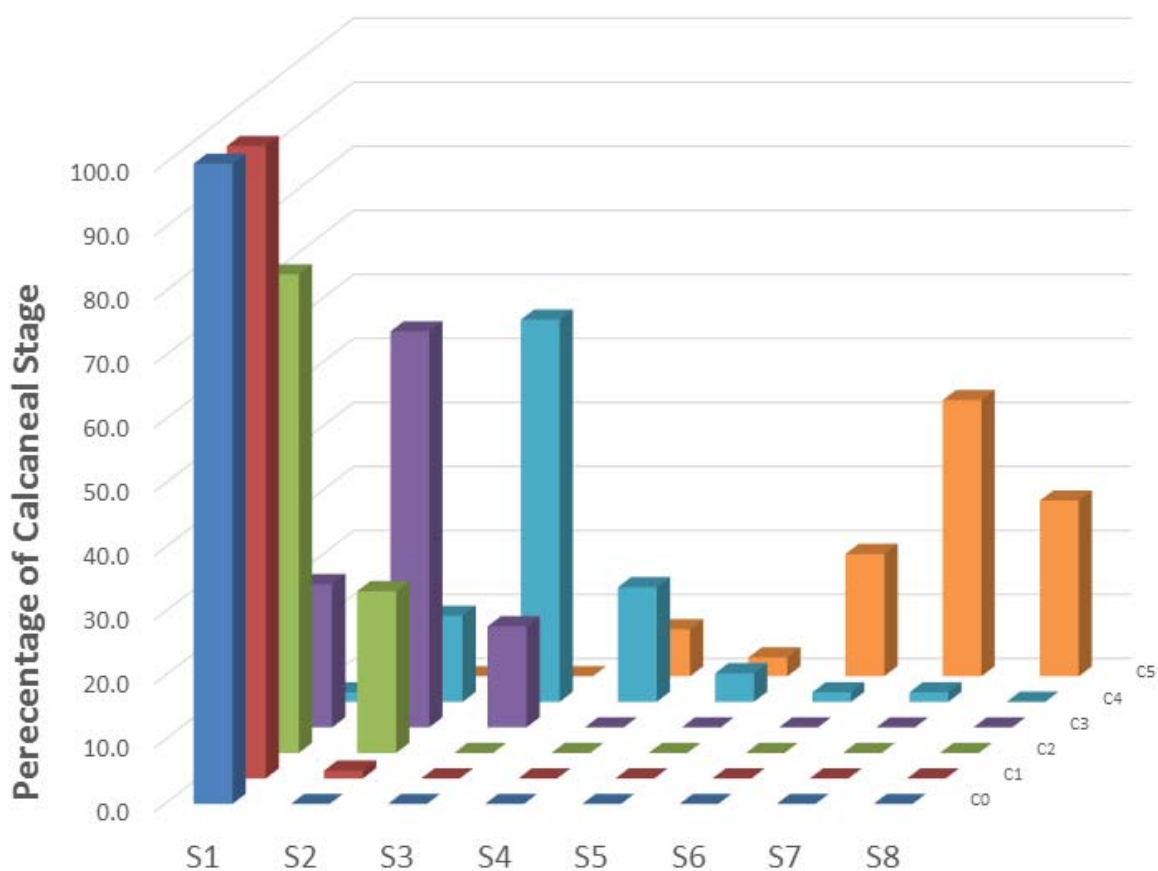


**Figure 2.3. Percentage of calcaneal stage corresponding to each Sanders stage**

The calcaneal stage is indicated by “C” followed by the stage number while the Sanders stage is indicated by “S” followed by the stage number. Each colored bar shows the



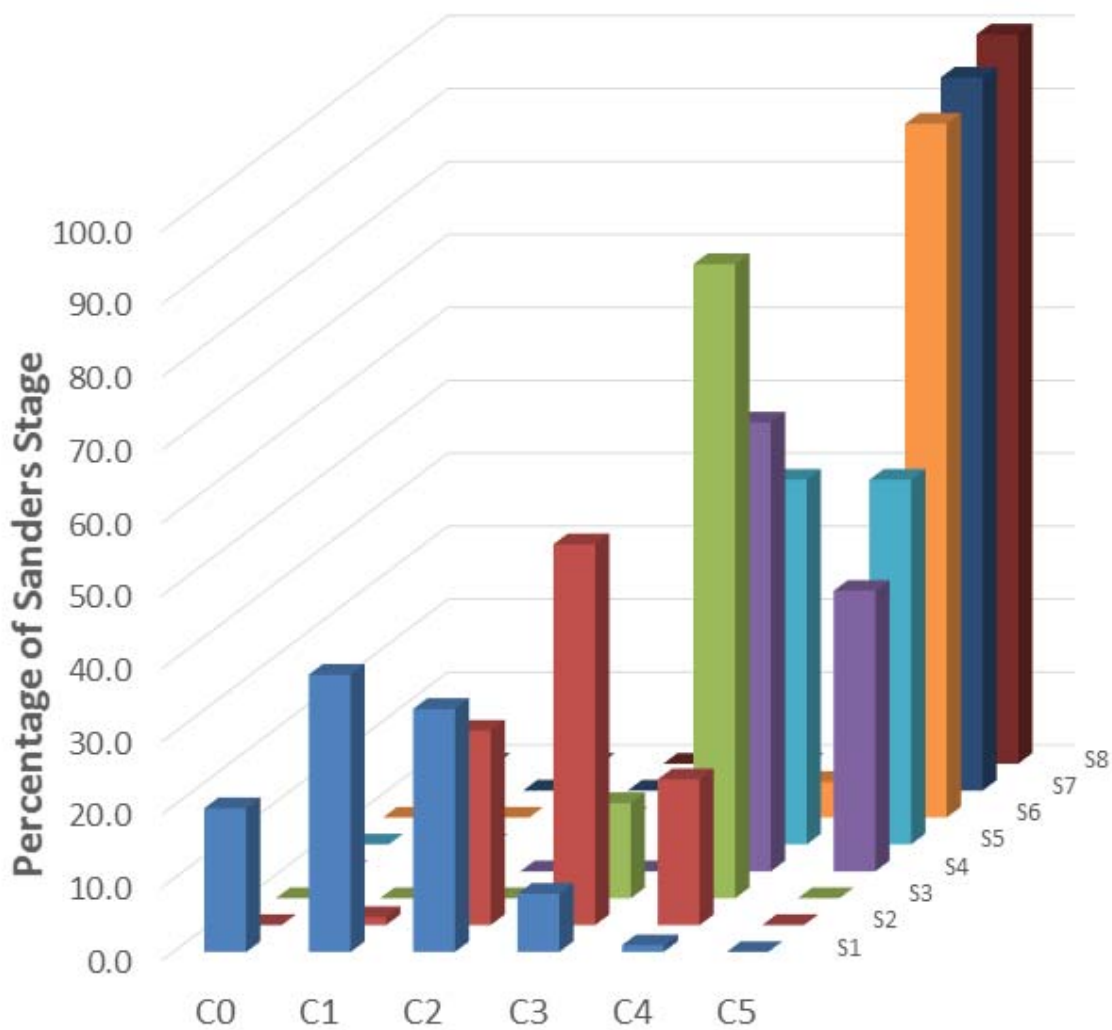


**Figure 2.4. Percentage of Sanders stage corresponding to each calcaneal stage**

Each colored bar shows the percentage of the Sanders stage that is associated with a particular calcaneal stage. For instance, 13% of Sanders 3 radiographs had corresponding calcaneal radiographs that were calcaneal stage 3, and 87% were calcaneal stage 4.

**Table 2.4. Percentage of Sanders stage corresponding to each calcaneal stage**

	S1	S2	S3	S4	S5	S6	S7	S8
C0	19.7	0.0	0.0	0.0	0.0	0.0	0.0	0.0
C1	38.0	1.1	0.0	0.0	0.0	0.0	0.0	0.0
C2	33.3	26.7	0.0	0.0	0.0	0.0	0.0	0.0
C3	8.0	52.2	13.0	0.0	0.0	0.0	0.0	0.0
C4	0.9	20.0	87.0	61.5	50.0	4.9	2.2	0.0
C5	0.0	0.0	0.0	38.5	50.0	95.1	97.8	100.0

As shown in Figures 2.3 and 2.4, there is a distribution of Sanders scores within calcaneal scores and vice versa. For instance, hand radiographs taken at the same time as the calcaneal stage 3 radiographs were either Sanders 1, 2, or 3. The calcaneal scores can be subdivided by their corresponding Sanders scores. The Sanders and calcaneal stages were combined and mean ages with respect to PHV were determined for combined stages with a sample size greater than 5. The mean ages with respect to PHV for each combined stage are shown in Figure 2.5 and Table 2.5.

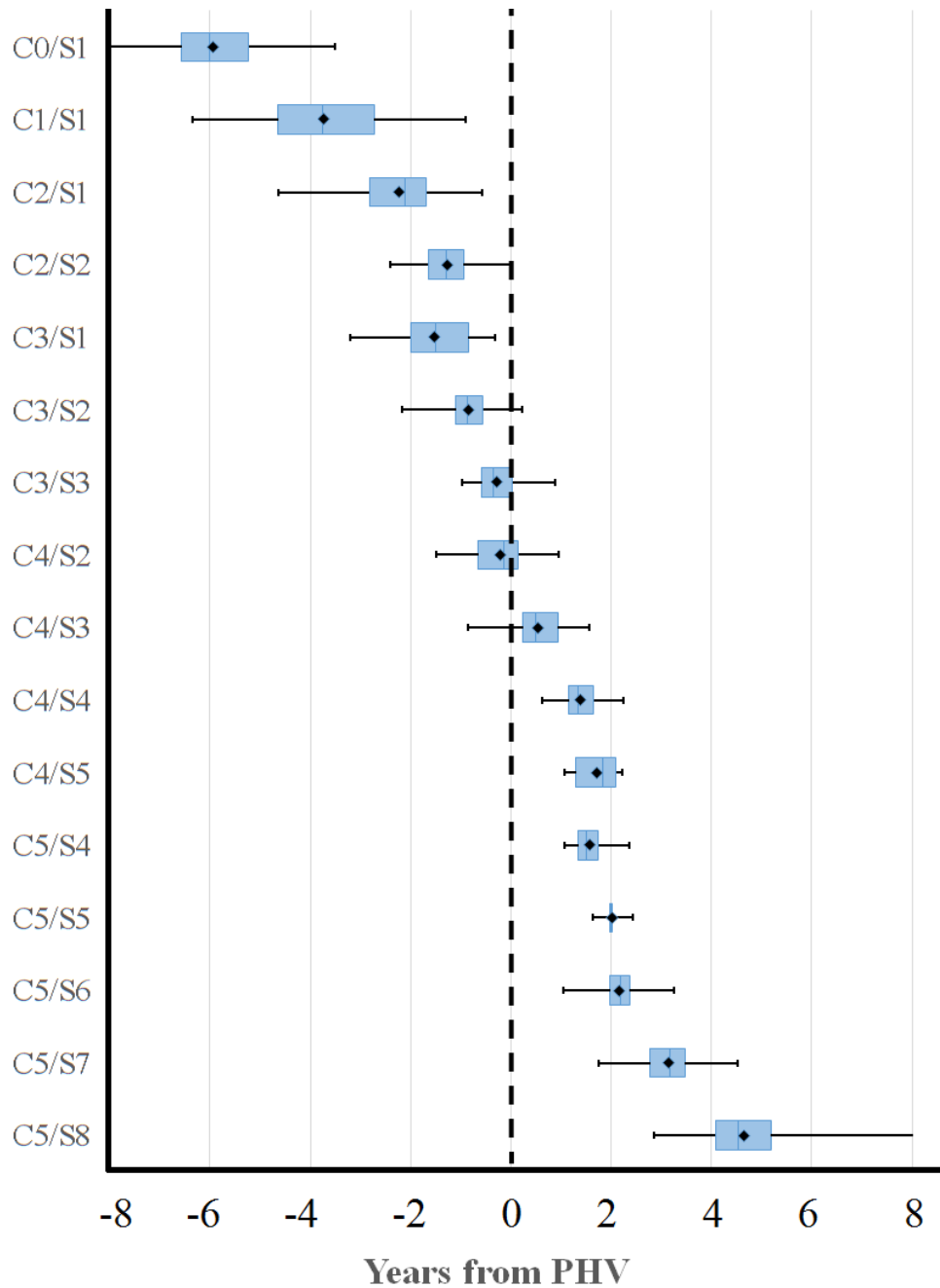


**Figure 2.5.** A box and whiskers plot of the age with respect to PHV for the combined calcaneal and Sanders stages. The calcaneal stage is indicated by “C” followed by the stage number while the Sanders stage is indicated by “S” followed by the stage number. The black lines represent the range for each examined sequence, while the blue box represents the middle 50% of data. The blue line in the middle of each box represents the

median, while the black diamond represents the mean. C0/S1 has the lower age range extended to -8 years from PHV to represent that it is a score of immaturity and children will have that score from birth. C5/S8 has the upper age range extended to +8 years from PHV to represent that it is a score of full maturity.

**Table 2.5 – Age from PHV for each combined calcaneal/Sanders stage**

		Timing Relative to PHV (yr)		
Stage	n	Mean	95% CI	Range
C0/S1	42	-5.94	-6.28 to -5.60	-8.55 to -3.51
C1/S1	81	-3.73	-4.01 to -3.45	-6.35 to -0.91
C2/S1	71	-2.23	-2.44 to -2.02	-4.64 to -0.57
C2/S2	24	-1.26	-1.50 to -1.02	-2.41 to 0.02
C3/S1	17	-1.52	-1.90 to -1.13	-3.20 to -0.32
C3/S2	47	-0.85	-1.00 to -0.69	-2.17 to 0.23
C3/S3	12	-0.28	-0.58 to 0.02	-0.97 to 0.88
C4/S2	18	-0.21	-0.50 to 0.07	-1.49 to 0.95
C4/S3	80	0.53	0.42 to 0.65	-0.84 to 1.56
C4/S4	24	1.39	1.22 to 1.56	0.62 to 2.24
C4/S5	6	1.72	1.32 to 2.11	1.07 to 2.23
C5/S4	15	1.58	1.41 to 1.75	1.08 to 2.37
C5/S5	6	2.01	1.81 to 2.22	1.63 to 2.43
C5/S6	39	2.17	2.04 to 2.31	1.06 to 3.24
C5/S7	88	3.15	3.03 to 3.27	1.75 to 4.53
C5/S8	56	4.65	4.41 to 4.88	2.85 to 6.95

Inter-rater reliability and intra-rater reliability for determination of the Sanders hand scores were calculated with average weighted  $\kappa$  values of 0.96 and 0.89, respectively.<sup>12</sup>

## **Discussion**

The period of peak height velocity represents the period of highest spinal growth rate and has been shown to be closely related to skeletal maturity.<sup>1, 2, 5, 6, 12, 41, 42</sup> Several studies have established that PHV is useful for predicting cessation of growth.<sup>31, 44</sup> Investigators have found strong evidence that skeletal maturity is more closely related to PHV than chronological age.<sup>2-4, 40-42</sup> At peak height velocity, maturity of individuals, regardless of sex, is very similar. Identification of PHV also has direct clinical implications. Sanders *et al.* found that the period of PHV has a high correlation with the curve acceleration phase of scoliosis and that posterior spinal fusions performed before PHV will result in crankshaft.<sup>1, 4</sup>

Both the Sanders and calcaneal systems can measure skeletal maturity as a series of regular stages with respect to PHV. The calcaneal stages progress at fairly regular intervals over a seven year period. The Sanders stages occur at irregular intervals, with Sanders stages 2-3 progressing at fairly regular intervals over 1 year periods beginning approximately 1 year before PHV, while Sanders stages 4-6 occur rapidly, often within the span of a single year. The stages of each system show significant correlation with each other. Sanders stage 2 and calcaneal stage 3 both occur 0.9 years before PHV while Sanders stage 3 and calcaneal stage 4 both occur approximately 0.5 years after PHV. The calcaneal system has four of its six stages in the time before PHV whereas the Sanders

system has two of its eight occurring before PHV. The presence of four stages prior to PHV allows for the calcaneal system to localize maturity within more narrow intervals in the time before PHV while the presence of six stages after PHV allows the Sanders system to localize maturity within more narrow intervals in the time after PHV.

The Sanders system and calcaneal system have a substantial period of overlap, particularly in the time around PHV. Although some stages of the calcaneal and Sanders systems share similar mean ages with respect to PHV, such as calcaneal stage 3 and Sanders stage 2, there are portions of each calcaneal stage and Sanders stage that do not overlap perfectly. For instance, as shown in Figures 2.3 and 2.4, there is a substantial percentage of calcaneal stage 3 radiographs that correspond to Sanders stage 1 or Sanders stage 4, in addition to Sanders stage 2. Calcaneal stage 3 can be subdivided by Sanders stages 1-3 to achieve resolution superior to examining calcaneal stage 3 alone. This applies for the other calcaneal and Sanders stages with substantial overlap, allowing the systems to be combined. The combined systems can be used to localize skeletal maturity relative to PHV with greater resolution and more narrow intervals than use of either system alone.

The Sanders stages correspond to specific references from the Greulich and Pyle hand atlas, as shown in Table 1. Therefore, the relationship between the calcaneal stages and the Sanders hand stages would also apply to the comparison of calcaneal stages to specific Greulich and Pyle reference radiographs and bone ages.

The Sanders method and calcaneal staging complement each other. The calcaneal system offers greater resolution in the time preceding PHV while the Sanders method provides



greater resolution of the time after PHV. When the systems are combined, they offer far superior resolution of maturity relative to PHV than either system alone.

## **Chapter 3 – Digital and Analog Markers of Skeletal Maturity: The Clinical Utility of the Thenar and Plantar Sesamoids**

### **Introduction**

The majority of skeletal maturity systems such as the Greulich and Pyle hand atlas, or the TW-III hand scores, rely on accurately judging a series of morphological changes of bones to establish skeletal maturity.<sup>9,22</sup> The sequence of regular morphological changes of an ossification center can be considered an analog radiographic feature. Analog radiographic features can create potential for inter-rater disagreement due to varying judgment of the morphological appearance. Depending on the complexity of the skeletal maturity system and the familiarity of the rater, this can result in large inter-rater errors, as described by Cundy *et al.* for the Greulich and Pyle system.<sup>13</sup>

Certain skeletal maturity systems also feature digital radiographic features, bony features that are either absent or present. Many bones can serve as digital systems of assessment, in that they are absent and later appear, or certain parts of them appear such as the epiphyses. Digital markers are simple, and can sometimes be used by themselves in the absence of other radiographic features. However, the majority of ossification centers appear early during development. The plantar and thenar sesamoids have unique potential to be considered for use as a digital assessment method because they develop later, around the time of PHV. The time period around the adolescent growth spurt is often of the most interest to the pediatric orthopedist, as this is the time period most associated with scoliosis curve progression, SCFE, and epiphysiodesis.<sup>4,33</sup>

Although digital distinctions are simple, they may not be specific enough for exclusive use. They can be difficult to localize temporally since they are either present or absent. When they first appear, it can be difficult to tell how long they have been present unless one has serial radiographs. They oftentimes need to be attached to analog distinctions to have value. For instance, in the article from Nicholson *et al.* outlining the ossification of the calcaneal apophysis, the appearance of the plantar sesamoids on an AP radiograph can help clarify whether a calcaneus is stage 2 or 3.<sup>37</sup> By themselves the plantar sesamoids are not specific enough to delineate a stage 2 calcanei from a stage 3 calcanei, and their presence should be relied upon secondary to the other characteristics of a stage 3 calcaneus. However, for an ambiguous calcaneal apophysis, they can be helpful in deciding the calcaneal stage.

The purpose of this study is to examine the information difference conveyed by digital and analog methods of maturity assessment, using the plantar and thenar sesamoids. We examine the sesamoids using three systems of measurement, one of which is digital and two of which are analog. We explore the information that can be ascertained using the plantar and thenar sesamoids in conjunction as a digital assessment. We also examine the relationship of the plantar sesamoids to calcaneal apophyseal stages and the thenar sesamoids to Sanders hand scores.

## **Materials and Methods**

We studied 742 serial foot and 694 serial hand radiographs from ninety-four children (forty-nine females and forty-five males) ages three to eighteen years, who were evaluated under the direction of Dr. T. Wingate Todd by the Brush Foundation at

Western Reserve University from 1926 to 1942.<sup>9, 11</sup> Four of the foot radiographs had the area of the plantar sesamoids visible but did not show the complete calcaneus. The children used in this study were the same as those used for establishment of the calcaneal system.<sup>37</sup> The Bolton-Brush study is described in chapter 1 as are the calculations for our present study.

The appearance of the plantar and thenar sesamoids was recorded based on three systems of measurement, one digital, and two analog. The grading schemes for assessing the plantar sesamoids are outlined in Figure 3.1 and the grading schemes for assessing the thenar sesamoids are shown in Figure 3.2. The first system of measurement, a digital system, grades the sesamoids based only on their absence or presence. The second system, an analog scale based on three morphologic grades, grades the sesamoids as either absent, present as a small ossification center on an AP radiograph or only visible on the lateral radiograph (for the plantar sesamoids), or larger than a small ossification center. The third system, an analog scale based on four morphologic grades, grades the sesamoids as absent, present as a small ossification center on an AP radiograph or only visible on the lateral radiograph (for the plantar sesamoids), larger than a small ossification center but not fully mature size, or fully mature (size and density no longer increase). The third system is only possible if serial radiographs are obtained in order to ascertain the final size of the sesamoids.

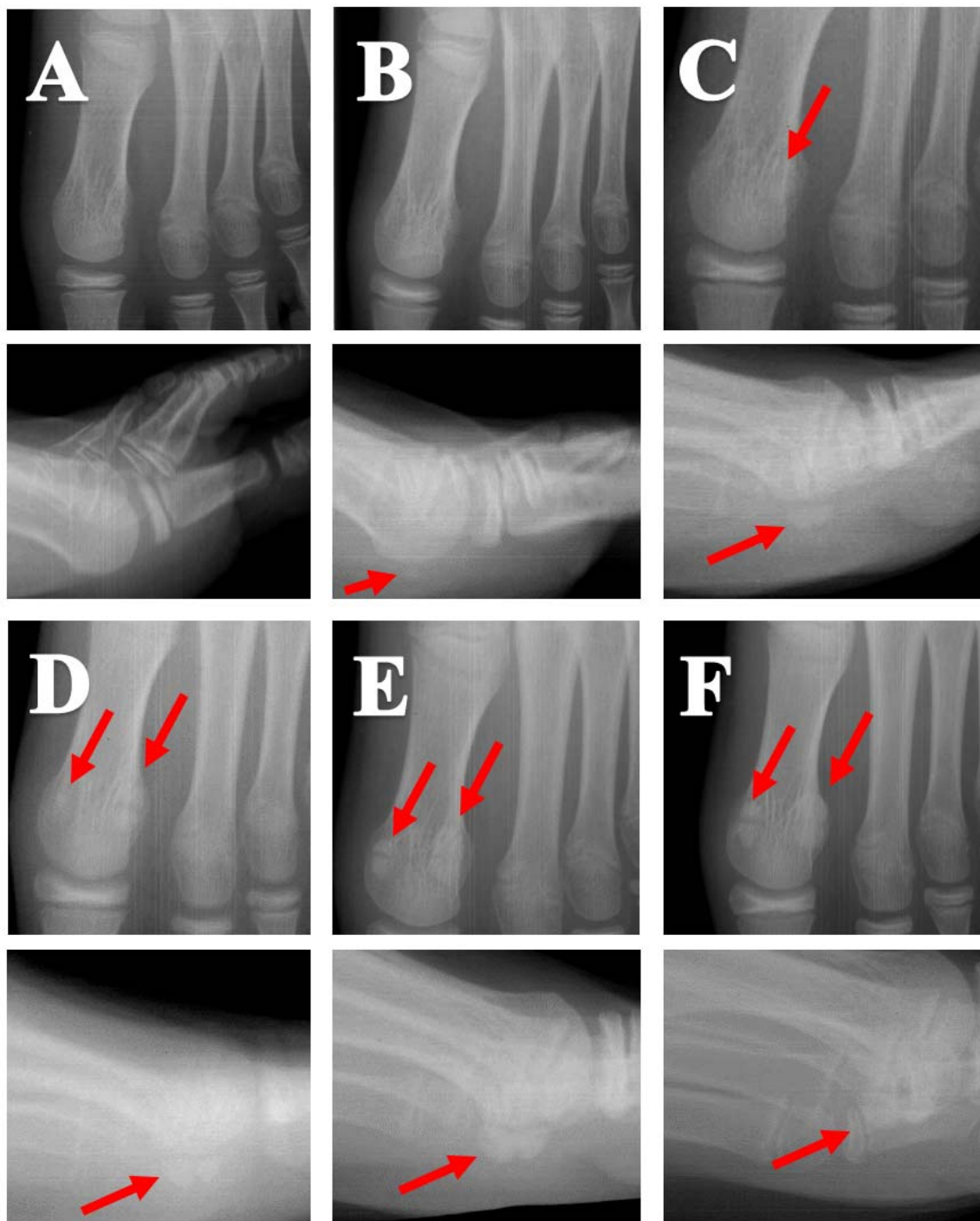


**Figure 3.1. The maturity schemes for judging the plantar sesamoid**

Plantar sesamoids are indicated by the red arrows.

Grading Scheme #1 – two point digital system. The plantar sesamoid is either absent (Figure A) or present (Figure B-F) on an AP and lateral foot radiograph. Figure B shows

that the plantar sesamoids can appear absent on an AP radiograph but still be present on the lateral, as indicated by the red arrow. In Figure C the plantar sesamoids are clearly present on the lateral radiograph but is only slightly visible on the AP radiograph. The medial plantar sesamoid is not visible on the AP radiograph.

Grading Scheme #2 – three point analog system. The plantar sesamoid is absent (Figure A), visible as only a small speck of ossification on an AP radiograph or only on the lateral radiograph (Figure B and C), or larger than a small speck of ossification (Figure D-F) on an AP radiograph of the foot.

Grading Scheme #3 – four point analog system. The plantar sesamoid is absent (Figure A), visible as only a small speck of ossification on an AP radiograph or only on the lateral radiograph (Figure B and C), or larger than a small speck of ossification but not yet mature size or density (Figure D and E), and is fully mature (Figure F). A sesamoid is considered mature when it no longer increases in size and density. There is a very small increase in size of the medial plantar sesamoid from Figure E to Figure F. This method is only possible with serial radiographs in order to determine the mature size since there is significant variation in final size of the plantar sesamoid for each child.

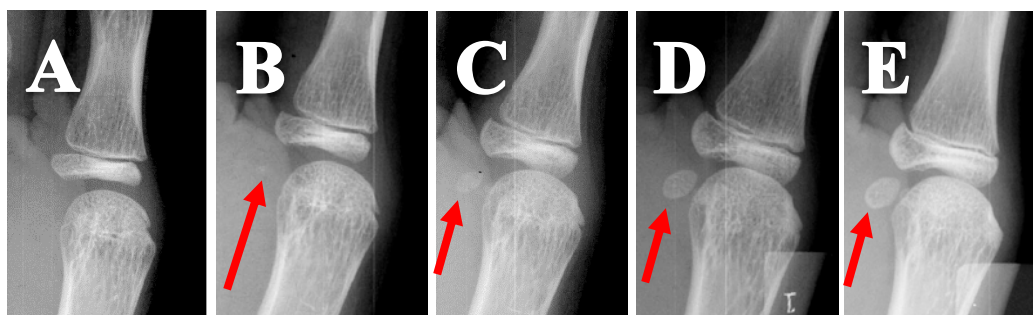


**Figure 3.2. The maturity schemes for judging the thenar sesamoid**

Thenar sesamoids are indicated by the red arrows.

Grading Scheme #1 – two point digital system. The thenar sesamoid is either absent (Figure A) or present (Figure B-E) on an AP hand radiograph.

Grading Scheme #2 – three point analog system. The thenar sesamoid is absent (Figure A), visible as only a small speck of ossification (Figure B), or larger than a small speck of ossification (Figure C-E) on an AP radiograph of the hand.

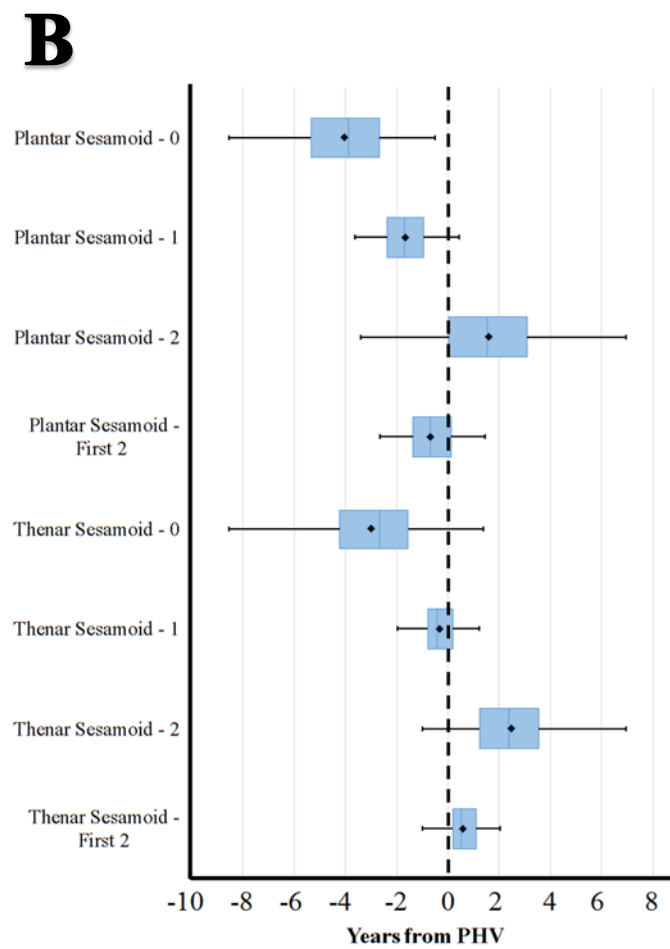
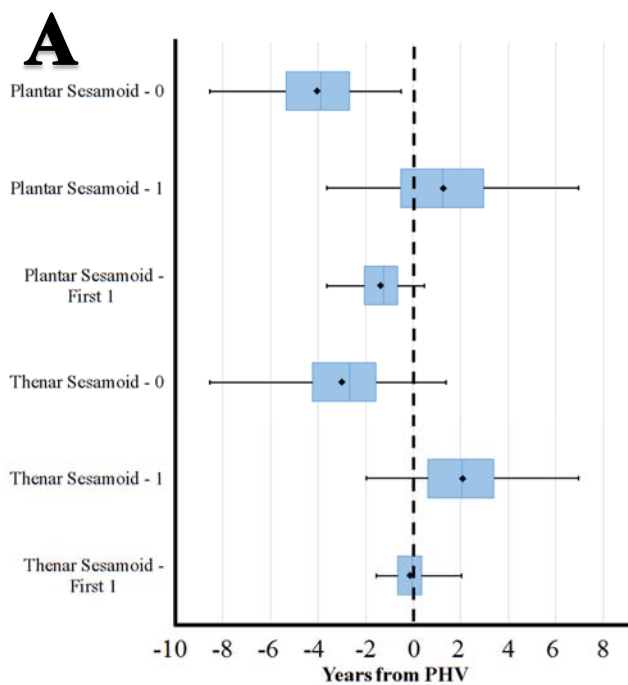
Grading Scheme #3 – four point analog system. The thenar sesamoid is absent (Figure A), visible as only a small speck of ossification (Figure B), or larger than a small speck of ossification but not yet mature size or density (Figure C and D), and is fully mature (Figure D). A sesamoid is considered mature when it no longer increases in size and density. This method is only possible with serial radiographs in order to determine the mature size since there is significant variation in final size of the thenar sesamoid for each child.

The calcaneal scores and Sanders hand scores have been described previously.<sup>12, 37</sup> The grading scales are shown in Figures 1.1 and 2.1. Each hand radiograph was graded with a Sanders hand score and each foot radiograph was graded with a calcaneal score. Two observers, a fellowship-trained pediatric orthopedist and a medical student evaluated 75 randomly selected hand and foot radiographs for evaluation of the plantar and thenar sesamoids using the three grading scales described previously. For the four point scheme, the 75 images were bracketed by an image from 1-2 years before and after the radiograph of interest for comparison. Confidence intervals and unweighted  $\kappa$  were calculated using Microsoft Excel 2013.

## Results

The years from PHV for each stage of plantar and thenar sesamoid ossification by the three grading schemes are shown in Figure 3.3 and Tables 3.1-3.3. The plantar sesamoids first appear 1.67 years (95% CI, 1.90 to 1.43 years) before PHV. The plantar sesamoids are visible on a lateral radiograph of the foot before they are visible on an AP radiograph. The plantar sesamoids continue to increase in size over the next 2.7 years and reach their mature size on average 1.02 years (95% CI, 0.80 to 1.24 years) after PHV. The thenar sesamoids first appear 0.32 years (95% CI, 0.49 to 0.15 years) before PHV. The thenar sesamoids increase in size over the next 2.6 years and reach their mature size on average 2.25 years (95% CI, 2.11 to 2.39 years) after PHV. Both plantar and thenar sesamoids ossify over a similar length of time. However, the plantar sesamoids ossify approximately 1.4 years earlier than the thenar sesamoids. In addition, the plantar sesamoids are often not visible on an AP radiograph when they first appear.





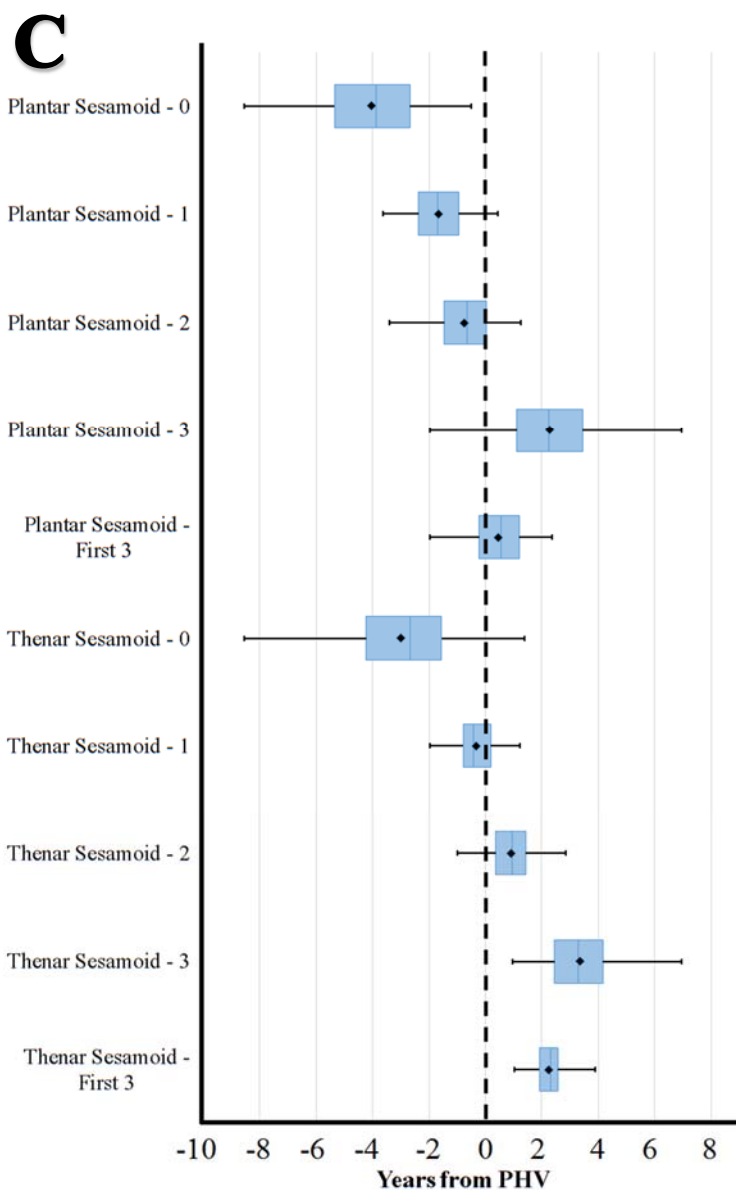


**Figure 3.3.** A box and whiskers plot of the age with respect to PHV for the plantar and thenar sesamoids using three grading schemes. The black lines represent the range for each examined sequence, while the blue box represents the middle 50% of data. The blue line in the middle of each box represents the median, while the black diamond represents the mean.

A). Grading Scheme #1 – two point digital system. The sesamoids were graded as either absent (0) or present (1).

B). Grading Scheme #2 – three point analog system. The sesamoids were graded as absent (0), present as a tiny speck of ossification on the AP view or only visible on the lateral (1), and larger than a tiny speck of ossification (2).

C). Grading Scheme #3 – four point analog system. The sesamoids were graded as absent (0), present as a tiny speck of ossification on the AP view or only visible on the lateral (1), and larger than a tiny speck of ossification but not fully mature size or density (2), and fully mature (3). This system requires serial radiographs to establish when the sesamoids no longer continue growing.

**Table 3.1 – Age from PHV for the thenar and plantar sesamoids – two point system**

		Timing Relative to PHV (yr)		
Stage	n	Mean	95% CI	Range
Plantar sesamoids absent	181	-4.04	-4.29 to -3.78	-8.55 to -0.52
Plantar sesamoids present	561	1.26	1.08 to 1.44	-3.64 to 6.95
Plantar sesamoids present - first appearance*	55	-1.35	-1.61 to -1.10	-3.64 to 0.48
Thenar sesamoids absent	291	-2.99	-3.21 to -2.77	-8.55 to 1.39
Thenar sesamoids present	403	2.08	1.90 to 2.25	-1.97 to 6.95
Thenar sesamoids present - first appearance*	72	-0.12	-0.27 to 0.04	-1.55 to 2.02

\*Sesamoids were included in the “first appearance” group if they were the first radiograph of that stage directly following a radiograph of a different stage.

**Table 3.2 – Age from PHV for the thenar and plantar sesamoids – three point system**

		Timing Relative to PHV (yr)		
Stage	n	Mean	95% CI	Range
Plantar sesamoids absent	181	-4.04	-4.29 to -3.78	-8.55 to -0.52
Plantar sesamoids only visible on lateral or as small ossification center on AP	56	-1.67	-1.90 to -1.43	-3.64 to 0.44
Plantar sesamoids larger than small ossification center	505	1.59	1.41 to 1.76	-3.40 to 6.95
Plantar sesamoids larger than small ossification center - first appearance*	66	-0.67	-0.90 to -0.45	-2.66 to 1.45
Thenar sesamoids absent	291	-2.99	-3.21 to -2.77	-8.55 to 1.39
Thenar sesamoids visible as small ossification center on AP	58	-0.32	-0.49 to -0.15	-1.97 to 1.22
Thenar sesamoids larger than small ossification center	345	2.48	2.31 to 2.65	-0.99 to 6.95
Thenar sesamoids larger than small ossification center - first appearance*	70	0.58	0.42 to 0.74	-0.99 to 2.02

\*Sesamoids were included in the “first appearance” group if they were the first radiograph of that stage directly following a radiograph of a different stage.

**Table 3.3 – Age from PHV for the thenar and plantar sesamoids – four point system**

		Timing Relative to PHV (yr)		
Stage	n	Mean	95% CI	Range
Plantar sesamoids absent	181	-4.04	-4.29 to -3.78	-8.55 to -0.52
Plantar sesamoids only visible on lateral or as small ossification center on AP	56	-1.67	-1.90 to -1.43	-3.64 to 0.44
Plantar sesamoids smaller than fully mature size	165	-0.48	-0.64 to -0.32	-3.40 to 2.00
Plantar sesamoids fully mature	340	2.58	2.42 to 2.75	-1.67 to 6.95
Plantar sesamoids fully mature - first appearance*	80	1.02	0.80 to 1.24	-1.67 to 2.81
Thenar sesamoids absent	291	-2.99	-3.21 to -2.77	-8.55 to 1.39
Thenar sesamoids visible as small ossification center on AP	58	-0.32	-0.49 to -0.15	-1.97 to 1.22
Thenar sesamoids smaller than fully mature size	124	0.91	0.78 to 1.04	-0.99 to 2.84
Thenar sesamoids fully mature	221	3.36	3.21 to 3.52	0.96 to 6.95
Thenar sesamoids fully mature - first appearance*	66	2.25	2.11 to 2.39	1.02 to 3.87

\*Sesamoids were included in the “first appearance” group if they were the first radiograph of that stage directly following a radiograph of a different stage.

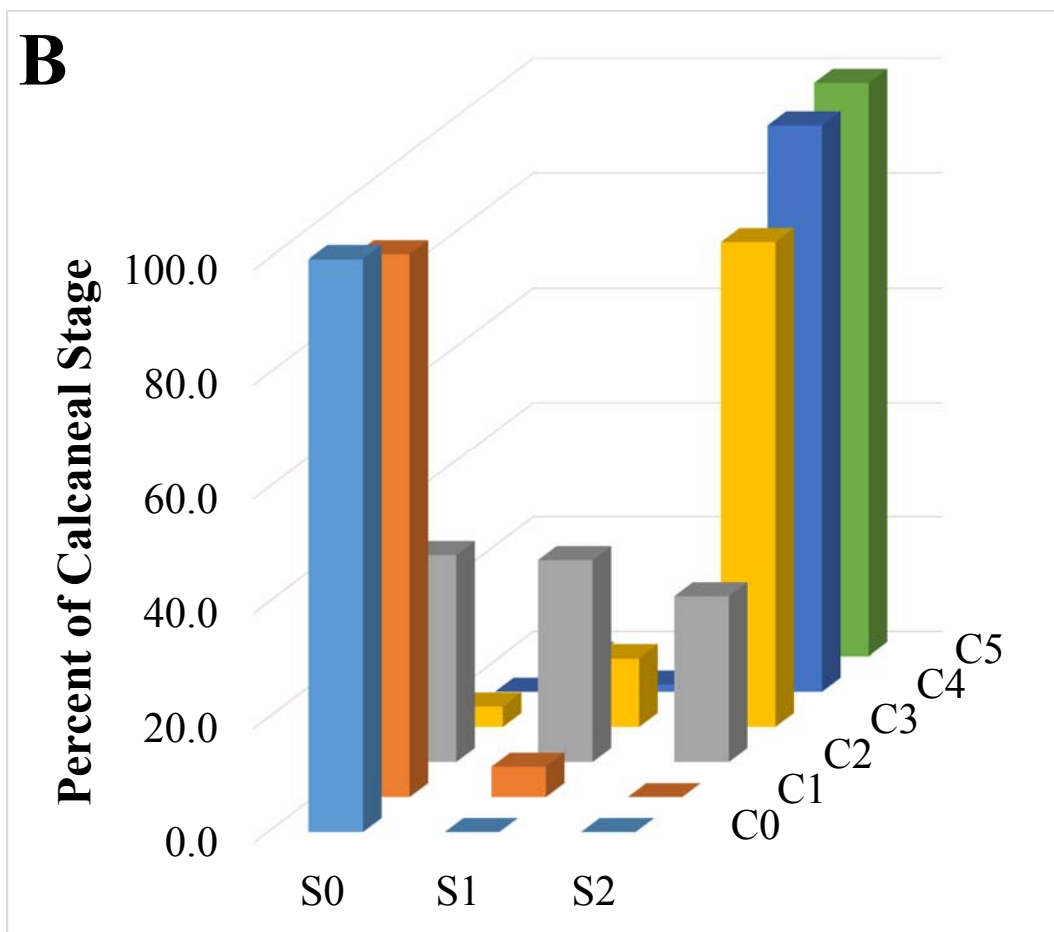
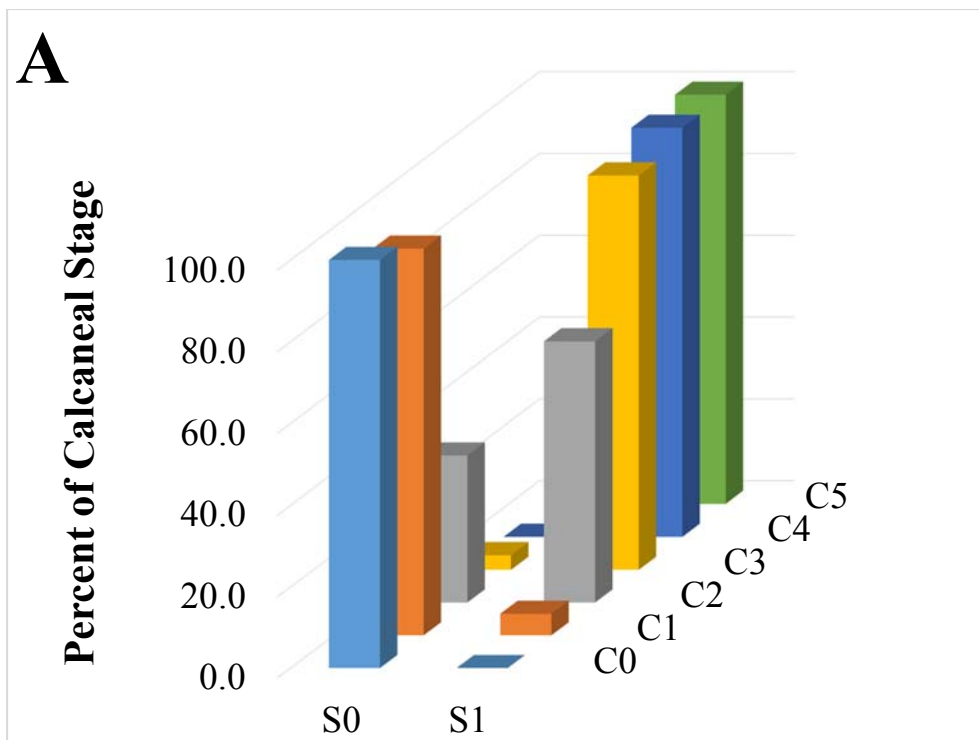
As shown in Figure 3.3A and Table 3.1, the two point or digital system provides limited information with respect to years from PHV, unless being followed with serial radiographs allowing for discernment of when the plantar or thenar sesamoids first appear. Based on the two point system, the plantar sesamoids first appear 1.35 years (95% CI, 1.61 to 1.10 years) before PHV and the thenar sesamoids first appear 0.12 years before (95% CI, 0.27 years before to 0.04 years after) PHV. These numbers are somewhat higher than those detailed by the analog systems because the first appearance of the digital system includes more mature forms of the sesamoids whereas analog systems only include small sesamoids in the first appearance.

The three point analog system provides more information regarding PHV than the digital method, as shown in Figure 3.3B and Table 3.2. The plantar sesamoids are only visible on the lateral radiograph or as a small puff of ossification within a narrow window with respect to PHV, with an average age of 1.67 years (95% CI, 1.90 to 1.43 years) before PHV. Plantar sesamoids larger than a puff of ossification, that are well-defined and radiopaque on an AP radiograph, first occur 0.67 years (95% CI, 0.90 years to 0.45 years) before PHV. The thenar sesamoids are only visible as a small puff of ossification with a mean age of 0.32 years (95% CI, 0.49 to 0.15 years) before PHV. The thenar sesamoids first become larger than a puff of ossification on average 0.58 years (95% CI, 0.42 to 0.74 years) after PHV.

The four point analog system provides the most information relative to the other two systems of assessment, as shown in Figure 3.3C and Table 3.3. The four point system furthers the information conveyed by the three point system by subdividing sesamoids that are larger than a puff of ossification into semi-mature and mature. Mature

sesamoids no longer increase in size or density. The mean age of the semi-mature plantar sesamoids was 0.48 years (95% CI, 0.64 to 0.32 years) before PHV. The first appearance of fully mature plantar sesamoids occurred 1.02 years (95% CI, 0.80 to 1.24 years) after PHV. The mean age of semi-mature thenar sesamoids was 0.91 years (95% CI, 0.78 to 1.04 years) after PHV. The first appearance of fully mature thenar sesamoids occurred 2.25 years (95% CI, 2.11 to 2.39 years) after PHV.

In regards to the calcaneal stages, the two point system shown in Figure 3.4A shows clearly when the plantar sesamoids appear. The majority of the plantar sesamoids appear during calcaneal stage 2, with 64% of calcaneal stage 2 having the plantar sesamoids present. 96% of calcaneal stage 3 have the plantar sesamoids present, and 100% of calcaneal stage 4 have the plantar sesamoids present. The three point scale shown in Figure 3.4B adds further information to the digital system. For instance, 28.8% percent of calcaneal stage 2 radiographs have plantar sesamoids that appear more mature than a faint puff of ossification on an AP radiograph, whereas 84.5% of calcaneal stage 3 radiographs have plantar sesamoids that are more mature than a puff of ossification on an AP radiograph. The four point system shown in Figure 3.4C provides the most detailed information about the size of the plantar sesamoids within each calcaneal stage.





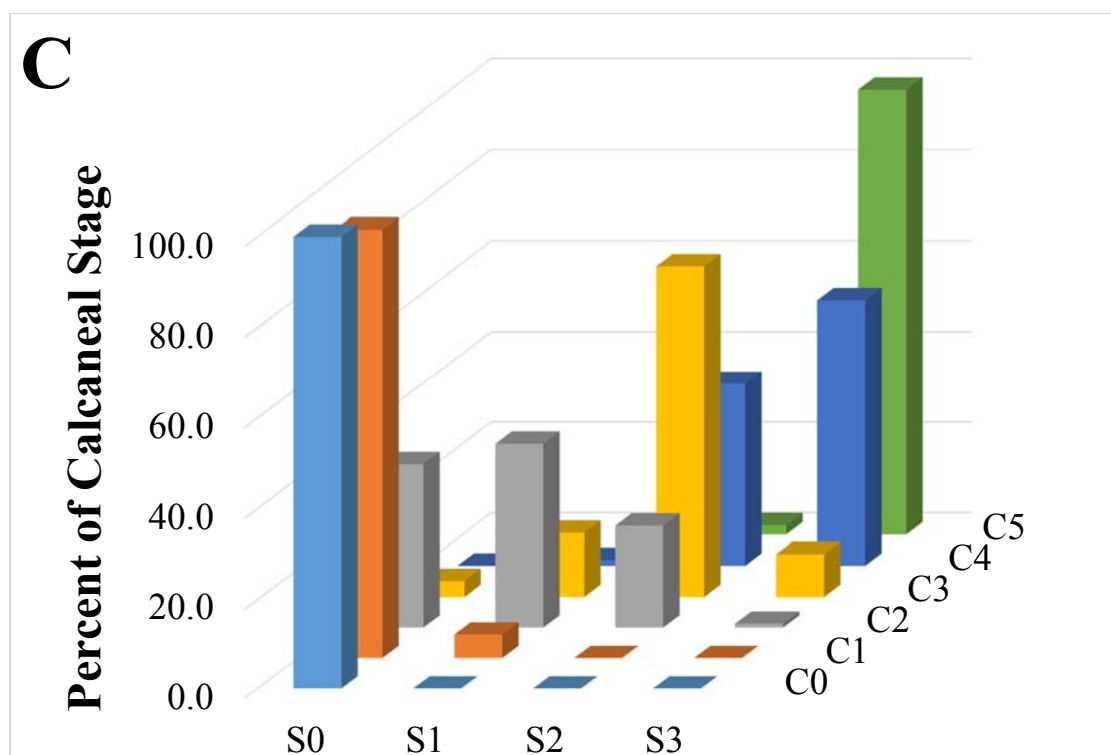


**Figure 3.4.** The distribution of the plantar sesamoids across calcaneal stages.

Calcaneal stages are listed on the right. Calcaneal stage 0 (C0), calcaneal stage 1 (C1), calcaneal stage 2 (C2), calcaneal stage 3 (C3), calcaneal stage 4 (C4), calcaneal stage 5 (C5).

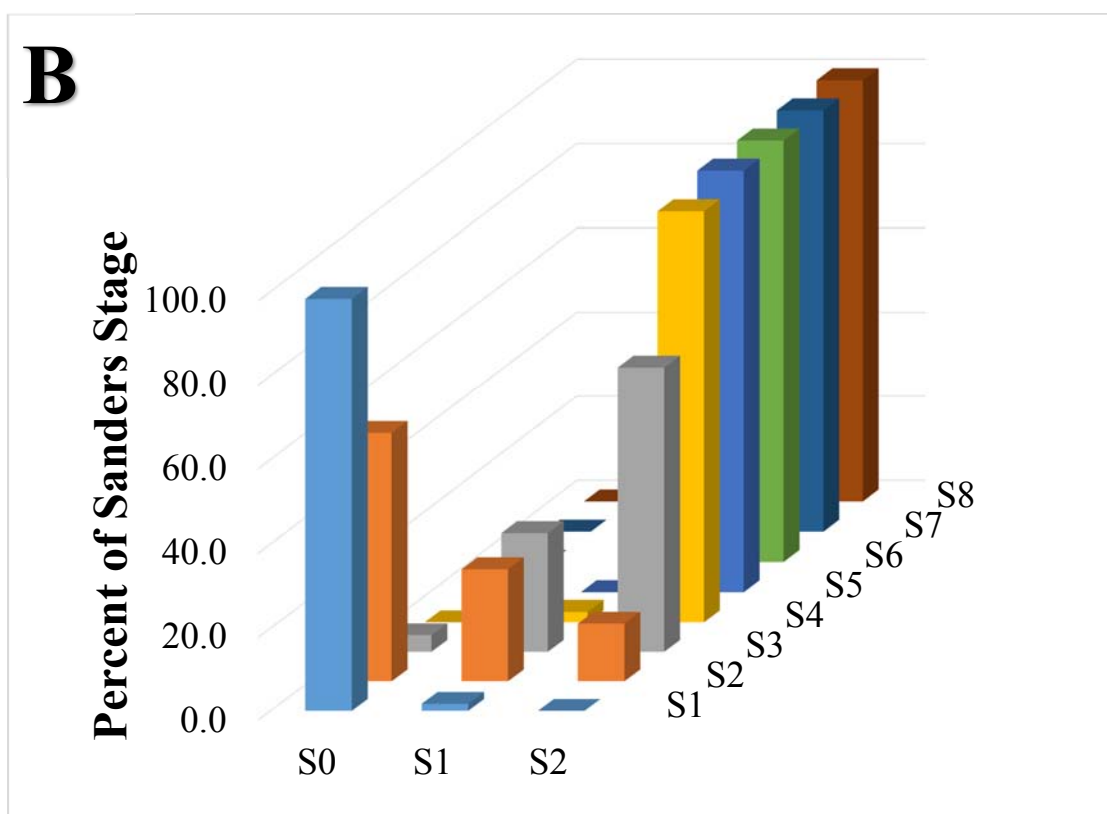
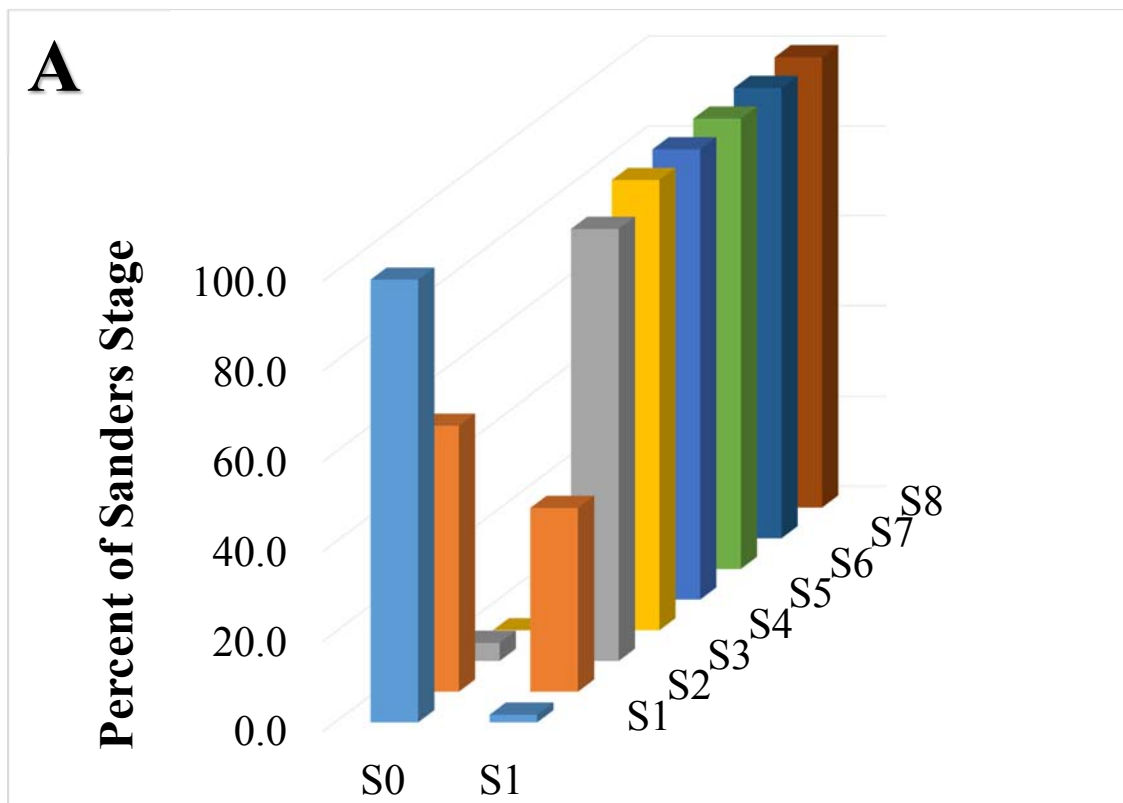
A). Grading Scheme #1 – two point digital system. The plantar sesamoids were graded as either absent (S0) or present (S1). A few plantar sesamoids begin to appear during calcaneal stage 1 with the majority appearing by calcaneal stage 2. By calcaneal stage 3 virtually all of the plantar sesamoids are present.

B). Grading Scheme #2 – three point analog system. The plantar sesamoids were graded as absent (S0), present as a tiny speck of ossification on the AP view or only visible on the lateral (S1), and larger than a tiny speck of ossification (S2). A few plantar sesamoids appear as a speck of ossification during calcaneal stage 1, with most developing during

calcaneal stage 2. By calcaneal stage 3, the plantar sesamoids have predominantly progressed past a small ossification center.

C). Grading Scheme #3 – four point analog system. The plantar sesamoids were graded as absent (S0), present as a tiny speck of ossification on the AP view or only visible on the lateral (S1), and larger than a tiny speck of ossification but not fully mature size (S2), and fully mature (S3). This system requires serial radiographs to establish when the sesamoids stop growing. This system offers additional information to the two more simple systems, for instance, indicating that during calcaneal stage 3 the majority of plantar sesamoids have not reached their mature size.

The two point system shown in Figure 3.5A shows clearly when the thenar sesamoids appear. The majority of the thenar sesamoids appear during Sanders stage 2, with 40.9% of Sanders stage 2 having the plantar sesamoids present. Only 4.0% of Sanders stage 3 do not have the thenar sesamoids present, indicating that the thenar sesamoids form during Sanders stage 2. The three point scale shown in Figure 3.5B adds further information to the digital system. For instance, Sanders stage 3 has 67.7% of thenar sesamoids that appear in a more mature form than a puff of ossification, whereas only 14.0% of the thenar sesamoids are more mature than a puff of ossification for Sanders stage 2. The four point system shown in Figure 3.5C provides the most detailed information about the size of the thenar sesamoids within each Sanders stage.



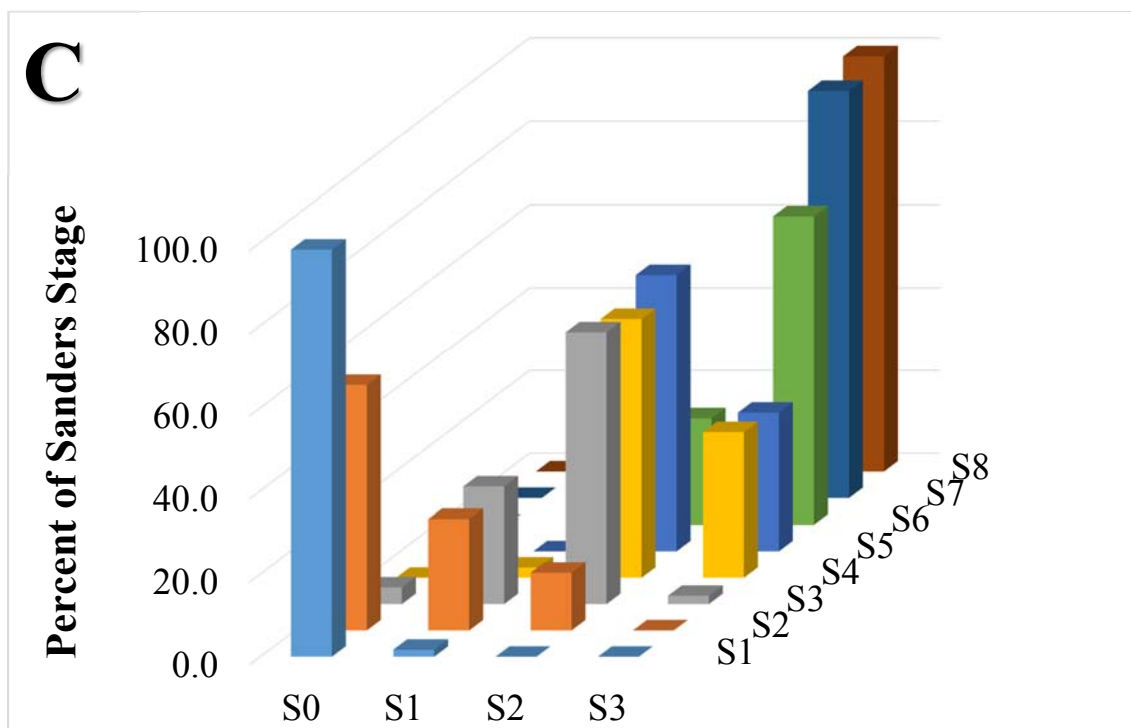


**Figure 3.5.** The distribution of the thenar sesamoids across Sanders stages.

Sanders stages are listed on the right. Sanders stage 1 (S1), Sanders stage 2 (S2), Sanders stage 3 (S3), Sanders stage 4 (S4), Sanders stage 5 (S5), Sanders stage 6 (S6), Sanders stage 7 (S7), Sanders stage 8 (S8).

A). Grading Scheme #1 – two point digital system. The thenar sesamoids were graded as either absent (S0) or present (S1). A few thenar sesamoids develop during Sanders stage 1, with the majority developing during Sanders stage 2.

B). Grading Scheme #2 – three point analog system. The thenar sesamoids were graded as absent (S0), present as a tiny speck of ossification on the AP view (S1), and larger than a tiny speck of ossification (S2). The thenar sesamoids mature during Sanders stage 2 and Sanders stage 3. By Sanders stage 3, the majority are larger than a small ossification center.

C). Grading Scheme #3 – four point analog system. The thenar sesamoids were graded as absent (S0), present as a tiny speck of ossification on the AP view (S1), and larger than a tiny speck of ossification but not fully mature size or density (S2), and fully mature (S3). This system requires serial radiographs to establish when the sesamoids stop growing. This system offers additional information compared to the previous two systems, indicating that the majority of thenar sesamoids do not become fully mature until Sanders stage 5.

The inter-rater  $\kappa$  and P, and the intra-rater  $\kappa$  and P for the three methods of grading the plantar and thenar sesamoids are shown in Table 3.4. P is the proportion of measurements that were the same between the two raters.

**Table 3.4 – Inter-rater reliability and intra-rater reliability**

	Inter-rater $\kappa$	Inter-rater P	Intra-rater $\kappa$	Intra-rater P
Plantar sesamoids - 4 point system	0.85	0.89	0.93	0.95
Plantar sesamoids - 3 point system	0.73	0.85	0.93	0.96
Plantar sesamoids - 2 point system	0.93	0.97	0.97	0.99
Thenar sesamoids - 4 point system	0.91	0.93	0.96	0.97
Thenar sesamoids - 3 point system	0.86	0.91	0.94	0.96
Thenar sesamoids - 2 point system	0.80	0.91	0.94	0.97

## Discussion

Many people are uncomfortable with analog distinctions, especially in the absence of additional data. Capping is easier to appreciate if you have x-rays that immediately precede and follow capping. Many people prefer digital distinctions, which have the advantage of clear distinction between the absent and present forms. Although digital distinctions are simple, they are often not specific enough for exclusive use. They sometimes need to be married to analog distinctions like the calcaneal score to add value.

The digital approach, considering the sesamoids as either absent or present, provides useful information regarding maturity, especially when the plantar and thenar sesamoids are considered together. Certainty is created about the degree of ossification because the distinction is all or nothing. It is easy to remember. In absence of serial radiographs it is difficult to assess maturity of the child relative to PHV since there are only two stages of ossification. However, a combination of these two simple digital markers can allow for deduction of maturity relative to PHV, due to the fact that the plantar sesamoids appear approximately 1.4 years earlier than the thenar sesamoids. If both sesamoids are absent, the child is likely at least 1.35 years before PHV. If the plantar sesamoids are present, and the thenar sesamoids are absent, the child is in between 1.35 years before PHV and 0.12 years before PHV. If both sesamoids are present, the child is after 0.12 years before PHV. Our data is in agreement with the observation by Dimeglio that the onset of puberty coincides with the appearance of the thenar sesamoids.<sup>35</sup>

The three grade system is an analog scale. The distinction between a puff of bone seen best on a lateral radiograph and more advanced ossification is not difficult. The information derived is richer than the digital system because identifying a puff of bone allows maturity to be localized with single radiographs rather than requiring both hand and foot radiographs. A plantar sesamoid that appears as a puff of ossification or only visible on the lateral radiograph indicates that the child is within 1.67 years to 0.67 years before PHV. A thenar sesamoid visible as a puff of ossification indicates that a child is between 0.32 years before PHV and 0.58 years after PHV.

The four stage system offers the most complete picture of sesamoid development by dividing sesamoids that are larger than a puff of ossification into those that are semi-mature and those that have reached mature size and density. However, the four-stage system is difficult to use without serial radiographs. The sesamoids vary significantly in final size between children, and cannot be discerned as having reached full growth until radiographs show no further increase in size and density. The difference between a semi-mature sesamoid and a completely mature one is difficult. The distinction exists and can be recognized, but is more suitable for research when the index radiograph can be bracketed with radiographs that come before and after.

Although the proportion of measurements in agreement (P) between the raters was similar for each grading scheme, the grading schemes with fewer grades in general had lower  $\kappa$  values than the grading schemes with more grades. The slightly lower  $\kappa$  of the schemes with fewer grading options is a reflection that when there are fewer options to choose from, there is an increased possibility that a measurement agreeing between raters is due to chance, which lowers  $\kappa$ . The four point scheme had a high inter-rater  $\kappa$  reflecting that the sesamoids can be consistently graded using this scheme if bracketing radiographs are available.

The thenar sesamoids and plantar sesamoids are useful as markers for adding certainty to analog systems, such as the Sanders and calcaneal scores. The plantar sesamoids can be used to differentiate calcaneal stage 1 from 2, and 2 from 3. Only 5.3% of calcaneal stage 1 radiographs have the plantar sesamoids present, even on a lateral radiograph. 64% of calcaneal stage 2 radiographs have the plantar sesamoids present, and 96.4% of calcaneal stage 3 radiographs have the plantar sesamoids present. If the



plantar sesamoids are present on a lateral radiograph, the calcaneus is significantly more likely to be calcaneal stage 2 than 1. The three point scale clarifies the distinction between calcaneal stage 2 and 3. Only 28.8% percent of calcaneal stage 2 radiographs have plantar sesamoids that appear more mature than a faint puff of ossification on an AP radiograph. However, 84.5% of calcaneal stage 3 radiographs have plantar sesamoids that are more mature than a puff of ossification on an AP radiograph. Thus, the presence of clearly defined radiopaque plantar sesamoids on an AP radiograph indicates that a calcaneus is more likely calcaneal stage 3 than 2.

The thenar sesamoids can be useful to differentiate Sanders stage 2 from Sanders 3, especially if capping is ambiguous. The majority of Sanders stage 3 radiographs (96.0%) had the thenar sesamoids present whereas only 40.9% of Sanders stage 2 radiographs had the thenar sesamoids present. The three point scale can further clarify the distinction between Sanders stage 2 and Sanders stage 3. Sanders stage 3 has 67.7% of thenar sesamoids that appear in a more mature form than a puff of ossification, whereas only 14.0% of the thenar sesamoids are more mature than a puff of ossification for Sanders stage 2. Thus, if the thenar sesamoids are larger than a puff of ossification, a hand is more likely to be Sanders stage 3 than stage 2.

As digital markers, the thenar and plantar sesamoids can provide limited information relative to timing of PHV by themselves. When the thenar and plantar sesamoids are considered together, the presence of the plantar sesamoid and absence of the thenar sesamoid indicates that a child is within 1.35 years before PHV. However, considering the thenar and plantar sesamoids as an analog three point scale allows significantly more information to be derived of maturity with respect to PHV without

serial radiographs. The four point system provides the most information, but is impossible to use without bracketing radiographs due to significant phenotypic variation in final size of the sesamoids. The two point and three point sesamoid grading scales also add certainty to analog scales such as the Sanders and calcaneal skeletal maturity systems. If the thenar sesamoids are larger than a puff of ossification, a hand is more likely to be Sanders stage 3 than stage 2. This may be especially useful because the presence of capping, which differentiates Sanders stage 3 from Sanders stage 2, can be difficult to appreciate, and sometimes absent in certain subjects. In regards to the calcaneal system, the presence of the plantar sesamoids on a lateral radiograph can differentiate calcaneal stage 1 from calcaneal stage 2, and radiopaque, clearly visible plantar sesamoids on an AP radiograph indicates that a calcaneus is calcaneal stage 3 as opposed to calcaneal stage 2.

## **Chapter 4 – Translating Between Systems of Skeletal Maturity: The Prognostic Power of Skeletal Maturity for Prediction of Contralateral SCFE**

### **Introduction**

Between 25-40% of children presenting with a unilateral SCFE develop a contralateral slip.<sup>7, 8, 33</sup> Those with uncomplicated SCFE develop hip deformity, but most are active for decades. If followed long enough, many go on to develop degenerative joint disease requiring a reconstructive procedure.<sup>45-49</sup> SCFE can be complicated by avascular necrosis, chondrolysis, and disabling pain resulting in early disability.<sup>48-50</sup> The severity of potential complications led Yildirim to conclude that prophylactic pinning is safer than observation of a contralateral hip.<sup>50</sup> Although prophylactic pinning prevents contralateral SCFE, it can result in infection, avascular necrosis, breakage of the implant or fracture of the femur, chondrolysis, and soft tissue irritation although the risks are small.<sup>8, 51</sup> It would be optimal to identify the risk of contralateral SCFE and offer prophylactic pinning to those at high risk for slipping. Skeletal maturity can be used to assess the risk for contralateral SCFE.

Two recent studies have shown that the modified Oxford hip score (MOHS) is predictive of contralateral SCFE development.<sup>7, 8</sup> Popejoy followed 260 patients treated for unilateral SCFE, of whom 64 went on to develop a contralateral slip. Fifty patients had a modified Oxford hip score of 16-18 at presentation, of whom forty-eight went on to develop a contralateral slip.<sup>8</sup> Stasikelis followed fifty patients seen for a unilateral slip,

and found that those with modified Oxford scores up to 21 were at elevated risk of contralateral slip, with lower scores having the most elevated risk.<sup>2</sup>

Although the modified Oxford score was strongly predictive of contralateral SCFE in these two studies, it is not widely used. The system is complex and uses variable numerical values for each radiographic feature examined.<sup>8,34</sup> The modified Oxford method has other difficulties associated with its use clinically. Oftentimes all five radiographic features are not clearly visible on a single radiograph, necessitating repeat radiographs. Furthermore, there is phenotypic variation among children. Some children have radiographic features that do not resemble those described by the modified Oxford method.

We compare the modified Oxford scoring system to other systems of skeletal maturity. We translate the stages of each system that correspond to modified Oxford hip scores most predictive of contralateral SCFE. We examine the utility of the TRC, calcaneal system, and Sanders hand scores for identifying children at risk of contralateral SCFE.<sup>12</sup>

## **Materials and Methods**

We studied 738 serial foot radiographs, 694 serial hand radiographs, and 686 serial AP hip radiographs from ninety-four children (forty-nine females and forty-five males) ages three to eighteen years, who were evaluated under the direction of Dr. T. Wingate Todd by the Brush Foundation at Western Reserve University from 1926 to 1942.<sup>9,11</sup> The children used in this study were the same as those used for establishment of the calcaneal system.<sup>37</sup> The Bolton-Brush study is described in chapter 1 as are

calculations for our present study. The calcaneal apophysis scoring has been described previously and is shown in Figure 1.1.<sup>37</sup> The Sanders method has been previously described and is summarized in Figure 2.1.<sup>12</sup> The Sanders stages correspond to Greulich and Pyle atlas standards, as shown in Table 2.1.

The modified Oxford hip score was described by Stasikelis and examines five of the features described in the full Oxford method.<sup>7,32</sup> The modified Oxford score grades three consecutive stages of maturation of the triradiate cartilage (TRC), ilium, femoral epiphysis, greater trochanter, and lesser trochanter. The total score ranges from 16-26. The modified Oxford scoring system is shown in Figure 4.1.

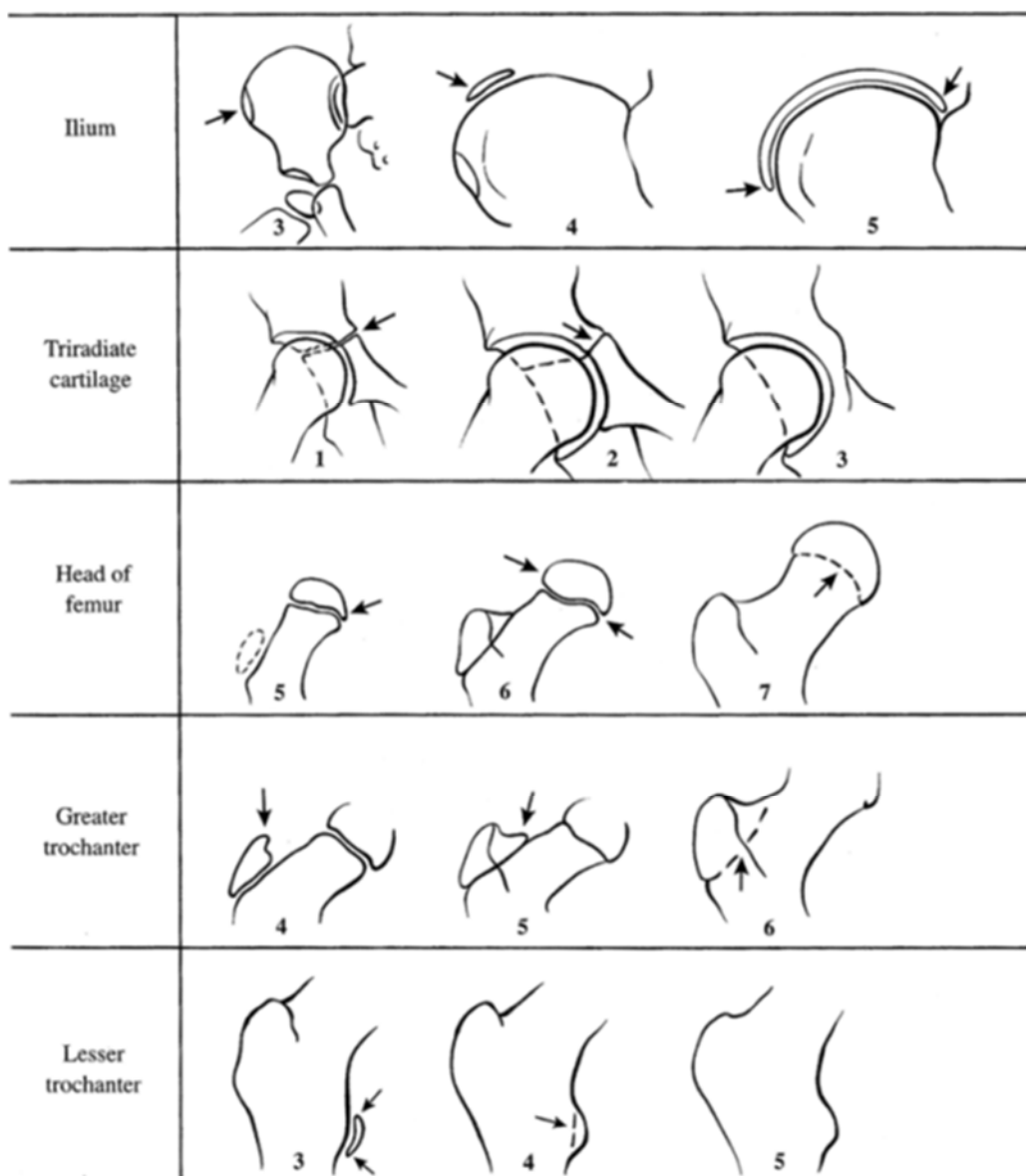


**Figure 4.1. The modified Oxford hip score**

Reprinted with Permission from Zide JR; Popejoy D; Birch JG. Revised Modified Oxford Bone Score: A Simpler System for Prediction of Contralateral Involvement in Slipped Capital Femoral Epiphysis. *Journal of Pediatric Orthopaedics*. 2011;31(2):159-164.

We had the advantage of having a full series of hip radiographs for each child.

This allowed us to determine the scores of some features that were unclear on the index

film. For instance, there were a number of index radiographs with a lesser trochanter with an unclear score. However, radiographs taken a year or two later clearly shows a 3 point lesser trochanter, the least mature in the series used by the modified Oxford method. This allowed us to assign a score of 3 to the index film as the trochanter couldn't have been more mature. We were also able to account for phenotypic variation in determination of our modified Oxford scores due to having serial radiographs. Several children did not follow the phenotypic patterns outlined in the modified Oxford method.

We graded each radiograph with their respective calcaneal stage, Sanders stage, modified Oxford hip score, and TRC status. There were 636 sets of calcaneal and hip radiographs taken at the same session. For the overlapping calcaneal and hip radiographs, the calcaneal scores were compared to modified Oxford hip scores and TRC status. 598 sets of hand and hip radiographs were taken at the same session. For the overlapping hand and hip radiographs, the Sanders hand scores were compared to modified Oxford hip scores and TRC status. 557 sets of calcaneal radiographs, hand radiographs, and hip radiographs were taken at the same session. For the 557 sets of overlapping calcaneal, hand, and hip radiographs, the combined calcaneal/Sanders scores were compared to the modified Oxford hip scores and the TRC status.

Calculation of  $\kappa$  for the calcaneal system was described in chapter 1.<sup>37</sup>

Calculation of  $\kappa$  for the Sanders hand scores was described in chapter 2.<sup>12</sup> Two individuals graded 686 AP hip radiographs for calculation of  $\kappa$  using the modified Oxford hip scores and TRC. Two individuals also graded 75 randomly selected AP hip radiographs that were shown singly, and 75 randomly selected AP hip radiographs that were shown with the hip radiographs from the years before and after for calculation of  $\kappa$

for determining TRC status. Microsoft Excel 2013 was used to calculate confidence intervals as well as  $\kappa$  coefficients.

## **Results**

The distribution of modified Oxford scores for each calcaneal stage is shown in Figure 4.2. A slow progression of hips from modified Oxford scores 16 to 18 is seen during calcaneal stages 0 to 2. Beginning with calcaneal stage 3, hips begin to mature more rapidly, with 36.3% reaching modified Oxford hip scores 19 and above. Calcaneal stage 4 consists of a wide range of hips with advanced modified Oxford hip scores, although a minority (11.4%) are modified Oxford hip scores 17-18. Calcaneal stage 5 consists entirely of mature hips that are modified Oxford hip scores 19 or higher.



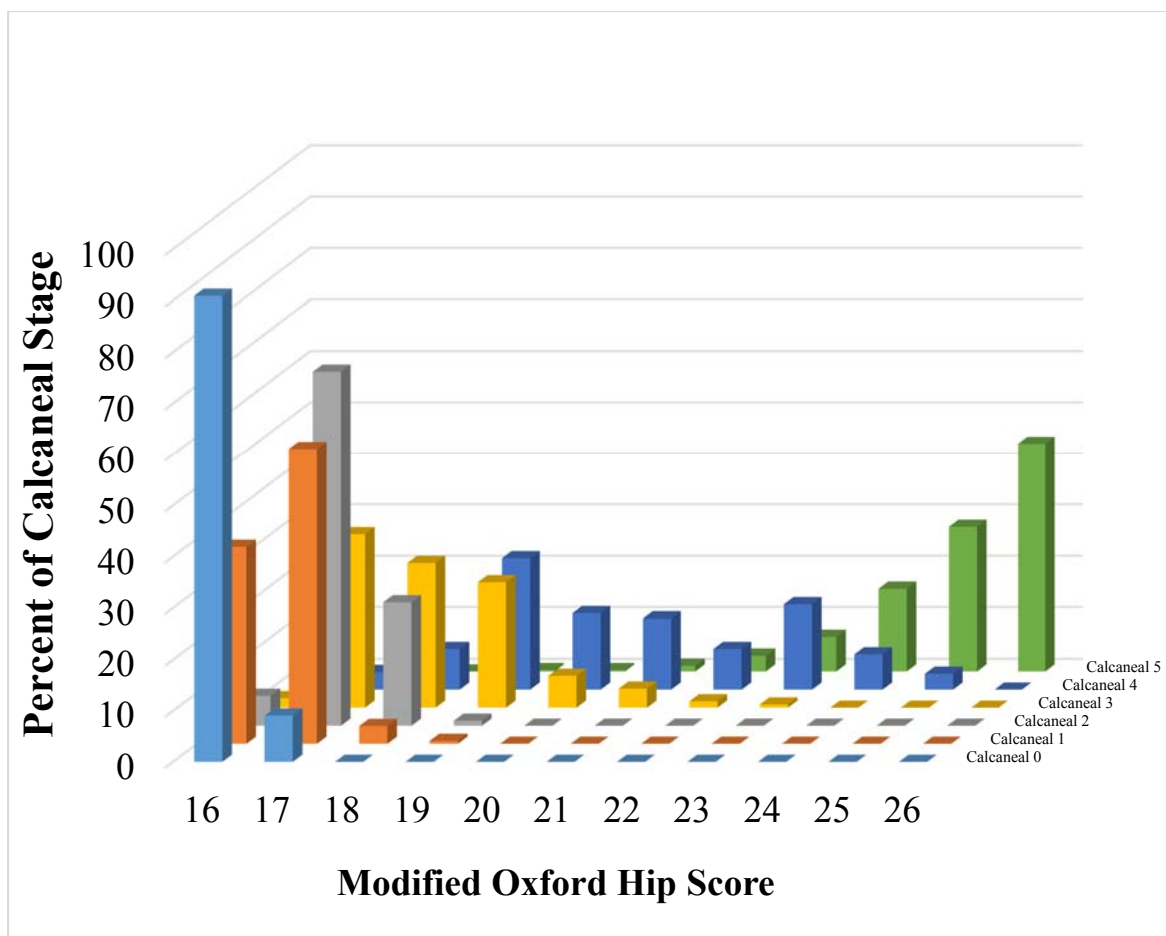


**Figure 4.2. Calcaneal stages compared to modified Oxford hip scores**

The percentage of radiographs for each calcaneal stage that has matching hip radiographs for each modified Oxford hip score.

The risk of contralateral SCFE for each calcaneal stage was calculated using the risk for each modified Oxford hip score described by Stasikelis and Popejoy and are shown in Figure 4.3 and Table 4.1.<sup>7,8</sup> Risk of contralateral SCFE was considerably elevated for calcaneal stages 0-3, over 50%. Risk of contralateral SCFE for calcaneal stage 4 remained significant at approximately 25%. Calcaneal stage 5 had negligible risk of contralateral SCFE.

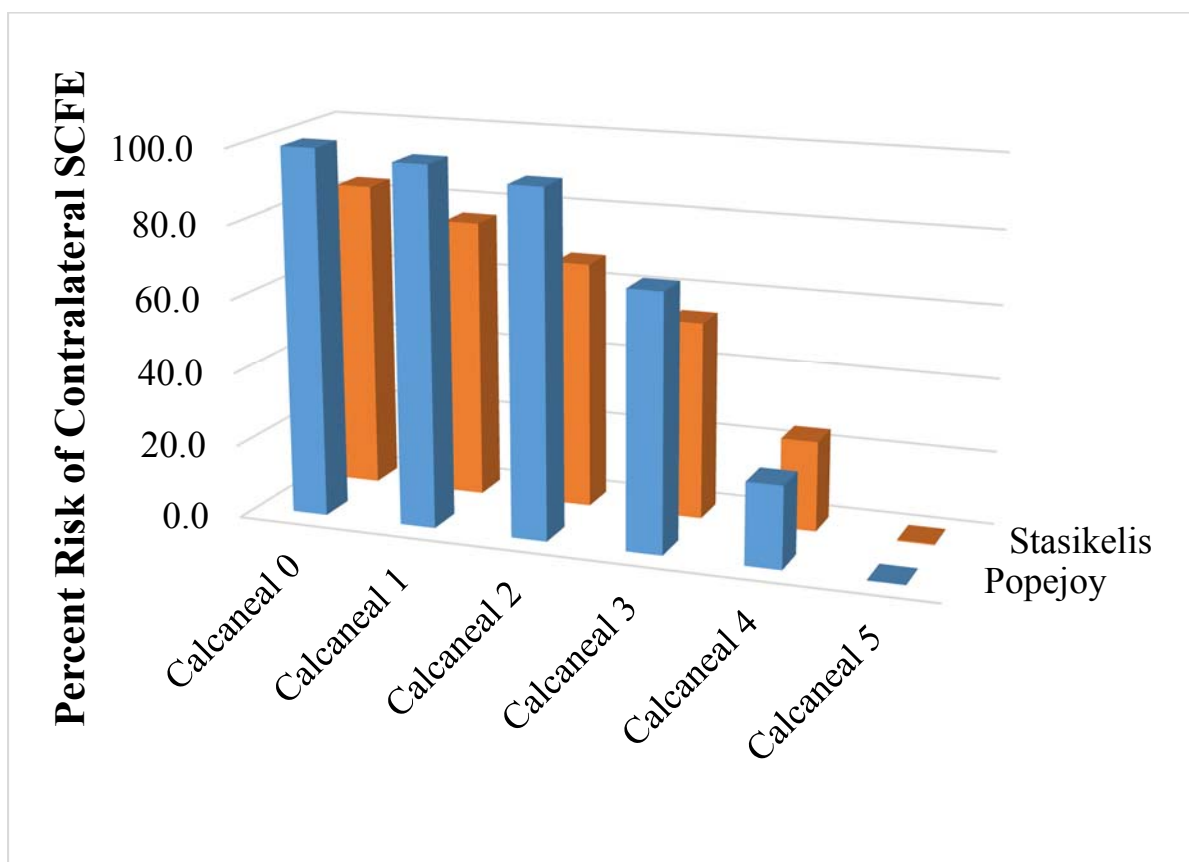


**Figure 4.3. Risk of contralateral SCFE for each calcaneal stage**

Risk of contralateral SCFE was calculated using data from Popejoy and Stasikelis based on the percent risk for each modified Oxford hip score and the percentage of each calcaneal stage corresponding to a particular modified Oxford hip score.

**Table 4.1. Percent Risk of contralateral SCFE for each calcaneal stage**

	Calcaneal 0	Calcaneal 1	Calcaneal 2	Calcaneal 3	Calcaneal 4	Calcaneal 5
Popejoy	99.7	97.4	93.8	69.6	22.3	0.2
Stasikelis	83.8	76.1	67.2	53.9	24.5	0.3

The distribution of modified Oxford scores for each Sanders hand score is shown in Figure 4.4. An orderly progression of modified Oxford scores is seen from Sanders stage 1 to 4. Sanders stages 1 and 2 correspond principally to modified Oxford hip scores from 16 to 18. Sanders stage 3 corresponds principally to modified Oxford hip scores 19 or higher, although a small percentage (12.4%) are modified Oxford hip scores of 17-18. All of Sanders stage 4 and higher radiographs correspond to modified Oxford hip scores of 19 or higher.

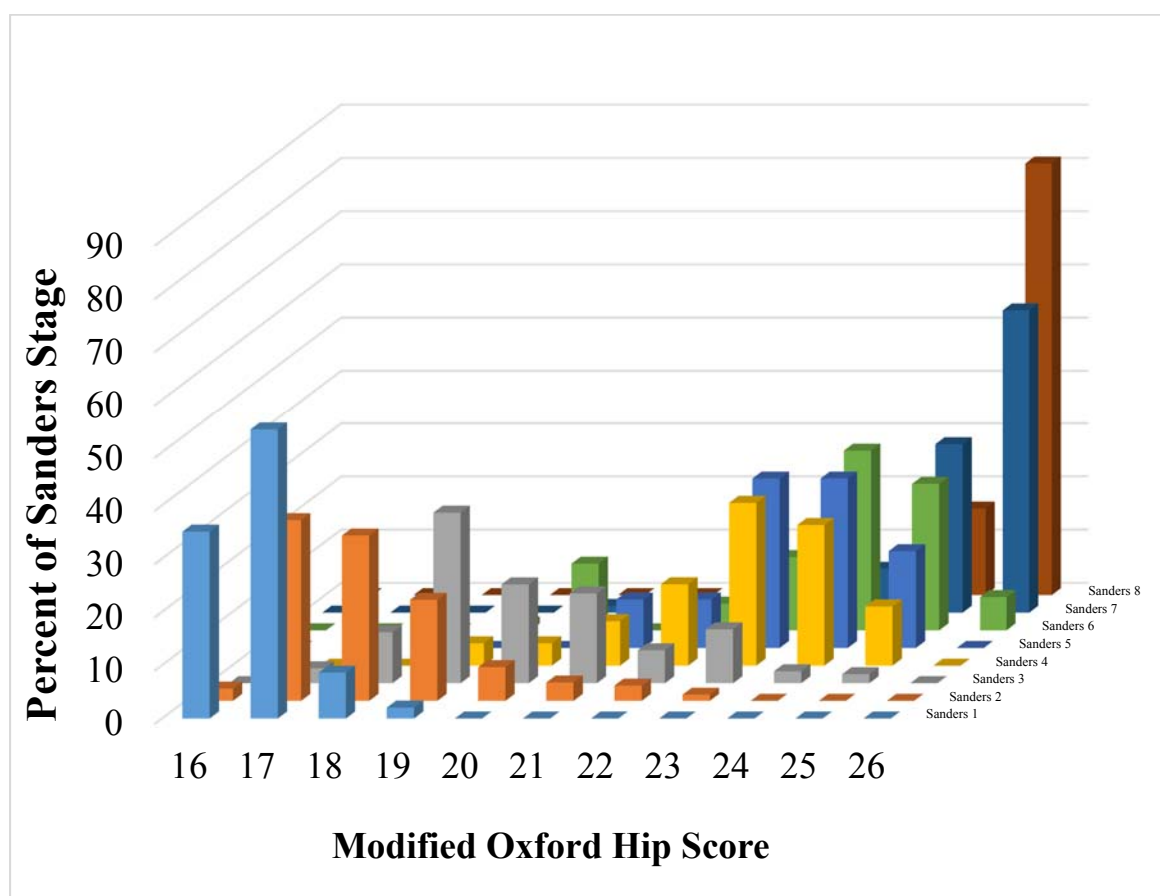


**Figure 4.4. Sanders hand scores compared to modified Oxford hip scores**

The percentage of radiographs for each Sanders hand score that has matching hip radiographs for each modified Oxford hip score.

The risk of contralateral SCFE for each Sanders hand score was calculated using the risk for each modified Oxford hip score described by Stasikelis and Popejoy and are shown in Figure 4.5 and Table 4.2.<sup>7,8</sup> Risk of contralateral SCFE was considerably elevated for Sanders hand scores 1 and 2, over 50%. Risk of contralateral SCFE for Sander hand score 3 remained significant at approximately 25%. Risk of contralateral SCFE for Sanders hand scores 4 or higher were negligible.

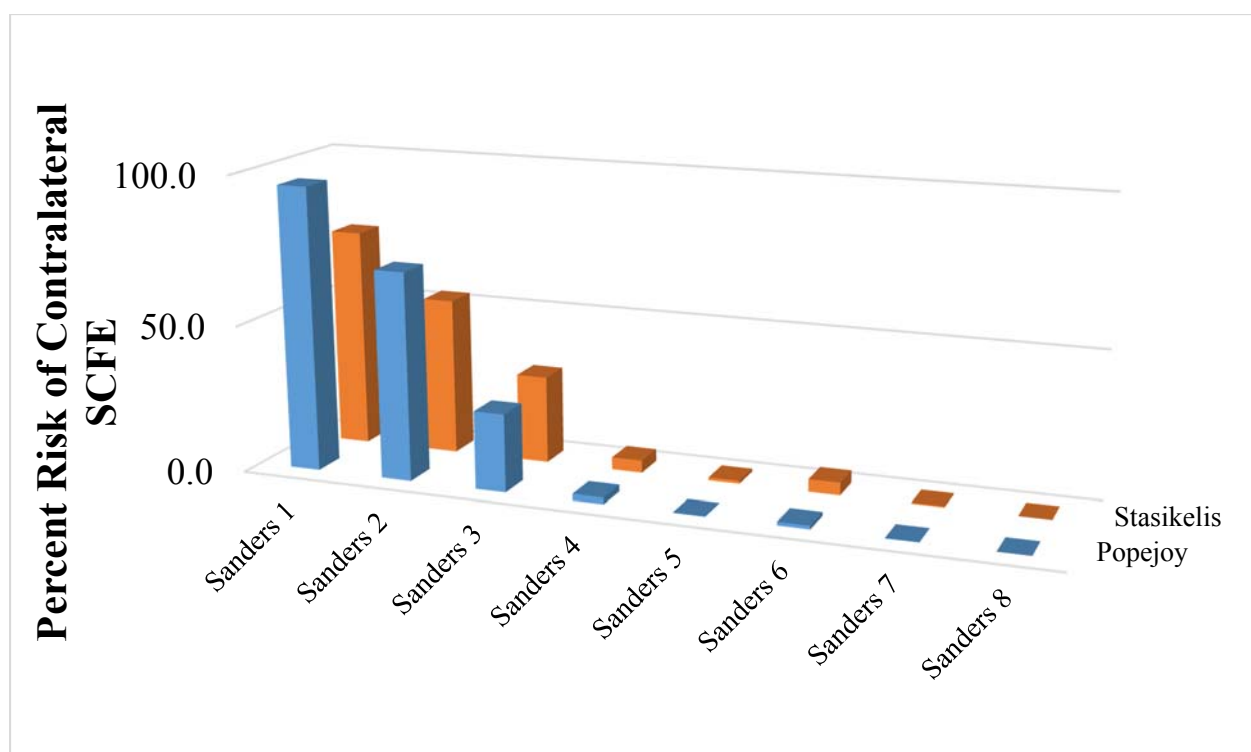


**Figure 4.5. Risk of contralateral SCFE for each Sanders hand score**

Risk of contralateral SCFE was calculated using data from Popejoy and Stasikelis based on the percent risk for each modified Oxford hip score and the percentage of each Sanders hand score corresponding to a particular modified Oxford hip score.

**Table 4.2. Percent Risk of contralateral SCFE for each Sanders hand score**

	Sanders 1	Sanders 2	Sanders 3	Sanders 4	Sanders 5	Sanders 6	Sanders 7	Sanders 8
Popejoy	95.9	70.3	26.1	2.3	0.2	1.2	0.1	0.0
Stasikelis	74.2	53.2	29.4	4.1	1.0	4.2	0.4	0.0

The distribution of modified Oxford scores for the combined calcaneal/Sanders scores is shown in Figure 4.6. C0/S1 to C3/S1 correspond principally to modified Oxford hip scores 16-18. Beginning with C3/S2, hips begin to progress to modified Oxford hip scores of 19 or higher. C4/S2 and C4/S3 are the transition stages that have a large range of intermediate modified Oxford hip scores. C4/S4 and higher stages correspond to mature modified Oxford hip scores.

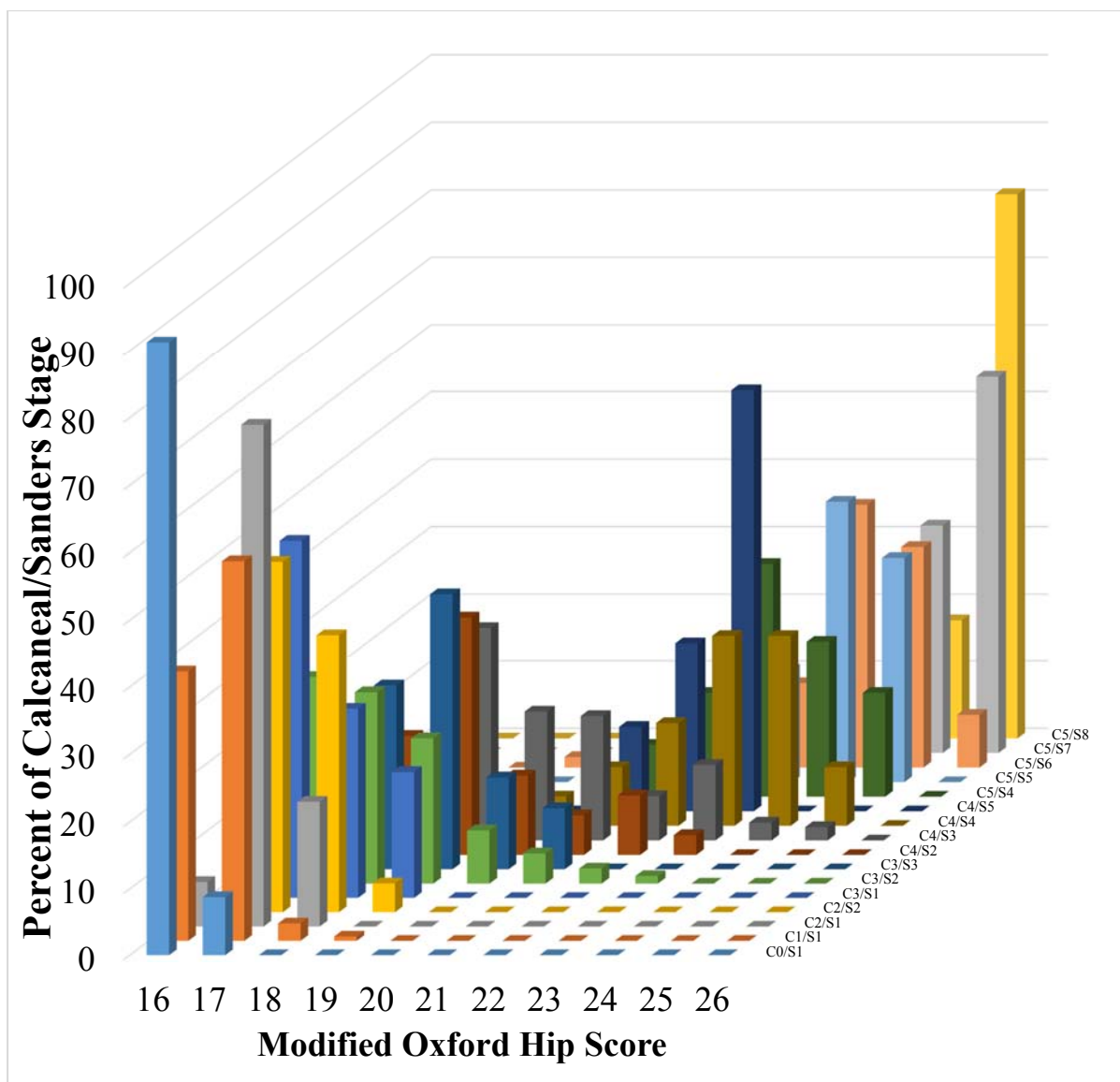


**Figure 4.6. Combined calcaneal/Sanders stages compared to modified Oxford hip scores**

The percentage of radiographs for each combined calcaneal/Sanders stage that has matching hip radiographs for each modified Oxford hip score. The calcaneal stage is indicated by C followed by the stage, and the Sanders stage is indicated by S followed by the stage.

The risk of contralateral SCFE for each calcaneal/Sanders stage was calculated using the risk for each modified Oxford hip score described by Stasikelis and Popejoy and are shown in Figure 4.7 and Table 4.3.<sup>7,8</sup> Risk of contralateral SCFE was considerably elevated up to calcaneal 4/Sanders 2, which had approximately 50% risk of contralateral SCFE. Risk remained significant for calcaneal 4/Sanders 3, which had approximately 25% risk of contralateral slip. Calcaneal 4/Sanders 4 and higher had negligible risk of contralateral slip.

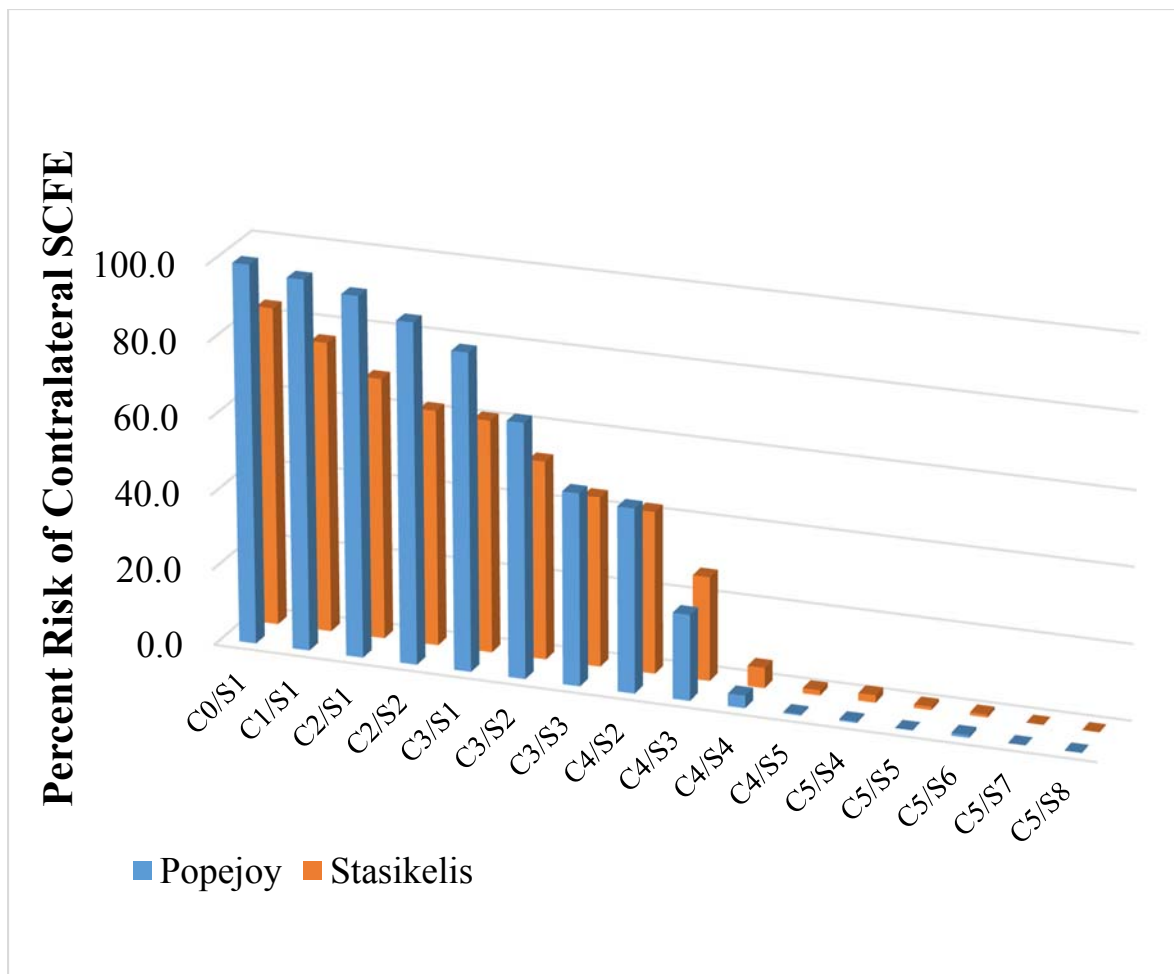


**Figure 4.7. Risk of contralateral SCFE for each calcaneal/Sanders stage**

Risk of contralateral SCFE was calculated using data from Popejoy and Stasikelis based on the percent risk for each modified Oxford hip score and the percentage of each calcaneal/Sanders stage corresponding to a particular modified Oxford hip score.



**Table 4.3. Percent Risk of contralateral SCFE for each calcaneal/Sanders stage**

	Popejoy	Stasikelis
C0/S1	99.7	83.9
C1/S1	97.5	76.5
C2/S1	95.0	68.8
C2/S2	89.8	62.2
C3/S1	83.7	61.3
C3/S2	67.3	52.4
C3/S3	50.8	44.8
C4/S2	48.4	42.5
C4/S3	22.5	27.3
C4/S4	3.3	5.3
C4/S5	0.4	1.4
C5/S4	0.4	2.0
C5/S5	0.1	0.9
C5/S6	0.8	0.8
C5/S7	0.0	0.0
C5/S8	0.0	0.0

The distribution of the TRC being open, closing or closed for each modified Oxford hip score is shown in Figure 4.8. The TRC begins closing during modified Oxford hip scores of 18. By modified Oxford hip scores of 22 the majority (86.5%) of TRC's are fully closed.

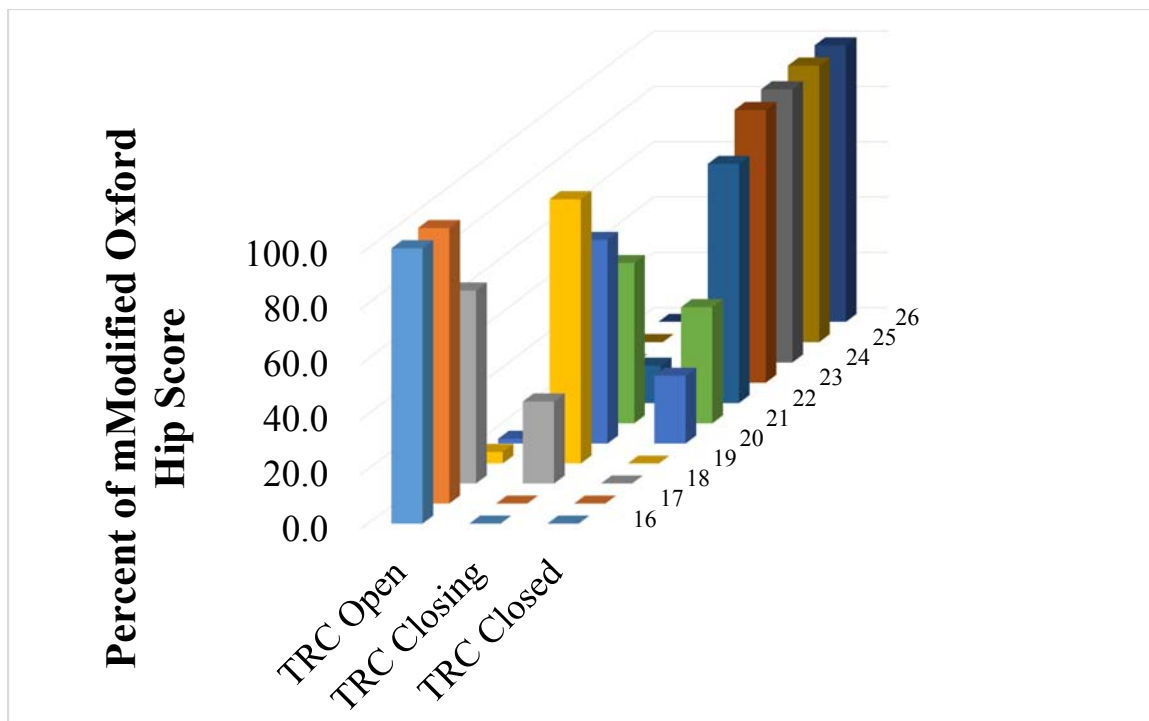


**Figure 4.8. Modified Oxford hip scores compared to TRC status**

The percentage of radiographs for each modified Oxford hip score that have corresponding hip radiographs with the TRC either open, closing, or closed.

The risk of contralateral SCFE for each TRC state was calculated using the risk for each modified Oxford hip score calculated by Stasikelis and Popejoy and are shown in Figure 4.9 and Table 4.4.<sup>7,8</sup> Risk of contralateral SCFE was considerable for an open TRC and remained significantly elevated for a closing TRC. Risk of contralateral slip was negligible for a closed TRC.

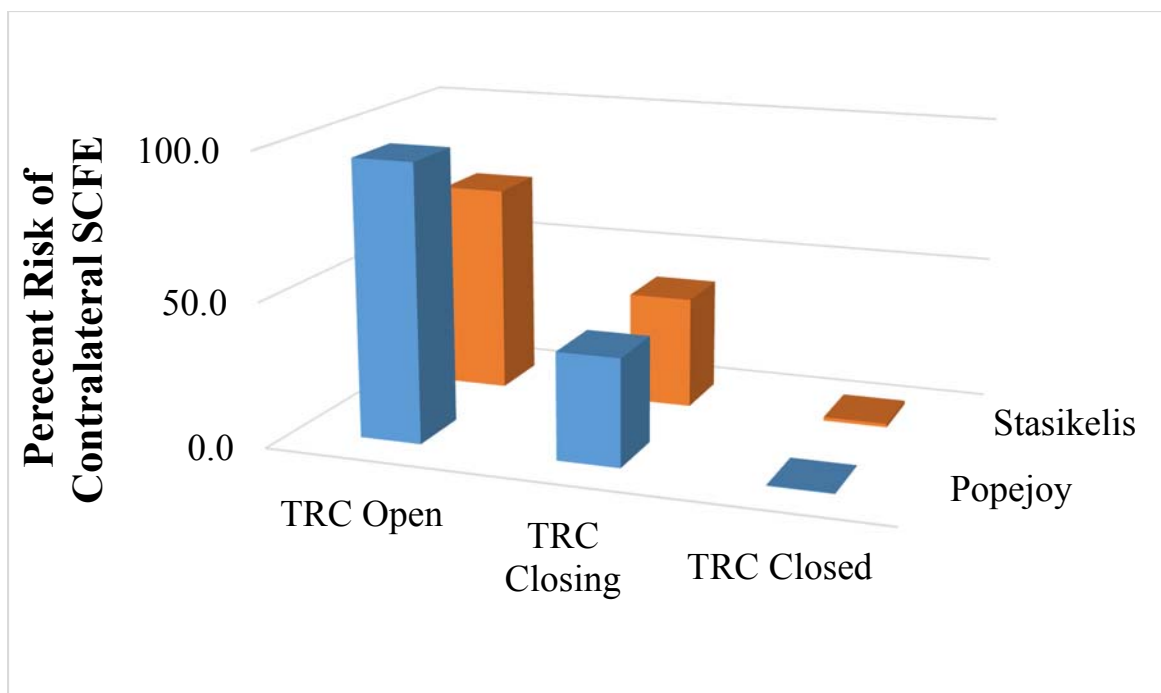


**Figure 4.9. Risk of contralateral SCFE for the TRC being open, closing, or closed**

Risk of contralateral SCFE was calculated using data from Popejoy and Stasikelis based on the percent risk for each modified Oxford hip score and the percentage of each TRC state corresponding to a particular modified Oxford hip score.

**Table 4.4. Percent Risk of contralateral SCFE for the TRC being Open, Closing, or Closed**

	TRC Open	TRC Closing	TRC Closed
Popejoy	95.5	36.9	0.2
Stasikelis	72.2	38.7	1.2

The distribution of the TRC being open, closing or closed for each calcaneal stage is shown in Figure 4.10. The TRC begins to close in calcaneal stage 2. A significant

percentage of TRC's are fully closed by calcaneal stage 4 (42.4%) and by calcaneal stage 5 virtually all TRC's are fully closed.

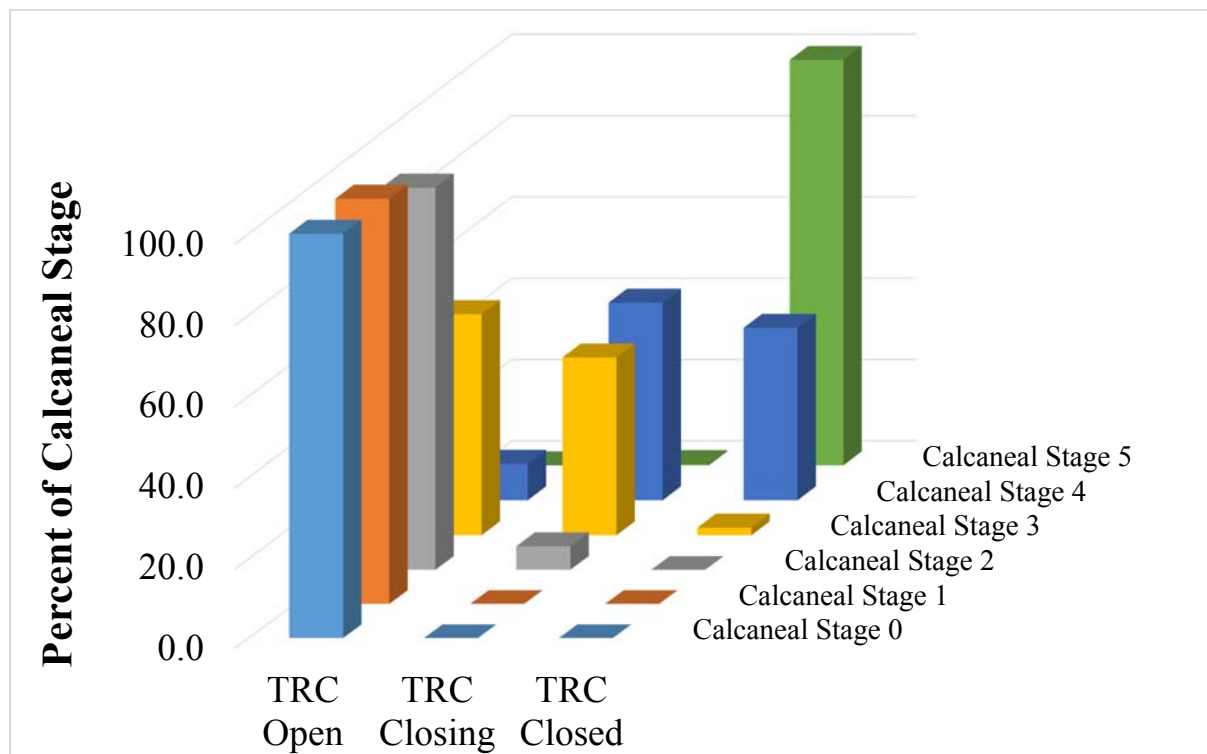


**Figure 4.10. Calcaneal stages compared to TRC status**

The percentage of radiographs for each calcaneal stage that have corresponding hip radiographs with the TRC either open, closing, or closed.

The distribution of the TRC being open, closing or closed for each Sanders hand score is shown in Figure 4.11. The TRC is closing principally during Sanders stage 2 and 3. By Sanders stage 4, the majority of TRC's are closed (90.3%) and by Sanders stage 5 or higher virtually all TRC's are closed.

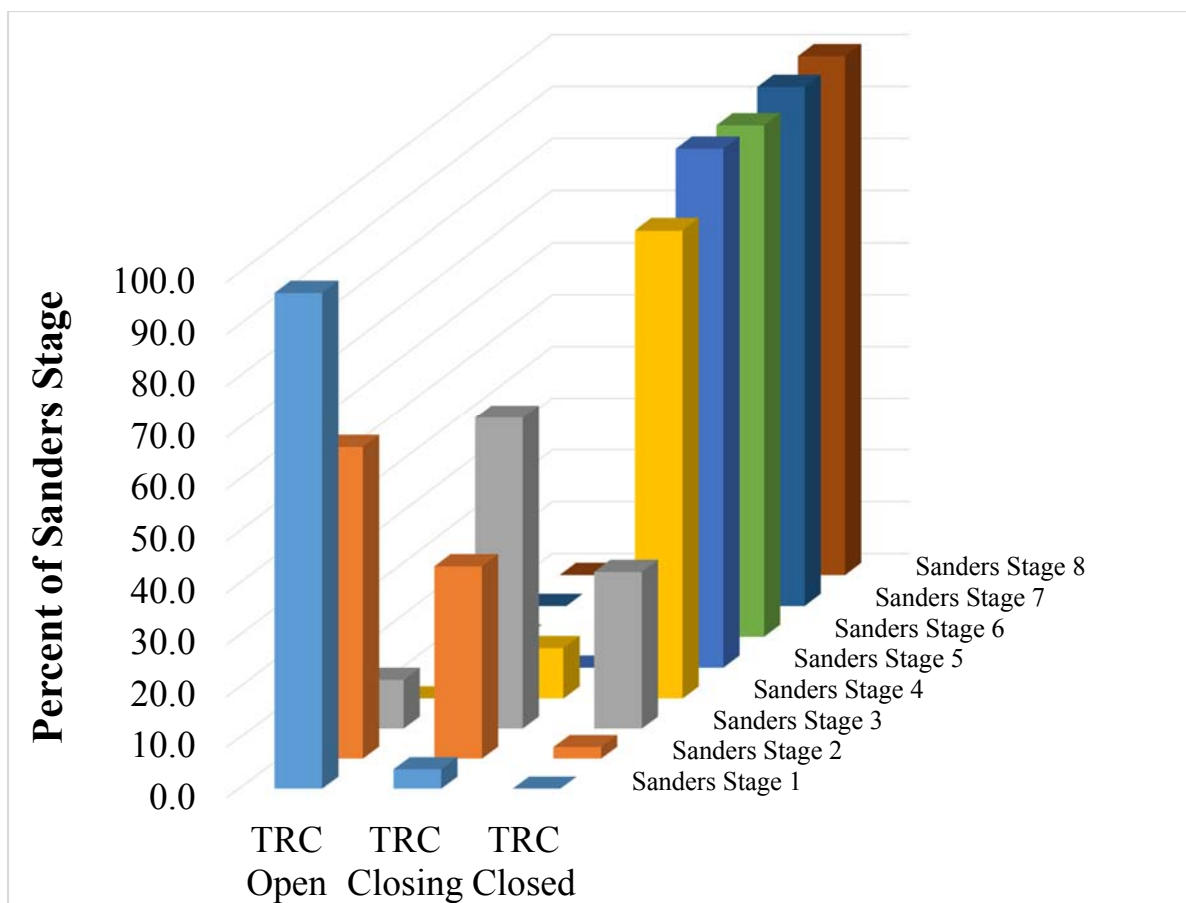


**Figure 4.11. Sanders hand scores compared to TRC status**

The percentage of radiographs for each Sanders hand score that have corresponding hip radiographs with the TRC either open, closing, or closed.

Age with respect to PHV for the modified Oxford system and the TRC are shown in Figure 4.12 and Table 4.5. A regular progression of modified Oxford hip scores and TRC status is seen with respect to PHV. Modified Oxford hip score 19 and the TRC closing occur approximately at the time of PHV. Age with respect to PHV for the calcaneal stages and Sanders scores are shown in chapter 2.

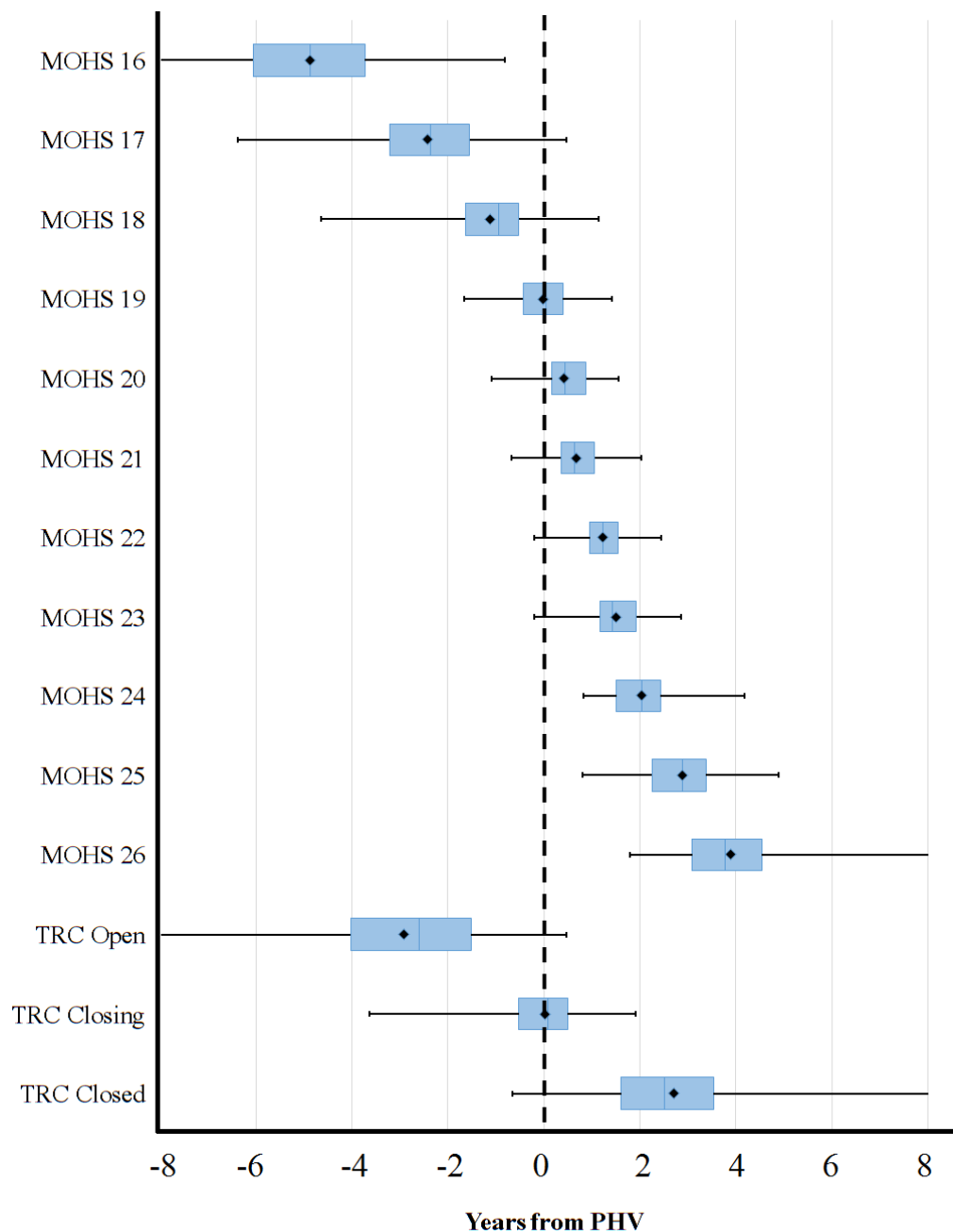


**Figure 4.12. Comparison of the modified Oxford system (MOHS) and TRC status with respect to PHV**

A box and whiskers plot of the age with respect to PHV for the modified Oxford hip scores and TRC status. The modified Oxford hip score is indicated by the number on the y-axis. The black lines represent the range for each examined sequence, while the blue

box represents the middle 50% of data. The blue line in the middle of each box represents the median, while the black diamond represents the mean. Modified Oxford hip score 16 and the TRC Open have their lower age ranges extended to -8 years from PHV to represent that they are scores of immaturity and children will have that score from birth. Modified Oxford hip score 26 and TRC Closed have their upper age ranges extended to +8 years from PHV to represent that they represent scores of full maturity.

**Table 4.5. Age from PHV for modified Oxford hip scores and the TRC**

		Timing Relative to PHV (yr)		
	n	Mean	95% CI	Range
<b>MOHS 16</b>	174	-4.87	-4.63 to -5.12	-8.55 to -0.82
<b>MOHS 17</b>	345	-2.42	-2.29 to -2.55	-6.39 to 0.47
<b>MOHS 18</b>	126	-1.12	-0.95 to -1.28	-4.64 to 1.15
<b>MOHS 19</b>	117	-0.01	0.10 to -0.13	-1.67 to 1.42
<b>MOHS 20</b>	57	0.42	0.59 to 0.26	-1.09 to 1.56
<b>MOHS 21</b>	50	0.68	0.84 to 0.53	-0.67 to 2.02
<b>MOHS 22</b>	37	1.24	1.46 to 1.02	-0.20 to 2.45
<b>MOHS 23</b>	74	1.51	1.63 to 1.38	-0.20 to 2.86
<b>MOHS 24</b>	81	2.04	2.20 to 1.89	0.83 to 4.18
<b>MOHS 25</b>	118	2.88	3.04 to 2.72	0.80 to 4.89
<b>MOHS 26</b>	193	3.90	4.06 to 3.75	1.80 to 7.22
<b>TRC Open</b>	618	-2.92	-2.77 to -3.06	-8.55 to 0.47
<b>TRC Closing</b>	228	0.02	0.12 to -0.08	-3.64 to 1.91
<b>TRC Closed</b>	531	2.71	2.83 to 2.59	-0.65 to 7.22

Inter-rater reliability for determination of individual modified Oxford scores was calculated with a weighted  $\kappa$  value of 0.77, with 87% of the ratings in agreement. Inter-rater reliability and intra-rater reliability for the TRC are shown in Table 4.6.

**Table 4.6 – Inter-rater reliability and intra-rater reliability for the TRC**

	Inter-rater $\kappa$	Inter-rater P	Intra-rater $\kappa$	Intra-rater P
Serial radiographs	0.86	0.91	0.88	0.92
Single radiographs	0.78	0.87	0.80	0.88
Serial vs single radiographs			0.72	0.81

## Discussion

Although factors such as age, body mass index, race, gender, and some systemic medical conditions (hypothyroidism and renal disease, among others) are associated with increased risk of developing a contralateral SCFE, many surgeons still have difficulty deciding which children are at highest risk of a contralateral slip and might benefit from prophylactic pinning.<sup>34</sup> Hagglund recommended that all patients with unilateral SCFE receive prophylactic contralateral pinning due to the high risk and the low morbidity of the procedure.<sup>52</sup> However, prophylactic pinning of all contralateral hips exposes all children to complications and unless they were likely to slip the other side, the risk would be unwarranted. Kocher recommended that prophylactic contralateral pinning should be done only if risk of a contralateral SCFE was >27%, and that children with less risk



should be observed.<sup>53</sup> Loder investigated the relation of Oxford bone age to SCFE, finding that SCFE occurs within a narrow window of bone age that is approximately half the width of the window of chronological age.<sup>33</sup> Although the Oxford bone score is strongly linked to SCFE, it is too complicated for clinical use, measuring nine regions surrounding the hip with various point ranges assigned to each region. Popejoy and Stasikelis suggest use of the modified Oxford hip score, which measures five regions surrounding the hip.<sup>7, 8</sup>

The modified Oxford method seems a promising approach to predicting the risk of contralateral slipping. Its use was first proposed by Stasikelis in 1999 and again more recently by Popejoy in 2012.<sup>7, 8</sup> Each study suggests that a modified Oxford hip score of 16-18 puts the contralateral hip at high risk for further slipping, greater than 50%. It is not widely used, perhaps due to the complexity of the scoring system.<sup>8</sup> Other difficulties of the modified Oxford method include phenotypic variation of radiographic features, and that all five radiographic features may not be present on a single radiograph or even on an AP and Frog Lateral. Many surgeons are expert at pinning SCFE. Fewer are expert at calculating an Oxford hip score. However, all surgeons who pin SCFE need to have a point of view concerning management of the side opposite a unilateral SCFE. At this time, most prefer to observe the opposite side until signs or symptoms of slipping are present.<sup>54</sup> This might not be the case if assigning risk for further slipping was straightforward and reliable.

As the Oxford score is complex, an alternative solution to determining risk of contralateral SCFE could be identification of another skeletal marker that correlates highly with low modified Oxford hip scores. Ossification of the calcaneal apophysis

provides an osteologic marker of skeletal maturation in relation to the modified Oxford method. The method is simple to use and closely resembles the widely used Risser sign. Calcaneal stages 0-2 almost entirely corresponded to the crucial modified Oxford score range of 16-18, and calcaneal stage 3 also corresponded to a significant percentage of hips that are modified Oxford scores of 16-18. We also relate the widely-used Sanders hand scores to the modified Oxford scores.

Sanders scores of 1 or 2 are associated with low modified Oxford hip scores and have substantial risk of contralateral slip. While our data clearly shows that calcaneal stages 0-3 or Sanders stages 1-2 have significant risk of contralateral slip, the risk of contralateral SCFE is more intermediate for calcaneal stage 4 or Sanders stage 3, approximately 25% for each, lower than the 27% threshold defined by Kocher.<sup>53</sup> For these crucial transition stages, we believe it beneficial to combine the calcaneal and Sanders systems for better localization of maturity and estimation of risk. Calcaneal stage 4 with a Sanders stage 2 hand, and a Sanders stage 3 hand with a stage 3 calcaneus both have significant risk of contralateral slip, approximately 50%. Calcaneal stage 4 with Sanders stage 3 has approximately 25% risk of contralateral slip. Higher combined stages, such as calcaneal stage 4 with Sanders stage 4 or above have negligible risk of contralateral slip.

Popejoy found that an open TRC is a significant predictor of contralateral slip, although less predictive than a modified Oxford score of 16-18.<sup>8</sup> Our comparison of the TRC with the overall modified Oxford hip score shows that the TRC first begins to close during modified Oxford hip scores of 18, and that closure is largely complete by the time a hip matures to modified Oxford hip scores of 22. Virtually all TRC's that remain wide

open are associated with modified Oxford hip scores 16-18. This explains why wide open TRC's are associated with extreme risk of contralateral slip, since they strongly correlate with modified Oxford hip scores of 16-18. In addition, our data shows that the TRC closes on average at PHV. Modified Oxford hip score of 19 also corresponds to time of PHV, indicating that at PHV the risk of contralateral SCFE begins to decrease. However, if a wide-open TRC is the only factor used to estimate modified Oxford hip scores and risk of contralateral SCFE, there will be a significant percentage of high risk contralateral SCFE's that are missed. A significant proportion of modified Oxford hip scores of 18 and 19 have the TRC in the process of closing. This indicates that a portion of children that have the TRC in the process of closing are still susceptible to contralateral SCFE. However, the process of the TRC closing continues until a modified Oxford hip score of 22. There needs to be a means of identifying the TRC's that are closing but are associated with elevated risk of contralateral SCFE.

In addition, it is often difficult to discern an open TRC from one that is closing. Readings obtained from single radiographs of the TRC were significantly different than readings obtained from the TRC viewed with TRC radiographs taken the years before and after the radiograph of interest. Rather than viewing the TRC as consisting of three states, which may be ambiguous, it could be helpful to consider the TRC as a digital marker, being either unambiguously closed or open. If the TRC is unambiguously open risk of contralateral SCFE is high and if the TRC is unambiguously closed risk of contralateral SCFE is low and there is certainty regarding clinical steps to be taken. However, if the TRC is closing, a hand or foot radiograph can be taken and the calcaneal and Sanders scores can be considered to add certainty. If we have a pelvis and hand and

a foot, we can make a very accurate estimate of slip risk, if the reader believes that modified Oxford hip scores predict risk and that we have accurately linked modified Oxford hip scores to the hand and foot radiographs.

A limitation of this study is that it involves normal children, and projections to SCFE using the data from Popejoy and Stasikelis are purely mathematical. A possible limitation of this study concerns the age of the collection used, that the radiographs may not be representative of modern children. However, our study design compares the calcaneal apophyseal ossification to the ossification sequence of the hip and pelvis, and the authors doubt that the order of the ossification sequences of the calcaneus, hip and pelvis has changed much over the last 80 years. In addition, we examine the relation of osteologic events compared to PHV. PHV allows males and females to be compared directly and would compensate for the earlier onset of puberty in modern children.

In summary, we found that the ossification of the calcaneal apophysis, Sanders hand scores, and the TRC can be used to predict modified Oxford hip scores. Considering the complexities of using the modified Oxford method, and the phenotypic variation inherent in the five radiographic features, we recommend the use of adjunct maturity systems for determining which children are at relatively high and relatively low risk of further slipping in unilateral SCFE. We recommend that if the TRC is clearly open, the child is considered to have high risk of contralateral slip and receives prophylactic pinning. If the TRC is clearly closed, the child does not need contralateral pinning. If the TRC is in the process of closing, or is unclear, a calcaneal radiograph or Sanders hand score can be obtained. If a calcaneus of stage 0-3 or Sanders stage 1-2 is seen, the child has elevated risk and should receive prophylactic pinning. If the calcaneus

is stage 4, or the hand is Sanders stage 3, the calcaneus and Sanders hand score should be considered jointly. Calcaneal stage 4 with a Sanders stage 2 hand, or a Sanders stage 3 hand with a stage 3 calcaneus should receive prophylactic pinning.

## **Discussion**

Skeletal maturity assessment allows prediction of remaining growth and is a central part of orthopaedic decisions such as timing of epiphysiodesis and prediction of AIS curve progression. Skeletal maturity was first described by Todd in his 1937 atlas of the hand.<sup>10</sup> The Todd atlas was followed by creation of several atlases that could be used to establish “bone age” based on regular changes of morphology in the hand, knee, and foot, including the widely-used Greulich and Pyle hand atlas and the lesser-known Hoerr atlas of the foot.<sup>9, 38, 55</sup> However, these atlases were created prior to the understanding of peak height velocity delineated by Tanner, which established the importance of the adolescent growth spurt, or specifically the timing of peak height velocity (PHV) as a uniform marker of maturity during adolescence.<sup>21-23, 56</sup> As noted by both Dimeglio and Sanders, the time intervals of the Greulich and Pyle atlas are problematic around the time of adolescence.<sup>12, 35</sup> Sanders found that children mature more rapidly at adolescence than the intervals between the “skeletal ages” of Greulich and Pyle suggest.<sup>12</sup> Loder found that the Greulich and Pyle standards are not applicable for white boys during late childhood or adolescence.<sup>19</sup>

Ossification of the calcaneal apophysis can determine skeletal maturity around the time of adolescence. Excursion of the calcaneal apophysis begins with appearance of the ossification center approximately five years prior to PHV, spread of the apophysis in a plantar-dominant fashion, regular changes to the appearance of the interval between the apophysis and metaphysis, and consistent patterns of fusion. These events can be divided into six stages that occur over a seven year period. Four of the six stages of calcaneal

apophyseal ossification occur prior to PHV, allowing time remaining to PHV to be predicted up to five years prior.

The Sanders hand scores also can identify the time period of PHV, and share areas of overlap with the calcaneal stages. Sanders stage 2 and calcaneal stage 3 both occur 0.9 years before PHV while Sanders stage 3 and calcaneal stage 4 both occur approximately 0.5 years after PHV. The Sanders system has two of its eight stages occurring before PHV. The presence of four stages prior to PHV allows for the calcaneal system to localize maturity within more narrow intervals in the time before PHV while the presence of six stages after PHV allows the Sanders system to localize maturity within more narrow intervals in the time after PHV. The areas of overlap of the calcaneal and Sanders stages allow the two maturity systems to be combined. For instance, a child with a stage 3 calcaneus may have a hand that is Sanders 2, 3, or 4. Depending on the combination of the calcaneal stage and Sanders hand score, maturity can be localized during more narrow intervals than use of either single system alone.

The calcaneal and Sanders systems are analog systems, relying upon a series of morphological changes. Many people are uncomfortable with analog systems, which sometimes require accurately identifying small morphological changes which may vary depending on the child. For instance, capping, the defining characteristic of Sanders stage 3, can be difficult to appreciate and sometimes appears to be absent in children followed with serial radiographs. Many people prefer digital distinctions, distinction that are all or nothing.

The plantar and thenar sesamoids are two digital distinctions occurring around time of PHV that offer ability to quickly deduce maturity without judging small

morphological changes. If both sesamoids are absent, the child is likely at least 1.35 years before PHV. If the plantar sesamoids are present, and the thenar sesamoids are absent, the child is in between 1.35 years before PHV and 0.12 years before PHV. If both sesamoids are present, the child is after 0.12 years before PHV. The presence of the sesamoids can also add clarity to existing maturity systems, particularly for stages that have morphological changes that are sometimes difficult to appreciate. The presence of the plantar sesamoids on a lateral radiograph indicates that a calcaneus is significantly more likely to be calcaneal stage 2 than 1. The presence of clearly defined radiopaque plantar sesamoids on an AP radiograph indicates that a calcaneus is more likely calcaneal stage 3 than 2. Sanders hand score 3 can be difficult to appreciate if capping is ambiguous. If the thenar sesamoids are larger than a puff of ossification, a hand is more likely to be Sanders score 3 than 2.

The calcaneal and Sanders systems have potential to simplify complex maturity systems that have known clinical uses, such as the modified Oxford hip score. Although low modified Oxford hip scores have been shown to be strongly associated with contralateral SCFE, the maturity system is difficult to use in practice due to a complex scoring system, difficulty in seeing the five required radiographic areas on a single radiograph, and morphological variation between children.<sup>7, 8, 34</sup> Calcaneal stages 0-3, and Sanders hand scores 1-2 are associated with modified Oxford hip scores indicating substantial risk of contralateral SCFE. Calcaneal stage 4 and Sanders hand score 3 are associated with modified Oxford hip scores indicating intermediate risk of contralateral SCFE, approximately 25%.



We have outlined a number of skeletal maturity systems, and ways in which they might be combined or substituted for each other. The question arises, which maturity system should be used, and when should combinations of maturity systems be used? A possible way to consider the use of maturity systems stems from the ideas of digital and analog. Digital distinctions are clear. The maturity indicator is certain, and the clinical association of the maturity indicator is strong. For instance, if the TRC is clearly wide open, the child is at high risk of contralateral SCFE, and further investigation of other maturity indicators is likely not necessary. However, there are often times when a maturity indicator is not clear, or the associated clinical question is in doubt. For instance, it can sometimes be difficult to distinguish calcaneal stage 2 from 3, or Sanders 2 from 3. This would be an example of an unclear maturity indicator, and at this time alternative maturity indicators could also be measured to provide additional resolution of maturity relative to PHV. There are also instances where the maturity indicator is clear, but the associated clinical implications are not. If a TRC is closing, the risk of contralateral SCFE is intermediate. An associated maturity marker could be examined to provide more clinical certainty about the probability of the child having a contralateral slip. For example, if the TRC is closing but the child is Sanders stage 2, the child is at high risk of contralateral SCFE. In areas of intermediate certainty regarding a clinical use, the improved power of combinations of multiple maturity systems can be leveraged.

While the majority of existing maturity systems focus on the mean, we believe that the range is important too. Many existing maturity systems only list the mean age of each stage without reporting the range. As shown in our analyses, the range of ages is often considerable within a single stage. Combining maturity systems allows the ranges

to be cut down considerably, allowing for much more precise localization of maturity.

Use of the hand and hip and foot together create certainty by clarifying areas of overlap and diminishing variation inherent from relying on a single marker. Using combinations of maturity systems, especially during times when a single maturity system is associated with an intermediate clinical probability, will allow for improved determination of maturity and better clinical accuracy.

We have described a new skeletal maturity assessment system, the calcaneal apophysis, and its utility for predicting PHV. We have also explored the relationships between several systems of maturity assessment, including the calcaneal apophysis, Sanders hand scores, modified Oxford hip scores, TRC, iliac apophysis, as well as plantar and thenar sesamoids. We have found that maturity systems used in conjunction provide improved localization of maturity relative to PHV, and better answer clinical questions such as risk of contralateral SCFE. Combinations of maturity systems are useful when maturity markers are unclear and for areas of intermediate clinical probability, to improve prediction. We predict that combinations of systems will answer other orthopaedic questions with improved accuracy over single maturity systems alone. We expect that the newly described calcaneal apophyseal system will also find further uses, particularly for scoliosis curve progression.

## **References**

1. Sanders JO, Little DG, Richards BS. Prediction of the crankshaft phenomenon by peak height velocity. *Spine*. 1997;22(12):1352-6.
2. Sanders JO. Maturity indicators in spinal deformity. *The Journal of Bone & Joint Surgery*. 2007;89(suppl\_1):14-20.
3. Sanders JO, Browne RH, Cooney TE, Finegold DN, McConnell SJ, Margraf SA. Correlates of the peak height velocity in girls with idiopathic scoliosis. *Spine*. 2006;31(20):2289-95.
4. Sanders JO, Browne RH, McConnell SJ, Margraf SA, Cooney TE, Finegold DN. Maturity assessment and curve progression in girls with idiopathic scoliosis. *The Journal of Bone & Joint Surgery*. 2007;89(1):64-73.
5. Hans SD, Sanders JO, Cooperman DR. Using the Sauvegrain method to predict peak height velocity in boys and girls. *Journal of Pediatric Orthopaedics*. 2008;28(8):836-9.
6. Marshall W, De Limongi Y. Skeletal maturity and the prediction of age at menarche. *Annals of human biology*. 1976;3(3):235-43.
7. Stasikelis PJ, Sullivan CM, Phillips WA, Polard JA. Slipped Capital Femoral Epiphysis. Prediction of Contralateral Involvement\*. *The Journal of Bone & Joint Surgery*. 1996;78(8):1149-55.
8. Popejoy D, Emara K, Birch J. Prediction of contralateral slipped capital femoral epiphysis using the modified Oxford bone age score. *Journal of Pediatric Orthopaedics*. 2012;32(3):290-4.
9. Greulich WW, Pyle SI. Radiographic atlas of skeletal development of the hand and wrist. *The American Journal of the Medical Sciences*. 1959;238(3):393.
10. Todd TW. *Atlas of Skeletal Maturation*. Baltimore, MD: The C. V. Mosby Company; 1937 1937.
11. Nelson S, Hans MG, Broadbent BH, Dean D. The brush inquiry: An opportunity to investigate health outcomes in a well-characterized cohort. *American Journal of Human Biology*. 2000;12(1):1-9.
12. Sanders JO, Houry JG, Kishan S, Browne RH, Mooney III JF, Arnold KD, et al. Predicting scoliosis progression from skeletal maturity: a simplified classification during adolescence. *The Journal of Bone & Joint Surgery*. 2008;90(3):540-53.
13. Cundy P, Paterson D, Morris L, Foster B. Skeletal age estimation in leg length discrepancy. *Journal of Pediatric Orthopaedics*. 1988;8(5):513-5.
14. Bull R, Edwards P, Kemp P, Fry S, Hughes I. Bone age assessment: a large scale comparison of the Greulich and Pyle, and Tanner and Whitehouse (TW2) methods. *Archives of disease in childhood*. 1999;81(2):172-3.
15. King D, Steventon D, O'Sullivan M, Cook A, Hornsby V, Jefferson I, et al. Reproducibility of bone ages when performed by radiology registrars: an audit of Tanner and Whitehouse II versus Greulich and Pyle methods. *The British journal of radiology*. 1994;67(801):848-51.
16. Büken B, Şafak AA, Yazıcı B, Büken E, Mayda AS. Is the assessment of bone age by the Greulich–Pyle method reliable at forensic age estimation for Turkish children? *Forensic science international*. 2007;173(2):146-53.

17. van Rijn RR, Lequin MH, Robben SG, Hop WC, van Kuijk C. Is the Greulich and Pyle atlas still valid for Dutch Caucasian children today? *Pediatric radiology*. 2001;31(10):748-52.
18. Hackman L, Black S. The reliability of the Greulich and Pyle Atlas when applied to a modern Scottish population. *Journal of forensic sciences*. 2013;58(1):114-9.
19. Loder RT, Estle DT, Morrison K, Eggleston D, Fish DN, Greenfield ML, et al. Applicability of the Greulich and Pyle skeletal age standards to black and white children of today. *American Journal of Diseases of Children*. 1993;147(12):1329-33.
20. Charles YP, Diméglio A, Canavese F, Daures J-P. Skeletal age assessment from the olecranon for idiopathic scoliosis at Risser grade 0. *The Journal of Bone & Joint Surgery*. 2007;89(12):2737-44.
21. Tanner JM, Davies PS. Clinical longitudinal standards for height and height velocity for North American children. *The Journal of pediatrics*. 1985;107(3):317-29.
22. Tanner J, Healy M, Goldstein H, Cameron N. Assessment of skeletal maturity and prediction of adult height (TW3). WB Saunders, London. 2001.
23. Tanner JM, Whitehouse R, Cameron N, Marshall W, Healy M, Goldstein H. Assessment of skeletal maturity and prediction of adult height (TW2 method): Academic Press London; 1975.
24. Cox LA. Tanner-Whitehouse method of assessing skeletal maturity: problems and common errors. *Hormone research*. 1996;45 Suppl 2:53-5. Epub 1996/01/01.
25. JC R. The Iliac apophysis; an invaluable sign in the management of scoliosis. *Clinical orthopaedics*. 1957;11:111-9.
26. Noordeen M, Haddad FS, Edgar MA, Pringle J. Spinal growth and a histologic evaluation of the Risser grade in idiopathic scoliosis. *Spine*. 1999;24(6):535-8.
27. Peterson L-E, Nachemson AL. Prediction of progression of the curve in girls who have adolescent idiopathic scoliosis of moderate severity. Logistic regression analysis based on data from The Brace Study of the Scoliosis Research Society. *The Journal of Bone & Joint Surgery*. 1995;77(6):823-7.
28. RISSER JC, FERGUSON AB. Scoliosis: its prognosis. *The Journal of Bone & Joint Surgery*. 1936;18(3):667-70.
29. Karol LA, Johnston CE, Browne RH, Madison M. Progression of the curve in boys who have idiopathic scoliosis. *The Journal of Bone & Joint Surgery*. 1993;75(12):1804-10.
30. Urbaniak J, Schaefer W, STELLING III F. Iliac apophyses: prognostic value in idiopathic scoliosis. *Clinical orthopaedics and related research*. 1976;116:80-5.
31. Little DG, Song KM, Katz D, Herring JA. Relationship of Peak Height Velocity to Other Maturity Indicators in Idiopathic Scoliosis in Girls\*. *The Journal of Bone & Joint Surgery*. 2000;82(5):685-.
32. Acheson R. The Oxford method of assessing skeletal maturity. *Clinical orthopaedics*. 1957;10:19.
33. Loder RT, Starnes T, Dikos G. The narrow window of bone age in children with slipped capital femoral epiphysis: a reassessment one decade later. *Journal of Pediatric Orthopaedics*. 2006;26(3):300-6.
34. Zide JR, Popejoy D, Birch JG. Revised Modified Oxford Bone Score: A Simpler System for Prediction of Contralateral Involvement in Slipped Capital Femoral Epiphysis. *Journal of Pediatric Orthopaedics*. 2011;31(2):159-64.

35. Diméglio A, Charles YP, Daures J-P, De Rosa V, Kaboré B. Accuracy of the Sauvegrain method in determining skeletal age during puberty. *The Journal of Bone & Joint Surgery*. 2005;87(8):1689-96.
36. Sauvegrain J, Nahum H, Bronstein H, editors. Study of bone maturation of the elbow]. *Annales de radiologie*; 1962.
37. Nicholson AD, Liu RW, Sanders JO, Cooperman DR. Relationship of Calcaneal and Iliac Apophysis Ossification to Peak Height Velocity Timing in Children. *The Journal of Bone & Joint Surgery*. 2015 2015-01-21 00:00:00;97:147-54.
38. Hoerr NL, Pyle S, Francis C. Radiographic atlas of skeletal development of the foot and ankle: a standard of reference: Thomas Springfield, IL; 1962.
39. Hackman L, Davies CM, Black S. Age estimation using foot radiographs from a modern Scottish population. *Journal of forensic sciences*. 2013;58(s1):S146-S50.
40. Song KM, Little DG. Peak height velocity as a maturity indicator for males with idiopathic scoliosis. *Journal of Pediatric Orthopaedics*. 2000;20(3):286-8.
41. Hauspie R, Bielicki T, Koniarek J. Skeletal maturity at onset of the adolescent growth spurt and at peak velocity for growth in height: a threshold effect? *Annals of human biology*. 1991;18(1):23-9.
42. Hägg U, Taranger J. Skeletal stages of the hand and wrist as indicators of the pubertal growth spurt. *Acta Odontologica*. 1980;38(3):187-200.
43. Parent A-S, Teilmann G, Juul A, Skakkebaek NE, Toppari J, Bourguignon J-P. The timing of normal puberty and the age limits of sexual precocity: variations around the world, secular trends, and changes after migration. *Endocrine reviews*. 2003;24(5):668-93.
44. Duval-Beaupère G, Dubousset J, Queneau P, Grossiord A. A unique theory on the course of scoliosis]. *La Presse Médicale*. 1970;78(25):1141.
45. Howorth B. Slipping of the capital femoral epiphysis. *Pathology. Clinical orthopaedics and related research*. 1965;48:33-48.
46. Murray R. The aetiology of primary osteoarthritis of the hip. 1965.
47. Jerre R, Billing L, Hansson G, Karlsson J, Wallin J. Bilaterality in slipped capital femoral epiphysis: importance of a reliable radiographic method. *Journal of Pediatric Orthopaedics B*. 1996;5(2):80-4.
48. Baghdadi YM, Larson AN, Sierra RJ, Peterson HA, Stans AA. The fate of hips that are not prophylactically pinned after unilateral slipped capital femoral epiphysis. *Clinical Orthopaedics and Related Research®*. 2013;471(7):2124-31.
49. Larson AN, Sierra RJ, Elizabeth MY, Trousdale RT, Stans AA. Outcomes of slipped capital femoral epiphysis treated with in situ pinning. *Journal of Pediatric Orthopaedics*. 2012;32(2):125-30.
50. Yildirim Y, Bautista S, Davidson RS. Chondrolysis, osteonecrosis, and slip severity in patients with subsequent contralateral slipped capital femoral epiphysis. *The Journal of Bone & Joint Surgery*. 2008;90(3):485-92.
51. Sankar WN, Novais EN, Lee C, Al-Omari AA, Choi PD, Shore BJ. What are the risks of prophylactic pinning to prevent contralateral slipped capital femoral epiphysis? *Clinical Orthopaedics and Related Research®*. 2013;471(7):2118-23.
52. Hägglund G. The contralateral hip in slipped capital femoral epiphysis. *Journal of Pediatric Orthopaedics B*. 1996;5(3):158-61.

53. Kocher MS, Bishop JA, Hresko MT, Millis MB, Kim Y-J, Kasser JR. Prophylactic pinning of the contralateral hip after unilateral slipped capital femoral epiphysis. *The Journal of Bone & Joint Surgery*. 2004;86(12):2658-65.
54. Mooney III JF, Sanders JO, Browne RH, Anderson DJ, Jofe M, Feldman D, et al. Management of unstable/acute slipped capital femoral epiphysis: results of a survey of the POSNA membership. *Journal of Pediatric Orthopaedics*. 2005;25(2):162-6.
55. Pyle SI, Hoerr NL. Radiographic atlas of skeletal development of the knee: a standard of reference: CC Thomas; 1955.
56. Tanner JM, Whitehouse R, Takaishi M. Standards from birth to maturity for height, weight, height velocity, and weight velocity: British children, 1965. I. *Archives of Disease in Childhood*. 1966;41(219):454.